ANTIGEN AGNOSTIC CO-STIMULATION FOR ENGINEERED TCR T-CELLS

By

Anton Dobrin

A Dissertation

Presented to the Faculty of the Louis V. Gerstner, Jr.

Graduate School of Biomedical Sciences,

Memorial Sloan-Kettering Cancer Center

in Partial Fulfillment of the Requirements for the Degree of

Doctor of Philosophy

New York, NY

April 2023

_____ _____

Michel Sadelain MD/PhD Date

Dissertation Mentor

Abstract

Adoptive cell therapy using chimeric antigen receptors (CARs) has been shown to be extremely efficacious in a number of relapsed and refractory blood cancers. Conversely, T-cell receptor (TCR) based adoptive cell therapy has so far not been as successful. While the two approaches differ in many aspects, including receptor structure, antigen structure and presentation, and cancer types treated, one key distinction is that TCR-based therapies do not contain autochthonous co-stimulatory support. As the addition of co-stimulation onto CARs was a key advance that led to clinical potency, I hypothesized that the addition of co-stimulation to the TCR would likely advance the utility of TCR-based therapies.

Initial strategies involved the direct fusion of co-stimulatory intracellular domains onto the TCR chains or onto CD3 molecules with which the TCR associates on the cell surface. While these strategies showed some promise *in vitro,* including increased cytokine secretion and proliferation, consistent with functional co-stimulation, *in vivo*, in a variety of tumour models, anti-tumour efficacy was not improved.

These observations suggested that a TCR independent co-stimulatory molecule would be a more viable strategy. To this end, we designed a receptor, “80BB”, that would provide co-stimulation through two extensively studied pathways, CD28 and 4-1BB, relying on the extracellular domain of CD80, a natural agnostic ligand for CD28, and the intracellular domain of 4-1BB. Engineered cells endowed with 80BB exhibited increased cytokine secretion, proliferation, and enhanced tumouricidal *in vitro*. In an aggressive B-ALL murine model, we observe improved anti-tumor efficacy, T-cell accumulation, decreased expression of dysfunction-associated genes and increased

expression of cytotoxicity genes following endowment of the 80BB receptor onto the therapeutic T-cells.

We further studied the interaction network of this new molecule, confirming that the 4-1BB domain is functional, that the extracellular CD80 domain binds to both canonical ligands, CD28 and CTLA-4, and that both of these interactions lead to 4-1BB co-stimulation. Finally, we showed that tumour infiltrating lymphocytes (TILs) endowed with 80BB were better able to control an autologous patient-matched tumour cell line *in vitro* and *in vivo* in a TCR agnostic manner.

Overall, through the work we translate key lessons from the CAR field to engineered TCR T-cells and TILs, significantly improving their preclinical efficacy.

Acknowledgements

I would like to thank my mentor Dr. Michel Sadelain for giving me the opportunity to work in his lab, providing the training, support, and independence for me to complete this work. I would like to further thank Dr. Michel Sadelain for sharing his experience and wisdom on the profession of science and translating scientific discoveries to the clinic.

I would like to thank Dr. Sjoukje van der Stegen for supervising me as a rotation student and welcoming me to the lab many years ago and providing arms-length advice over the years since then. I would like to thank Dr. Mohamad Hamieh for his role in the 80BB project, his seemingly endless knowledge of the field, and his generous advice. I would like to thank Dr. Nayan Jain for all his thought-provoking discussions on science, society, and future directions. I would also like to thank Pieter Lindenbergh for his helpful insights and perspective. I would like to also thank the many current and former members of the lab who provided pivotal advice and guidance – Drs. Yuzhe Shi, Zeguo Zhao, Justin Eyquem, Jorge Mansilla-Soto, Judith Feucht, Karlo Perica.

I want to thank my committee members, Dr. Morgan Huse and Dr. Andrea Schietinger for their advice and guidance through my PhD.

I would also want to thank the administration at Gerstner Sloan Kettering Graduate school for their assistance through out the process, especially David McDonagh, Linda Burnley, Michael Overholtzer and former dean, Ken Marians.

I would like to thank the MSKCC Dragon Boating team, coached by James Lozada and Akila Simon. Their motivation and lessons have been incredibly useful on and off the water.

Contents

List of Figures

List of Abbreviations

80BB	CD80 – 4-1BB fusion molecule
ACT	Adoptive cell therapy
AAV	Adeno associated virus
ATAM	Artificial T-cell-activating adapter molecules
B-ALL	B-cell acute lymphoblastic leukemia
BCG	Bacillus Calmette Guerin [vaccine]
BiTE	Bispecific T-cell Engager
CAR	Chimeric antigen receptor
CLL	Chronic lymphocytic leukemia
CCR	Chimeric costimulatory receptor
CTL assay	Cytotoxic T Lymphocyte assay
CD	Cluster of differentiation
CRISPR	Clustered regularly interspaced short palindromic repeats
CTLA-4	Cytotoxic T-lymphocyte-associated protein 4
DC	Dendritic cell
GFP	Green fluorescent protein
HIT	HLA independent TCR
HDR	Homology directed repair
HLA	human leukocyte antigen
IL	Interleukin
IRES	Internal ribosome entry site
iv	Intravenous
KO	Knock out
LNGFR	Low-affinity nerve growth factor receptor
NSG	NOD (nonobese diabetic) scid gamma [mouse]
REP	Rapid expansion protocol
scFv	Single-chain variable fragment
TCR	T-cell receptor
TCR Vβ1	T-cell receptor variable chain beta 1
TIL	Tumour infiltrating lymphocyte
WT	Wildtype

Chapter 1 – Introduction

There is ample evidence that cancer progression is antagonized by a functional immune system[1]. Immunotherapies, which comprise a broad class of therapeutics that attempt to augment the anti-tumour response including adoptive cell therapies, immune checkpoint blockade therapies, cancer vaccines, agonist antibodies and BiTEs, capitalize on and stimulate this intrinsic immune property[2-4]. Over the last 15 years, the field of immunotherapies has led a number of highly specific therapies that have graduated beyond clinical trials and have been proven to lead to improved patient outcomes across a diverse array of cancer malignancies, including melanomas, leukemias, lymphomas, bladder cancers, breast cancers, esophageal cancers, liver cancer, lung cancers and many others[5, 6]. While highly efficacious, these therapies are still limited to a relatively small number of malignancies and do not induce responses in all patients treated. Investigations are underway to broaden their applicability and increase their efficacy while decreasing adverse events.

Cancer vaccines

Coleys' Toxins composed of live and inactivated bacteria injected into inoperable tumours is the earliest documented case of immunotherapy[4, 7, 8]. A more contemporary, clinically approved, therapy uses the Bacillus Calmette Guerin (BCG) vaccine injected directly into the bladder to induce an immune response and treat bladder cancers[9, 10]. Cancer vaccines are therapeutics that are postulated to both directly attack the cancer and indirectly induce the development of a patient's own immune response against their tumour[2, 10, 11].

Another cancer vaccine strategy takes advantage of antigen presenting dendritic cells (DCs) that are loaded with patient-specific antigens *in vitro* and subsequently re-infused, possibly along with adjuvants to activate a T-cell in an inflammatory context[12, 13]. Sipuleucel-T is an approved DC vaccine, in which DCs are isolated from a patient, pulsed with prostate-specific protein and a cytokine, and subsequently re-infused[14]. The exact mechanism has not been clearly delineated, but likely involves the presentation of antigens to T-cells, and the initiation of T-cell anti-tumour response[15]. While beneficial, the overall survival benefit of Sipuleucel-T is 4.1 months, and no further DC vaccines have been approved[16-18]. In light of additional developments in the field of immunotherapy, combinations of antigen-loaded DC cells and checkpoint blockade therapies are under investigation[19, 20]. The advent of mRNA technology has also allowed for the development of *in situ* cancer vaccines where an mRNA coding for a tumour neoantigen or tumour associated antigen is injected into the patient[21, 22]. DCs and other antigen presenting cells (APCs) express the mRNA and induce the development of a *de novo* immune response. mRNA vaccines are highly promising, and clinical trials are ongoing alone or in combination with other immunotherapies[21, 22].

Immune checkpoint blockade antibodies

Immune checkpoint blockade antibodies are a highly successful clinical approach that takes advantage of an already-present T-cell repertoire[5, 23]. They have been licensed for a number of indications including melanoma, non-small cell lung cancer, renal clear cell carcinoma and others[5]. Upon activation, T-cells express inhibitory molecules to limit their activation, such as PD-1 or CTLA-4, which bind tumour-expressed inhibitory PD-

L1 or compete for co-stimulatory CD80, respectively[24, 25]. Checkpoint blockade therapies act by blocking these inhibitory proteins from interacting with their ligands, either by biding the inhibitory proteins directly (ipilimumab, nivolumab) or by binding their ligands (atezolizumab, durvalumab)[5]. There is evidence to suggest that the two most common targets, PD-1 or CTLA-4 lead to therapeutic improvements through different mechanisms[26]. CTLA-4 blockade abolishes the inhibitory role of CTLA-4 during initial T-cell priming and leads to fresh T-cell influx into the tumour, while the PD-1 pathway inhibitors are though to act on pre-existing T-cells, leading to their increased activity[5]. Some studies have also suggested that CTLA-4 blockade is able to bind tumour microenvironment associated Tregs and lead to their ablation via antibody mediated cytotoxicity[5]. Since this therapy depends on triggering a more potent immune endogenous immune response, tumour mutational burden is a correlate of outcome in patients receiving immune checkpoint blockade therapies[27]. Efforts to increase the efficacy of this therapy have led to the ongoing investigations of other T-cell inhibitory checkpoints have investigated including Lag3 (relatlimab), and Tim3 (cobolimab)[28, 29].

TIL therapies

Immune checkpoint blockade antibodies seek to re-functionalize an immune response directly within a patient. Tumour infiltrating lymphocyte (TIL) therapy conversely uses T-cells isolated from a tumour resection and cultured in stimulatory conditions *in vitro* for therapy[30, 31]. Typically, the T-cells are expanded in high dose IL-2 and subsequently re-infused with the patient receiving further IL-2 to bolster the immune response. Similarly to checkpoint blockade, this approach takes advantage of a natural

polyclonal TCR repertoire already present within a patient. TILs have recently been identified as more efficacious than second-line checkpoint blockade therapy, although given the associated pre-conditioning and post-condition regiment, 100% of the TIL-treated patients had grade 3 or higher adverse events[32]. Efforts to make TILs independent of exogenous cytokines, which are a major source of adverse events, have focused on engineering TILs to constitutively or inducibly express their own IL-2 or IL-12[33, 34]. TILs engineered to express IL-2 did not exhibit increased persistence, while IL-12 secretion was associated with hepatic toxicity. There are ongoing clinical trials to investigate TILs co-infused with checkpoint blockade therapies or expressing a chimeric co-stimulatory receptor to advance this therapy further[35, 36].

TCR engineered therapies

While TILs and immune checkpoint blockade use a naturally developed T-cell repertoire, TCR engineered therapies are adoptive cell therapies where an exogenous T-cell receptor (TCR) is introduced onto healthy T-cells to redirect them towards novel targets[37]. Unlike strategies that rely on the endogenously generated T-cell repertoires, this strategy also allows for engineering of the TCR itself via affinity optimization and the targeting of self-antigens[38, 39] or further cell engineering to bolster cell efficacy[40].

Clinical relevance of TCR-targeted adoptive cell therapies

Similarly to TIL and checkpoint blockade therapies, TCR-engineered adoptive cell therapies allow for the targeting of intracellular antigens, possibly including single nucleotide polymorphisms and tumour driver mutations, but unlike those therapies, they

can be engineered with a carefully selected and engineered TCR targeting an essential mutation, such as mutant KRAS[37, 41, 42]. Other TCR therapies focused on tissue-restricted self-antigens such as MART-1 or cancer germline antigens, such as NY-ESO-1 which are though to be targetable with acceptable safety profiles[37]. While this remains a highly promising therapeutic modality, the patient outcomes have been limited, especially when compared to chimeric antigen receptor based adoptive cell therapies[40, 43, 44]. Factors such as insufficient adoptive T-cell proliferation, limited persistence, highly differentiated starting cells and poor function within an inhibitory tumour microenvironment have all been implicated in poor T-cell therapeutic function[37, 40]. The lack of co-stimulatory ligands within the tumour microenvironment is likely another reason behind poor T-cell efficacy[45]. Tumour-intrinsic factors, such as loss of HLA expression or changes in the proteasomal processing of proteins have also led to treatment ineffectiveness, suggesting a polyclonal approach may be required to prevent tumour escape[37, 46].

TCR structure and function

The TCR is composed of two TCR chains (α and β) which contain no known signalling motifs, associated with a complex of CD3 signalling proteins composed of CD3ζζ, CD3εδ and CD3εγ dimers[47, 48]. The two TCR chains are composed of constant regions and variable regions that are pseudo randomly generated through a series of genetic rearrangements and mutations in each developing T-cell in the thymus. The TCR uses its variable regions to bind and detect antigens presented through human leukocyte antigens (HLAs), a set of proteins expressed on the vast majority of human cells. T-cells that fail to generate a surface-expressed TCR or a TCR that shows excessive self-reactivity to self peptides do not persist.

Unlike the TCR chains, the CD3 molecules do not undergo rearrangement or mutations, but endowed with immunoreceptor tyrosine-based activation motifs (ITAMs) which are responsible for initiating the downstream signalling pathways[49]. TCRs require CD3 chains for cell-surface expression and interact through a series of charged residues in their transmembrane regions[48]. To ensure that each TCR heterodimer is equipped with the requisite assortment of CD3 chains, the CD3εδ and CD3εγ dimers are equipped with intracellular retention signals that are inactivated by subsequent CD3ζζ dimer binding, which is the last and limiting step of TCR cell surface expression[50]. In a complete TCR/CD3 complex, there are 10 ITAMs, a feature that has been shown to be essential for the TCR's high sensitivity, allowing for the detection of as few as 1-10 peptide targets[51-53]. 3 ITAMs come from each of the CD3ζ chains, and the remainder of the CD3 proteins are endowed with 1 ITAM each. While the precise individual roles have not been entirely elucidated, there is evidence that the different ITAMs are not interchangeable[54, 55]. Furthermore, there are a number of other signalling sites present on various CD3 components, such as the CD3ε basic rich stretch (BRS) and proline-rich sequence (PRS), which have been shown to interact with downstream proteins Lck and Nck, respectively[56]. The CD3ε BRS and the CD3ζ BRS have also been shown to interact with the inner leaflet of the cell membrane in resting T-cells, controlling access to the signalling motifs contained therein[56].

TCR antigen recognition and co-receptors

The TCR recognizes peptides presented by HLA class 1 or class 2 molecules, which largely present digested peptides sampled from the cytoplasm or Golgi and endosomes respectively. All cells except for gametes and red blood cells present class 1

HLAs, while class 2 HLA expression is more restricted. HLA class 2 is limited to professional antigen presenting cells and T-cells in humans, however other cell types can upregulate class 2 HLA molecules upon interferon-γ stimulation. T-cells are restricted to specificity for either class 1 or class 2 HLA molecules based on the co-receptor they carry. As part of development, T-cells are endowed with either a CD8 or CD4 co-receptor, which allows them to bind class 1 or class 2 HLA molecules. A classical T-cell activation model suggests that the co-receptor recruits Lck to the TCR-HLA complex, however recent evidence that not all co-receptors are endowed with Lck highlights that this may not be required, and the co-receptor may largely serve a role in stabilizing the TCR-HLA interaction[57-59].

TCR signalling

Three models of TCR activation that explain the TCR's exquisite sensitivity have been proposed, and the process likely involves features from all three models. The kinetic proof-reading model posits that a series of relatively slow reversible steps have to occur prior to commitment occurring in the form of an irreversible signalling step[49]. Upon TCR-HLA interaction, Lck must be recruited to the complex, and phosphorylates the ITAMs on the CD3 chains. One version of the model suggests that the TCR-HLA complex sequentially interacts with multiple co-receptors until it encounters one with a bound Lck, which requires that TCR-HLA interaction persist for a certain duration until this process is complete[57]. The phosphorylated ITAM motifs in turn recruit Zap70, which must also be phosphorylated by Lck for activity. Zap70 further propagates the signalling cascade by targeting *linker for activation of T-cells* (LAT), which is an adaptor protein that recruits multiple further signalling proteins, including PLCy1, Grb2, Gads, ultimately

leading to NFAT, NF-kB and AP-1 signalling[60]. The outcome of NF-kB and AP-1 signalling pathways appears digital regardless of the strength of antigen binding, while the NFAT pathway appears to have a graded response[61-63]. The phosphorylation of LAT has been hypothesized to be the irreversible signalling step that commits the T-cell to a digital TCR response[60].

Another TCR signalling model, the kinetic segregation model suggests that the ITAMs of CD3 are stochastically phosphorylate and dephosphorylated by various free kinases and phosphatases, such as CD45, present near the cell membrane[49]. Upon successful interaction between a TCR and its peptide-HLA target, the large and rigid extracellular domain of CD45 forces its exclusion from the TCR-HLA contact area, which leads to increased localized ITAM phosphorylation and subsequent signalling as described above. In line with this model, there is evidence that the various splice variants of CD45, which have been associated with T-cell differentiation and memory states, contribute to the differential sensitivities observed in those cells directly by the size of their extracellular domains[64].

Finally, the third model of TCR signalling involves a structural change upon TCR-HLA binding, which is transmitted to the CD3 complex, and in turn leads to signalling[47]. It has been suggested that this structural change gets propagated to the CD3 complex and leads to the membrane associated CD3ζ and CD3ε chains to dissociate from the membrane and become accessible for subsequent signalling. Recent structural work comparing a TCR bound to its target and an unbound one found few changes, disfavouring this model[47].

Exogenous TCR engineering considerations

As T-cells naturally express an endogenous TCR, an exogenously introduced TCR can mispair, limiting its efficacy and possibly lead to novel off-target reactivity[65, 66]. In light of these limitations, multiple strategies have been proposed to minimize this mispairing, including the use of murine constant chains, human γδ constant regions in the exogenous TCR, and the addition of exogenous cysteines leading to artificial disulfide bonds[67-70]. While these strategies minimize mispairing, the endogenous and exogenous TCRs still compete for a limited number of CD3 complexes and limited signalling machinery, possibly leading to decreased efficacy[71]. With the advent of programmable genetic engineering, it is now possible to edit out the endogenous TCR from T-cells, simultaneously resolving possible mispairing concerns and competition for limited cell surface expression capacity[66, 72].

Co-stimulation

Beyond just stimulation with an appropriate peptide-HLA, full T-cell activation requires a co-stimulatory signal 2, which acts as an additional check on spurious T-cell activation[73]. The most well characterised co-stimulatory protein is CD28, which interacts with its ligands CD80 and CD86 found on professional antigen presenting cells, such as DCs, macrophages and B cells. CD80 and CD86 have also been found on activated T-cells, although the significance of this unknown[74]. CD28 is though to signal largely through the same pathways and gene networks that are triggered by the TCR, leading to quantitative as opposed to qualitative signalling differences[75]. A multitude of benefits have been attributed to CD28 signalling. CD28 is required for increased IL-2 secretion,

T-cell proliferation, T-cell survival post activation, and increased sensitivity to antigen[75]. Studies have shown that CD28 co-stimulation leads to increased glycolysis and increased mitochondrial mass[76, 77]. CD28 expression on T-cells has been shown to be required for immune checkpoint blockade therapy efficacy[78]. Finally, T-cells endowed with CD28 co-stimulation were shown to be resistant to CTLA-4-mediated inhibition[79]. Efforts are underway to develop strategies that would deliver co-stimulation to the tumour microenvironment, such as by using an agonist antibodies or mutated CD80, designed to interact with tumour-associated PD-L1 at high affinity[80, 81].

Another well characterized co-stimulatory ligand is 4-1BBL. 4-1BBL binds to 4-1BB, which is expressed on activated T-cells[82, 83], leading to its trimerization, and signalling via TNFR-Associated-Factor (TRAF) adapter proteins. 4-1BB signalling has been shown to synergize with CD28 co-stimulation leading to improved T-cell cytokine secretion, proliferation, and apoptosis resistance[84, 85]. The use of agonist antibodies against 4-1BB have been shown to lead to improved tumour clearance in murine models, and clinical investigations are underway [86-88]. To avoid possible systemic affects, a recent strategy uses a bispecific antibody targeting a tumour associated antigen, HER-2, delivering 4-1BB co-stimulation only to T-cells that are present in the HER2+ tumour microenvironment[89]. Clinical trials are in progress to also evaluate whether the *in-situ* delivery of other co-stimulatory ligands, including OX40, GITR, CD40, and ICOS[88].

Chimeric antigen receptor (CAR) therapies

CARs are a clear example of the benefits of co-stimulation. While modern CARs are a highly efficacious, licensed adoptive cell therapeutic, early CAR therapies without autochthonous co-stimulation exhibited limited efficacy[90, 91].

The first CAR designs, termed 1st generation CARs, were composed of the variable fragments of an antibody fused onto either the TCRα and β chains or a single chain variable antibody fragment (scFv) directly onto CD3ζ[92-94]. Contrary to the TCR, these receptors do not require HLA mediated presentation of their targets and are able to respond to cell-surface expressed antigens, allowing one receptor to be applicable to a broad patient population, regardless of the patients' HLA backgrounds. While able to redirect T-cell cytotoxicity, 1st generation CARs could not lead to sustained T-cell function. A key advance was the additional fusion of CD28 or 4-1BB co-stimulation onto the CAR leading to greatly improved efficacy[95, 96]. These 2nd generation CARs have been successful in the clinic against hematological malignancies including multiple myeloma, diffuse large B cell lymphoma (DLBCL), acute lymphoblastic leukemia. While CD28 and 4-1BB impart different features onto CAR T-cells in preclinical studies, the clinical outcomes between the two co-stimulatory domains are remarkably similar[97].

This design has been extended to contain multiple co-stimulatory motifs either on-board the CAR (3rd generation CARs)[98] or expressed orthogonally[99-101], cytokine-secreting CARs (armoured CARs)[102], CARs incorporating synthetic logical gates based on notch signalling (SynNotch CARs)[103] or hypoxia within the tumour microenvironment[104]. The therapeutic properties of CARs have been investigated and

optimized through scFv affinity optimization[105, 106], linker length optimization[105, 107], hinge-transmembrane modifications[108, 109], and co-stimulation[107, 110, 111] and stimulation domain mutations[108, 112].

Bispecific T-cell engagers (BiTEs)

T-cells can also be redirected directly inside a patient using bispecific T-cell engagers (BiTEs), which are proteins that have two antibody-derived binding regions, binding a T-cell via its CD3, and a target of interest. Unlike CARs, these molecules do not need to be made specifically for each patient, leading to decreased cost, increased speed and ease of manufacture[113]. The thorough study and clinical approval of an anti-CD19 BiTE allows for comparisons to anti-CD19 CARs, which highlights the inferior efficacy of BiTEs[114], a limitation at least partially attributable to the inability of these molecules to deliver co-stimulatory signals[115]. To address this limitation, there have been recent promising studies that infuse two BiTEs simultaneously, both against the same tumour antigen, but one targeting CD3 and the other driving CD28 signalling[81, 115, 116].

Limitations of CAR therapies

While CAR therapies are highly efficacious, they target extracellular antigens which allows for broad applicability but also restricts possible targets. CARs can be redirected against some tumour-associated antigens, such as CD19, which are restricted to the tumour and other non-essential cells, thus permitting their ablation[117]. Conversely, other tumour associated antigens, most prominently ERBB2, are expressed at low levels on some essential tissues, leading to serious adverse events due to on-target off-tumour toxicity from CAR therapy[118]. To overcome these limitations, CARs can incorporate

logic gates, restricting cytotoxicity only when multiple targets are expressed on a particular cell[103, 119], but this approach is limited when the tumour is proximate to similar healthy tissue[120]. The ideal target would be exclusively tumour-expressed with no expression in any healthy tissue. TCR-like CARs, which recognize a peptide within the context of an HLA molecule, similar to how a TCR functions, but with the co-stimulatory benefits of a CAR allow for the targeting of an intracellular cancer neoantigen while sparing healthy tissues[121]. While promising, initial TCR-like CARs were shown to interact largely with the HLA as opposed to the peptide fragment, permitting multiple peptide mutations, leading to weaker specificity than TCRs and raising the risk of off-target antigen recognition[122].

Delivery of co-stimulation to TCR T-cells

In light of the well validated importance of co-stimulation for T-cell function, and the need for complementary therapies to CAR T-cells allowing for intracellular antigen targeting, there have been efforts to engineer more potent TCR-targeted therapies. The modifications can be broadly grouped into two broad categories: the expression of independent co-stimulatory molecules and the addition of costimulation onto the TCR structure itself.

TCR-independent co-stimulation

Chimeric co-stimulatory receptors (CCRs) are synthetic molecules, similar to CARs but missing a stimulatory (CD3ζ) domain[91]. They rely on the expression of a tumour-associated but not necessarily tumour-restricted target to endow T-cells with

additional co-stimulation. One of the earliest examples of TCR-orthogonal co-stimulation was reported by Krause et al[123]. They illustrated that T-cells endowed with a CCR against a tumour-expressed antigen (G_{D2}) exhibit preferential expansion and increased IL-2 secretion. Building on the work of Krause et al and others, CCRs have been shown to be effective, and there is an ongoing a clinical trial evaluating the benefit of endowing polyclonal TILs with a CCR[35].

Co-stimulation can also be delivered by a *switch receptor*, which converts an inhibitory signal, such as PD-1, CD200, FasL or TGFβ into positive co-stimulation[124-127]. Such receptors serve two functions at once: competitively blocking an inhibitory signal and simultaneously delivering co-stimulation. Similar to CCRs, these switch receptors require their target to be present to exert a function, as illustrated in by Oda et al[125] and Roth et al[127], in the absence of appropriate target, CD200 and TGFb respectively, the switch receptors do not lead to improved T-cell function.

TCR-associated co-stimulation

Beyond CCRs and switch receptors that require additional tumour-associated targets, there have been efforts to develop one receptor, which similar to a CAR, delivers both signal 1 and signal 2 from one target. Early designs sought to simultaneously engineer co-stimulation onto T-cells and simultaneously prevent mispairing and competition for cell-surface expression with the endogenous TCR. Zhang et al developed a single chain TCR in which the exogenous TCR variable domains are linked together into a structure similar to an scFv, and the entire structure is fused onto a transmembrane domain (either CD3ζ or CD28) and endowed with CD28 co-stimulation and CD3ζ

leading to a CAR-like construct[128]. Their constructs were expressed but showed significantly reduced sensitivity compared to a control TCR. Whether this was an artifact of the single-chain format not binding antigen as well or due to decreased signalling ability of this design was not investigated. Other groups have illustrated that CAR T-cells have decreased sensitivity compared to TCR T-cells, which can be reversed if CAR designs taking advantage of the full CD3 complex are used[129]. These findings were further confirmed with another TCR[130].

An alternative design was reported by the lab of Reno Debets in two publications in which the extracellular portions of both the TCR α and TCR β proteins were fused to CD28 and CD3ζ or CD3ε. T-cells endowed with the TCR-CD28-CD3ζ were able to exert cytotoxicity against peptide-pulsed targets, but not endogenously expressed antigen[131]. Conversely, T-cells endowed with the wildtype TCR, which would be expected to mispair, were able to exert cytotoxicity against both sets of targets. Their follow up work illustrated that TCR-CD28-CD3ε designs exhibited increased sensitivity compared to TCR-CD28-CD3ζ designs, and T-cells endowed with TCR-CD28-CD3ε exhibited increased *in vivo* anti tumour efficacy compared to T-cells endowed with the wildtype TCR[132]. While suggestive, their engineered TCR was designed to avoid mispairing with the endogenous TCR present in T-cells, while the control TCR would be expected to compete for cell surface expression and mispair, preventing an evaluation of whether the co-stimulatory domain was functional in this structure.

T-cell engineering technologies

To augment T-cell function one must be able to introduce novel genetic material into the T-cells of interest, and this has been accomplished through a variety of means. The most validated strategies, used in clinically licensed CAR T-cell therapies, is to take advantage of γ-retroviral or lentiviral abilities to permanently integrate into a patient's genome[133-135]. A major difference between these strategies is that lentiviruses have an ability to cross the nuclear membrane, while γ-retroviruses require the division-associated nuclear membrane dissolution. The two viruses also favour integrating into different areas of the genome, with γ-retroviruses having a propensity to integrate into transcriptional start sites, while lentiviruses tend to integrate into genes actively undergoing transcription[136, 137]. While the pseudo-random integration near or into actively transcribed genes raises possible safety concerns, T-cells are believed to be largely resistant to oncogenesis, even when transduced with retroviral vectors encoding oncogenes[138]. The pseudo random integration leads to variability of transgene expression within a single therapeutic product, which may lead to sub-optimal levels of CAR or TCR expression[139, 140]. While retroviruses and lentiviruses have been the most clinically applied strategies, T-cells can be modified with a number of tools, including adeno associated viruses[141] and transposons[142].

The discovery of programmable genetic editors, including zinc finger nucleases, TALENs and most recently, CRISPR/Cas9 have allowed for precise T-cell engineering by taking advantage of homology directed repair (HDR). This strategy requires the delivery of a genetic editor and a novel template with homology to the region of interest,

delivered using an AAV or directly as single stranded or double stranded DNA[143]. Upon cleavage of the T-cell genome, the cell performs HDR using the newly delivered vector as a template. This is a very precise method to introduce a new transgene or mutation at a specific site within the cell genome, ensuring that oncogenes are avoided, and simultaneously increases control over transgene expression leading to a more efficacious product[139, 143]. In the context of TCR therapies, these strategies are particularly useful because they allow for the simultaneous knockout of the endogenous TCRα and knock-in of a novel TCR, simultaneously decreasing competition for the CD3 complex and risk of mismatch[42, 144, 145]. These strategies are actively being investigated in the clinic[42, 146, 147].

While more precise, there is evidence that these strategies may rarely lead to off-target modifications within the cell genome, especially if multiple DNA edits are performed simultaneously[148, 149]. This had prompted the development of an alternative editing strategy, termed PASTE, that only requires DNA nicking instead of double strand cleavage to insert a small integration site (attB), which is subsequently used to insert a larger insert using Bxb1 integrase[150].

NY-ESO-1

NY-ESO-1, also known as cancer testis antigen 1, is a well characterized, commonly associated tumour antigen, not thought to be expressed on normal somatic tissues[151]. It was initially described in an esophageal cancer, but since then identified in ovarian, bladder, breast, gastric, lung, skin, prostate and other cancers. It has been well studied in engineered TCR clinical trials, with minimal toxicities reported[37, 151]. Its broad

clinical relevance, and breadth of available clinical and preclinical data make it an ideal target for preclinical studies, especially in the context of the most frequently found HLA allele – HLA-A2:01.

Motivation for thesis studies

TCR-targeted adoptive T-cell therapies are a complementary approach to CAR-targeted adoptive T-cell therapies allowing the targeting of intracellular antigens but have so far not exhibited the same potency exhibited by CAR T-cells. While there are many differences between the two approaches, one critical difference is the lack of co-stimulation on TCR-targeted T-cells.

CD28 is a highly potent co-stimulatory molecule, which has been shown to increase T-cell cytokine secretion, proliferation, metabolism and lead to improved efficacy of TCR-targeted therapies endowed with target-dependant CCRs or switch receptors. While designs incorporating the CD28 intracellular domain onto the TCR structure have been studied, the experimental set up prevented confirmation of whether the costimulation was functional. Furthermore, the designs were shown to have decreased sensitivity compared to the wildtype exogenous TCR, which would be expected to compete for limited cell surface expression and mispair with the endogenous TCR, hinting at possible design limitations.

In chapter 3, I develop and evaluate CD28 co-stimulation when directly fused onto the TCRα and β chains or onto the CD3, leading to its association with the endogenous TCR/CD3 complex. Using recently developed T-cell engineering strategies, the

endogenous TCR or CD3 was ablated, allowing for the precise delineation of any contributions from the costimulation. A TCR-CD28 fusion would allow for streamlined one-step genetic delivery of both a novel TCR and co-stimulation into T-cells for adoptive cell therapy, while a CD3-CD28 fusion would allow for target-agnostic co-stimulation delivery into T-cells.

In chapter 4, I develop and evaluate a novel orthogonal co-stimulatory molecule that simultaneously delivers CD28 and 4-1BB co-stimulation, a combination that has been shown to be synergistic, in an antigen-independent manner. The molecule was designed to function as a target-independent co-stimulatory molecule and incorporate switch receptor features. I show that this molecule functions in the context of TCR-based CARs, TCRs, and importantly in a polyclonal TIL population isolated from a patient sample against their autologous tumour.

Chapter 2 - Methods

Cell lines and cell culture

NALM6 B-ALL leukemia cells and U266 multiple myeloma were obtained from ATCC and transduced to express firefly luciferase-GFP. NALM6 (NY-ESO-1+ and CD19+) cells for CD19 HIT and NY-ESO-1 TCR experiments for Incucyte assays were generated by sequential transduction and sorting with NY-ESO-1-P2A-mCherry, HLA-A0201-P2A-mTangerine and β2m-P2A-mKate. NALM6 cell lines with decreased CD19 densities were previously described[11]. SK-Mel-37 were provided by the Ludwig Center for Immunotherapy at Memorial Sloan-Kettering Cancer Center. SK-Mel-37 and SK-Mel-956A was transduced to express firefly luciferase-GFP or Incucyte® Nuclight Red (Essen BioScience) for Incucyte analysis. All cell lines were maintained in RPMI-1640 medium (Corning) supplemented with 10% FBS except for SK-Mel-956A, which were maintained in medium supplemented with 20% FBS (Neuromics), 10 mM HEPES (Invitrogen), 2 mM L-glutamine (Gibco), 1× NEAA (Invitrogen), 1 mM sodium pyruvate (Invitrogen), 100 U/ ml penicillin, 100 µg/ ml streptomycin (Corning). NALM6 media was supplemented with 50 µM β-mercaptoethanol (Gibco). Cells were regularly tested for mycoplasma.

T-cell activation, gene targeting and transduction

Buffy coats from healthy volunteer donors were obtained from the New York Blood Center. Peripheral blood mononuclear cells (PBMCs) were isolated by density gradient centrifugation using Lymphocyte Separation medium (Corning), subsequently T-cells were isolated using a Pan T-cell isolation kit (Miltenyi Biotec). Cells were activated

using CTS Dynabeads™ CD3/CD28 activation beads (ThermoFisher) at a 1:1 Bead:T-cell ratio. T-cells were cultured in RPMI-1640, supplemented with 10% FBS, and 100 U/ ml penicillin, 100 µg/ ml streptomycin and 2 mM L-glutamine with 3000 units IL-7 (Miltenyi Biotec) and 100 units IL-15 (Miltenyi Biotec) at a starting concentration of $1x10^6$ T-cells/mL. Cells were cultured in a 37°C incubator with 5% CO_2. 48 hours after T-cell activation, CD3/CD28 beads were magnetically removed, cells were resuspended in P3 buffer Cas9 ribonuclearprotein (RNP) and relevant gRNA were co-delivered using the Nucleofector II device (Lonza). Following electroporation, cells were resuspended in 1mL of X-Vivo 15 (Lonza) media without serum,
100 U/ ml penicillin, 100 µg/ ml streptomycin and 3000 units IL-7 and 100 units IL-15 per $1x10^7$ T-cells pre-electroporation. Recombinant AAV6 donor vector (Signagen) was added at an MOI of $4x10^4$ per viable T-cell, assuming a 66.6% viability after electroporation. Twenty-four hours later, T-cells were mixed with a titrated amount of SFG γ-retroviral vector, diluted to $1.5x10^6$ T-cells/mL in T-cell media, and plated onto non-tissue culture treated 6-well plates (Falcon) pre-coated with Retronectin (Takara, T100B). Plates were centrifuged for 1 hour at 300g. Cell cultures were replenished with additional T-cell media as needed to maintain a density of $1–1.5 \times 10^6$ cells/ml, with fresh 3000 units IL-7 and 100 units IL-15 replenished every 48 hours. For assays using sorted CD4 or CD8 T-cells or co-receptor matched T-cells, column-based depletion of bulk transduced T-cells was performed using either CD4 Microbeads (Miltenyi Biotec) or CD8 Microbeads (Miltenyi Biotec) as per the manufacturer's instructions. For assays using CD3 modified cells, cells were sorted using LNGFR Microbeads (Miltenyi Biotec) as per the manufacturer's instructions.

Autologous patient-derived tumors and Tumour-Infiltrating Lymphocyte (TILs) culture

All the patients signed an approved informed consent before providing tissue samples. Patient samples were collected on a tissue-collection protocol approved by the MSK Institutional Review Board. Single-cell suspensions from patients' tumors were obtained by digesting the tumor samples with 2 mg/ml type I collagenase (ThermoFisher), 2 mg/ml type V hyaluronidase (Sigma-Aldrich), and 200 U/ml type IV deoxyribonuclease I (Sigma-Aldrich) in serum-free RPMI 1640 using a GentleMACs Octo Dissociator (Miltenyi Biotec) and viably frozen at −80°C prior to use. Patient-derived SK-Mel-956A melanoma cells were generated by culturing fresh single-cell suspension from a patient in RPMI-1640 with 20% FCS (ThermoFisher), and 100 U/ ml penicillin, 100 µg/ ml streptomycin and subsequently cultured as described above.

TILs rapid expansion protocol (REP) was adapted from Dudley et al[57]. Briefly, TILs were resuspended in 2mL of Complete Medium (RPMI-1640, Corning; 25mM HEPES, Invitrogen; 10% Human Serum, GeminiBio; 1× NEAA, Invitrogen; 1x Glutamax, Gibco; 100 U/ ml penicillin, 100 µg/ ml streptomycin Corning), with 6,000 IU/mL of rhIL-2 (Miltenyi Biotec). rhIL-2 was added twice weekly, and cells were split once media colour indicating cell growth. On day 14, cells were resuspended in 15mL of 1:1 mixture of complete media and AIM V Medium (Thermo Fisher Scientific) per 5 x 10^5 cells and co-cultured with 5 x 10^6 irradiated (50 Gy) allogeneic PBMC feed cells from 5 pooled donors with 3,000 IU rhIL-2 (Miltenyi Biotec) and 30ng/mL OKT3 (Biolegend) as previously reported[57]. On day 3 post activation, cells were transferred to non-tissue culture treated 6-well plates (Falcon) pre-coated with Retronectin (Takara) at 5

x 10^6 cells / well in 2mL of 1:1 RPMI 1640/AIM V media and γ-retroviral vector encoding LNGFR or 80BB. Cells were centrifuged for 1 hour at 300g. Fresh media was given to cells twice weekly. 11 days post transduction, T-cells were bead sorted to remove any residual PBMCs using a human pan T-cell isolation kit (Miltenyi Biotec) and used for subsequent experiments.

Vector constructs and production

The Lau155 NY-ESO-1 specific TCRβ and TCRα chains was cloned into the SFGγ retroviral vector separated by an P2A sequence and followed by an internal ribosome entry site (IRES) and eGFP. TCR-28 constructs were made by further insert the intracellular coding sequence of CD28 at the end of the TCRβ and TCRα coding sequences. Linkers 1 and 2 were composed of 5x(GGGGS) or 5x(EAAAK) and fused directly after the TCRβ and TCRα before the CD28 intracellular motif. Linker 3 was designed by appending GGSLEDEKSALQTEIANLLSEKESLEGG and GGSLEDEKSALQTEIANLLSEKESLEGG to the TCRβ and TCRα sequences respectively.

The cDNA containing the extracellular domain and transmembrane domain of CD3ζ or CD3ε were fused to the intracellular amino acids of CD28, followed by intracellular domain of either CD3ζ or CD3ε to create $CD3\zeta^{pCD28}$ or $CD3\varepsilon^{pCD28}$. The cDNA containing the extracellular domain, transmembrane and intracellular domain of CD3ζ or CD3ε were fused to the intracellular amino acids of CD28 to create $CD3\zeta^{dCD28}$ or $CD3\varepsilon^{dCD28}$. The constructs were inserted into the SFGγ retroviral vector followed by P2A LNGFR.

The cDNA containing the extracellular domain, transmembrane domain, and first four intracellular amino acids of human CD80 and the corresponding intracellular domain of human 4-1BB were cloned into the SFGγ retroviral vector to express of CD80-4-1BB fusion molecule (80BB). Constructs encoding truncated human CD80 (ΔCD80) were created using the cDNA corresponding to the extracellular domain, transmembrane domain and first four intracellular amino acids of CD80, while FL-CD80 was generated by cloning the cDNA of full-length human CD80, into the SFGγ retroviral vector. Human ΔCTLA4, constructs were generated by cloning cDNA corresponding to the extracellular domain, transmembrane domain and 7 first intracellular amino acids of CTLA4. Truncated CD28 (ΔCD28) construct was generated by cloning the CD28 extracellular domain and transmembrane domain. LNGFR reporter was described previously[29]. Viral supernatant was produced as previously described[20]. Briefly, vesicular stomatitis virus glycoprotein G pseudotyped retroviral supernatants derived from transduced gpg29 fibroblasts (H29) were used to construct stable retroviral-producing cell lines[29]. Supernatant from stable retroviral-producing cell lines was collected and concentrated using Retro-X (Takara) as per the manufacturer's protocol.

The CD19 specific HIT (19-HIT) receptor AAV construct was made as described previously, based on a pAAV-GFP backbone (Cell Biolabs)[11]. To allow for NY-ESO-1-specific TCR-delivery into the endogenous TRAC locus using a TCR donor AAV, the complete TCRβ-P2A-TCRα sequence of an NY-ESO-1 TCR (Clone Lau 155, 1G4 LY or SB95) was cloned after the splice acceptor site and P2A sequence into the previously described pAAV-*TRAC*-1928z[35,58]. AAV6 viruses were produced and quantified by SignaGen.

Cas9 protein, RNP formation and AAV6

Cas9 protein (40 μM) was obtained from the QB3-Berkeley Macrolab core facility. RNP was prepared by mixing Cas9 protein and total gRNA at 1:2 molar ratio and incubated in 37 °C water bath for 15 min and immediately used for T-cell electroporation. gRNAs were purchased from Synthego with 2′-*O*-methyl 3′-phosphorothioate modifications in the first and last three nucleotides, with the following target sequences: TRAC: 5′-CAGGGTTCTGGATATCTGT, TRBC: 5'-GCAGUAUCUGGAGUCAUUGA, CD28, 5'-CACCAAAAUCUUGUUUCCUG and 5'-UCACCAAAAUCUUGUUUCCU, CTLA4: 5'-UUCCAUGCUAGCAAUGCACG, 5'-ACACAAAGCUGGCGAUGCCU, 5'-CCGGGUGACAGUGCUUCGGC, CD3ε: 5'-CAUGGAGAUGGAUGUGAUGU, CD3ζ: 5'-. CCTGCTGGATCCCAAACTCTGCT. gRNA was resuspended with TE buffer at 40 μM.

Knock-out efficiencies were evaluated by flow cytometry (TRAC, CD28, CD3) or by inference of CRISPR Editing (ICE) for CTLA4 (Synthego). For inference of CRISPR Editing (ICE), primers were designed that bind 150 bp 5' and 3' of the anticipated cut sites Fwd: GGGTGTGGAGAGGGGAAGGGG, Rvs: GCCCAGGTAGTATGGCGGTGGG). Genomic DNA from CTLA4 knockout and control cells was isolated using a DNeasy kit (Qiagen), and the region of interest was amplified using Q5 polymerase (NEB). PCR product was verified on a gel and purified using a Nucleospin column (Macherey-Nagel). PCR product was submitted for sanger sequencing using the PCR primers, and resultant traces were input into ICE analysis software (Synthego).

T-cell proliferation assay

NALM6 or NALM6^{ESO} were used as targets for repetitive stimulation assays. For *in vitro* expansion assays, 1 × 10^5 19-HIT+ or TCR+ T-cells were co-cultured with 2 × 10^5 NALM6 targeT-cells (ratio 1:2; E:T) in 500µL of T-cell media with no exogenous cytokines. Every 2 days, cells were analyzed by flow cytometry to determine 19-HIT or TCR+ percentage and counted using Countbright beads (Invitrogen). T-cells were replated at 1 × 10^5 HIT+ or TCR+ T-cells and re-stimulated with 2 × 10^5 NALM6 until cells ceased proliferating in response to stimulation.

For TILs proliferation assay, T-cells were stained with CellTrace Violet (CTV) assay as per the manufacture protocol (ThermoFisher) and stimulated with autologous unlabeled targets at an E:T ratio of 1:2 with no exogenous cytokines. 5 days later, CTV dilution was measured by flow cytometry.

Cytotoxicity Assays

For repetitive cytotoxic assay using an Incucyte S3, 2 x 10^4 NALM6 cells were plated per well onto a 96-well plate precoated with fibronectin (Sigma-Aldrich) for 1 hour at room temperature. 1 x 10^4 19-HIT or TCR+ T-cells were added to each well in a final volume of 200µL T-cell culturing media. Plates were briefly centrifuged and cultured in an Incucyte S3 inside a 37°C incubator with 5% CO_2. Every 2 days, 100µL of media from preceding culture was collected and added to new plate containing 2 x 10^4 NALM6 cells in 100µL fresh media until T-cells failed to control fresh NALM6 cells.

For TIL melanoma cytotoxic assays, 5 x 10^3 SK-Mel-956A cells were plated onto a fibronectin-coated plate. Twenty-four hours later, 2 x 10^4 TILs were added on the plate

for a final volume of 200µL. 100 µL of co-culture was added new 96-well plate containing 5 x 10^3 SK-Mel-956A cells. Wells of interest were imaged on an Incucyte S3 every 2 hours.

Tumour was quantified by red-fluorescent surface area measured by Incucyte S3 software (Essen BioScience) and normalized to the red-fluorescent surface area after each tumour cell addition.

For luciferase-based cytotoxicity assays, engineered T-cells or TILs were co-cultured with luciferase-GFP transduced targets at labelled ratios co-cultured in triplicates at the indicated effector : target ratios in a final volume of 100µL with 2 × 10^4 targeT-cells. Eighteen hour later, 100µl luciferase substrate (Bright-Glo; Promega) was added to each well. Emitted light was detected in a luminescence plate reader (Agilent BioTek S1L) and lysis was calculated using the formula 100 × (1 −(RLU_{sample})/(RLU_{target} alone).

T2 targets cells were incubated for 1 hour at 37°C with 10µM NY-ESO-1 peptide (SLLMWITQV) or FLU peptide (GILGFVFTL) unless otherwise labelled at a density of 1 × 10^6 cells per mL.

Cytokine Analyses

1 × 10^5 19-HIT+ or TCR+ T-cells were co-cultured with 2 × 10^5 NALM6 or $NALM6^{ESO}$ targeT-cells as indicated for each experiment in 200µL culturing media in the presence of IL-2 receptor blocking antibody (B-B10, ThermoFisher). For OKT3 stimulation assays, plates coated with OKT3 antibody overnight and washed twice with PBS. After 24 hours of co-culture, 40µL aliquots of supernatant were collected. Cytokines were measured using a BD Cytometric Bead Array (CBA), as per the

manufacturer protocol. Samples were measured on a BD LSR Fortessa and analyzed using BD FCAP software (BD bioscience).

Flow Cytometry

19-HIT expression was measured with Alexa-Fluor-647-conjugated goat anti-mouse (ab')2 antibody (Jackson ImmunoResearch). TCR was detected using NY-ESO-1 tetramers (MBL International). T-cell phenotypes were evaluated using BUV395 mouse anti-human CD4 (SK3, BD), BUV805 mouse anti-human CD8 (SK1, BD), PE mouse anti-human CD80 (2D10, Biolegend), BB515 mouse anti-human CD28 (CD28.2, BD), BV480 mouse anti-human PD-1 (EH12.1, BD), PerCp-eFluor710 mouse anti-human LAG3 (3DS223H, eBioscience), BV785 mouse anti-human Tim3 (F38-2E2, Biolegend), BV421 mouse anti-human CTLA4 (BNI3, Biolegend), APC-Cy7 mouse anti-human CD45 (2D1, Biolegend) or PE mouse anti-human CD45 (2D1, Biolegend), PE/Dazzle-594 mouse anti-human LNGFR (ME20.4, Biolegend). Countbright beads (Invitrogen) were used to determine the absolute number of cells according to the manufacturer's protocol. 7-AAD or DAPI was used to exclude dead cells (Biolegend). FcR Blocking Reagent mouse (Miltenyi Biotec) was used to block Fc receptors.

NALM6 expression of CTLA4, CD80, were evaluated using antibodies listed above, and PE- mouse anti-human CD86 (BU63, Biolegend), PE- mouse anti-human 4-1BBL (5F4, Biolegend), PerCP-Cy5.5 mouse anti-human PD-L1 (29E.2A3, Biolegend). HLA-A2 was stained using PE mouse anti-human HLA-A2 (BB7.2, Biolegend).

For protein binding assays, 1×10^5 T-cells were co-cultured with serially diluted human CD28-Fc protein (BPS Bioscience) or human CTLA4-Fc protein (BPS

Bioscience) for 30 minutes at room temperature, washed with flow buffer (2% FBS in PBS) then stained with mouse anti-human IgG Fc (QA19A42, Biolegend) for 10 minutes at room temperature. Cells were washed twice. Flow cytometric data were acquired on a 5-laser Aurora (Cytek Biosciences) and analyzed in FlowJo v10.8.1 (Treestar). Experiments were done under the same gain settings and the machine was calibrated using QC beads daily. Cell sorting was performed on a BD FACSAria cell sorter.

Mouse systemic tumour models

All experiments were performed under a protocol approved by the MSKCC Institutional Animal Care and Use Committee.

For all models, male and female 8–12-week-old NOD/SCID/IL-2Rγ-null (NSG) mice (Jackson Laboratory) were used. F or B-ALL models, mice injected via tail vein with 5 x 10^5 firefly luciferase-GFP transduced NALM6 (or NALM6^{2000} or NALM6^{200} or NALM6^{ESO}) cells per mouse. For disseminated melanoma models, male and female 8–12-week-old NOD/SCID/IL-2Rγ-null (NSG) mice (Jackson Laboratory) were injected via tail vein with 5 x 10^5 firefly luciferase-GFP transduced SK-Mel-37 cells. For multiple myeloma models, male and female 8–12-week-old NOD/SCID/IL-2Rγ-null (NSG) mice (Jackson Laboratory) were injected via tail vein with 5 x 10^5 firefly luciferase-GFP transduced U266 cells. Engineered T-cells were injected at the indicated doses. For patient-matched TIL experiments, mice were injected via tail vein with donor matched 5 x 10^5 firefly luciferase-GFP transduced SK-mel-956A. One week later, TILs transduced with 80BB or LNGFR were injected at the indicated doses.

Tumour engraftment was confirmed using bioluminescence imaging measured on the Xenogen IVIS Imaging System (Xenogen). Living Image software (Xenogen) was used to analyze acquired bioluminescence data. Mice were monitored and sacrificed upon evidence of hind-limb paralysis or other clinical signs of distress. Injections of tumour cells and T-cells and imaging was performed by double-blinded investigators.

For ex vivo T-cell characterization 4-5 mice per group were sacrificed at the indicated timepoints post T-cell injection, and cell were extracted from the lung, spleen, femur, tibia, and/or fibula as indicated. After PBS wash, RBC lysis was performed using ACK buffer (Lonza) and washed again. Mouse cell depletion was performed as per the manufacturer's protocol (Miltenyi Biotec). Cells were then stained for flow cytometry as described above.

For HLA-A2 expression level assessments and cell counts, lung tissue was surgically isolated from mice, and processed using a Miltenyi Tumor Dissociation Kit, human (Miltenyi) on a Miltenyi gentleMACS™ Octo Dissociator. Mouse cell depletion was performed as per the manufacturer's protocol (Miltenyi Biotec). Cells were then stained for flow cytometry as described above.

For single-cell RNA sequencing analysis, 5 Mice per group were injected with NALM6 tumour as described above and treated with 1×10^5 or 5×10^4 19-HIT+ T-cells per mouse on day 4 post tumour injection. On day 9 post T-cell injection, bone marrow cells were isolated as described above. Cells from mice within one condition were pooled and labelled with PE mouse anti-human CD45 (2D1, Biolegend) and TotalSeq™-B0251 anti-human Hashtag 1 Antibody (Biolegend) in 19-HIT treated mice or

TotalSeq™-B0254 anti-human Hashtag 4 Antibody (Biolegend) in 19-HIT^{80BB} treated mice. Cells were FACS sorted for CD45+ GFP- cells (human T-cells, excluding NALM6). Cells from different conditions were pooled together at a balanced ratio and submitted for 10X 3' RNA sequencing.

Single-cell transcriptome sequencing and analysis

Cells were stained with Trypan blue and Countess II Automated Cell Counter (ThermoFisher) was used to assess both cell number and viability. Following QC, the single cell suspension was loaded onto Chromium Next GEM Chip G (10X Genomics PN 1000120) and GEM generation, cDNA synthesis, cDNA amplification, and library preparation of 15-21,000 cells proceeded using the Next GEM Single Cell 3' Kit v3.1 (10X Genomics PN 1000268) according to the manufacturer's protocol. cDNA amplification included 11 cycles and 10 µL of the material was used to prepare sequencing libraries with 8-10 cycles of PCR. Indexed libraries were pooled equimolar and sequenced on a NovaSeq 6000 in a PE28/88 run using the NovaSeq 6000 S2 or S4 Reagent Kit (100 or 200 cycles) (Illumina). An average of 21 thousand paired reads was generated per cell.

Amplification products generated using the methods described above included both cDNA and feature barcodes tagged with cell barcodes and unique molecular identifiers. Smaller feature barcode fragments were separated from longer amplified cDNA using a 0.6X cleanup with aMPure XP beads (Beckman Coulter catalog # A63882). Feature barcode libraries were constructed using the 3' Feature Barcode Kit (10X Genomics PN 1000276) according to the manufacturer's protocol with 10 cycles of PCR. Indexed libraries were pooled equimolar and sequenced on a NovaSeq 6000 in a

PE28/88 paired end run using the NovaSeq 6000 S4 Reagent Kit (200 cycles) (Illumina). An average of 56 million paired reads was generated per sample.

Raw fastq data was processed by Cell Ranger (v6.1.1) multi command with reference assembly GRCh38, to demultiplex cells to original hashtags and to obtain gene counts. The two doses were aggregated with Cell Ranger aggr command. The count matrix was imported into R (v4.0.2) and analyzed with Seurat R package (v4.0.4). Cells were filtered by (1) over 200 unique genes and below 5000 unique genes expressed; (2) below 20000 total genes molecules; (3) below 12% UMIs derived from the mitochondrial genome; (4) doublets detected by DoubletFinder(v2.0). Principal component analysis (PCA) was performed using a set of 1000 top variable genes and then dimensionality reduction was performed using UMAP algorithm with top 18 PCAs. Seurat assigned cluster identities were used to exclude cells clustering separately, not expressing canonical T-cell markers, and positive for canonical B-ALL markers.

T-cell metabolic Assays

1 x 10^6 engineered 19-HIT+ T-cells were co-cultured with 2 x 10^6 NALM6 cells in 2mL of culturing media and no exogenous cytokine. Every 72 hours, cells were replated at 1 x 10^6 19-HIT+ T-cells per 2 x 10^6 CD19+ NALM6. After 3 total stimulations, cells were counted, and resuspended in XF RPMI (Agilent) supplemented with 10mM glucose (Agilent), 2mM glutamine (Agilent), 1 mM sodium pyruvate (Agilent) at 1 x 10^5 cells / 40 µL. Cells were plated onto a poly-L-Lysine coated plate (Fisherbrand), spun down and media was added to a final volume of 180µL. Cells were analyzed as per the manufacturer's protocol using the Mito Stress Assay kit (Agilent) and

the Glycolytic Rate Assay kit (Agilent). Assays were run on the Seahorse XFe96 Analyzer (Agilent).

Statistics

All experimental data are presented as mean ± s.e.m. No statistical methods were used to predetermine sample size. Appropriate statistical tests were used to analyze data, as described in the figure legends. Statistical analysis was performed on GraphPad Prism v.9 software and R v.4.

Chapter 3 – Delivery of CD28 costimulation directly to the TCR/CD3 complex

TCR α and β chains fused to CD28 are expressed on the cell surface

The co-endowment of co-stimulation onto 1st generation chimeric antigen receptors (CARs) leading to 2nd generation CARs was critical to CARs' clinical successes[91] and the benefits of TCR-independent co-stimulation in the form of CCRs and switch receptors have been well documented[123, 125, 127]. We set out to endow a T-cell receptor (TCR) with CD28 co-stimulation that would in principle deliver both signal 1 and signal 2 upon TCR binding to its cognate antigen without the need for additional ligands, similar to a 2nd generation CAR. To this end, we designed a retroviral construct which encodes for an anti-NY-ESO-1 TCR, with the CD28 intracellular domain fused onto both the α and β chains and a GFP reporter protein ("TCR-28", Fig. 3.1A). These constructs were used to transduce T-cells which had their endogenous TCR ablated by CRISPR/Cas9 TRAC editing. TCR-28 was well expressed on the cell surface of T-cells, although a consistent and statistically significant decrease in both TCRβ chain and tetramer staining was noted compared to control TCR-transduced TCR-wT-cells (Fig. 3.1B). This difference was not due to differences in vector transduction, as GFP expression MFI and percentage was not lower in TCR-28 cells compared to TCR-wt T-cells (Fig. 3.1B).

To further excluded transduction variabilities, we took advantage of a CRISPR/Cas9 knock-in protocol that allows for targeted genetic delivery of a gene into

Figure 3.1: TCR α and β chains fused to CD28 are expressed on the cell surface

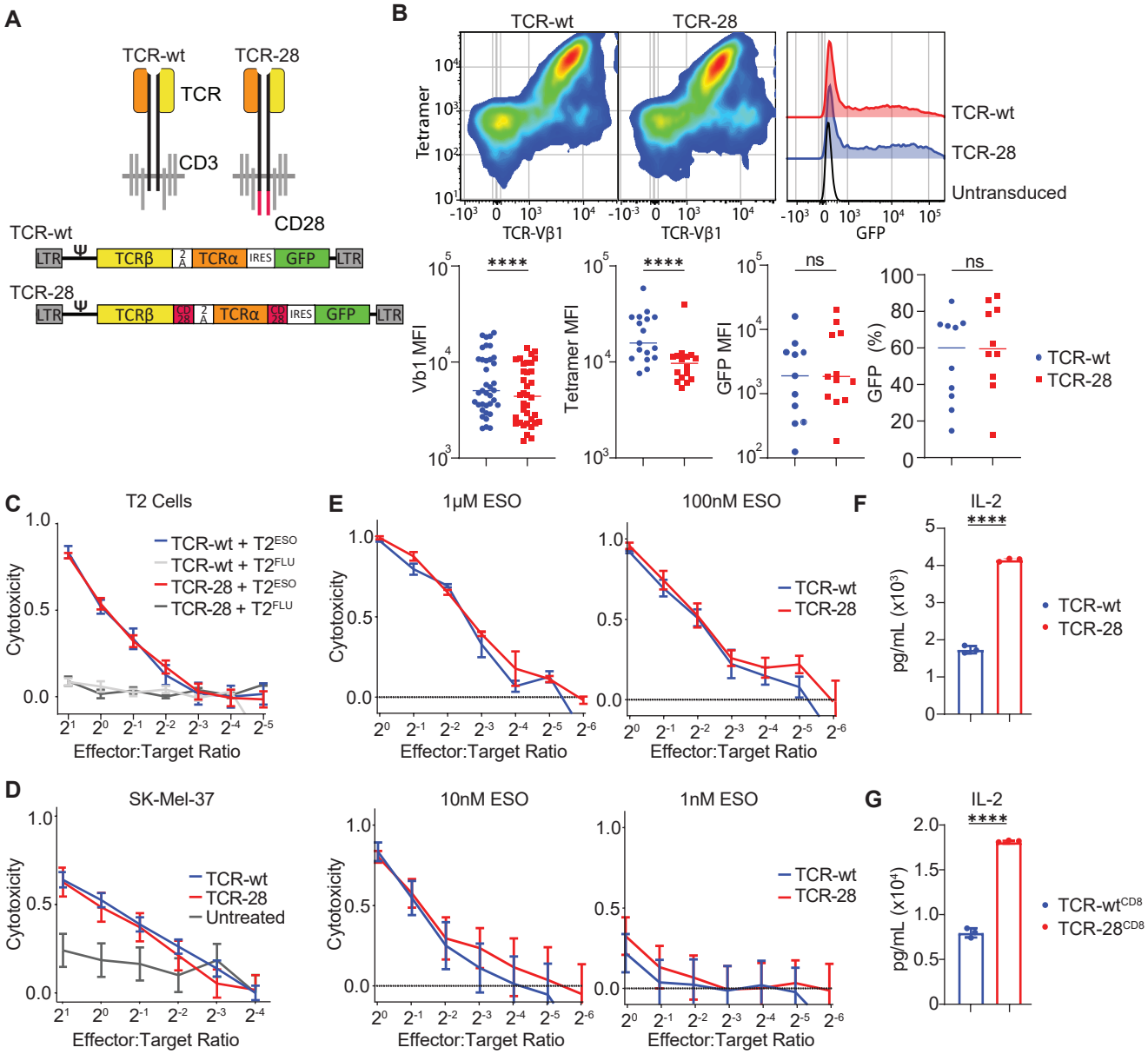

A, top, diagram of wildtype TCR complex ("TCR-wt") and TCR with CD28 fused to both the TCRα and TCRβ chains ("TCR-28"). Bottom, diagram of retroviral construct. **B,** top-left, flow profiles of T-cells modified to express TCR-wt and TCR-28 and stained with NY-ESO-1 tetramer and anti-TCR-Vβ1. Top-right, GFP flow profiles of T-cells modified to express TCR-wt and TCR-28. Bottom, quantification of anti-TCR-Vβ1, Tetramer, and GFP MFI, and GFP percentage in T-cells modified to express TCR-wt and TCR-28. Data representative of 10 human donors. **C,** *In vitro* cytotoxicity assay at titrated effector: target ratios of T2 cells pulsed with 10μM NY-ESO-1 peptide or off-target FLU peptide. Data representative of 3 human donors. **D,** *In vitro* cytotoxicity assay against SK-Mel-37, a cell line that endogenously expresses HLA-A2 and NY-ESO-1. **E,** *In vitro* cytotoxicity assay of T2 cells pulsed with titrated NY-ESO-1 peptide concentrations at an E:T ratio of 1:1. **F,** IL-2 cytokine levels detected in supernatant 24 hours after TCR-wt or TCR-28 T-cells are exposed to NY-ESO-1 pulsed T2 cells. **G,** IL-2 cytokine level detected in supernatant 24 hours after TCR-wt^{CD8} or TCR-28^{CD8} T-cells are exposed to NY-ESO-1 pulsed T2 cells. *P* values were determined by two-tailed t-test (F, G). Data are mean ± sem. * p<0.05, ** p<0.01, *** p<0.001, **** P<0.0001.

the *TRAC* locus, ensuring precise gene expression (Ext. Data Fig. 3.1A). Expression analyses with these constructs confirmed our retroviral findings that fusion of CD28 onto the TCR α and β chains led decreases in both TCRβ chain and tetramer cell surface staining (Ext. Data Fig. 3.1B). We further evaluated whether the addition of a spacer between the TCR α and β chains and the CD28 domain abrogated the cell surface staining decrease. Constructs incorporating a flexible linker composed of 5 repeats of GGGGS or an α-helix linker composed of 5 repeats of EAAAK fused to both TCR chains, or a β-sheet linker isolated from the proteins fos and c-jun fused to the TCR α and β chains respectively, still led to decreased TCRβ chain and tetramer staining at comparable GFP expression levels (Ext. Data Fig. 3.2A, B, C, D). These findings prompted us to continue our study with a linker-less construct.

Given the decreased cell surface expression, we next wanted to evaluate whether the TCR-28 construct exhibited any augmented *in vitro* cytotoxicity. Both T2 cells (TAP deficient, HLA-A2+) pulsed with NY-ESO-1 peptide and SK-Mel-37 cells (HLA-A2+, NY-ESO-1+) were equivalently lysed by either TCR-28 and TCR-wt suggesting that the decreased TCRβ chain and tetramer staining were not indicative of decreased cytotoxicity (Fig. 3.1C, D). Furthermore, titrating the peptide concentration used to pulse T2 cells confirmed similar sensitivities between TCR-28 and TCR-wt T-cells, as T2 cells were equivalently lysed between the two constructs at all tested concentrations (Fig 3.1E). Using IL-2 as a readout of CD28 function, we observed that TCR-28 T-cells secrete significantly more IL-2 than control TCR-wT-cells consistent with functional CD28 signalling (Fig 3.1F). Initial *in vivo* studies in an immunocompromised NSG mice implanted with NALM6^{ESO} B-ALL cells transduced to express high levels of HLA-A2

Extended Data Figure 3.1

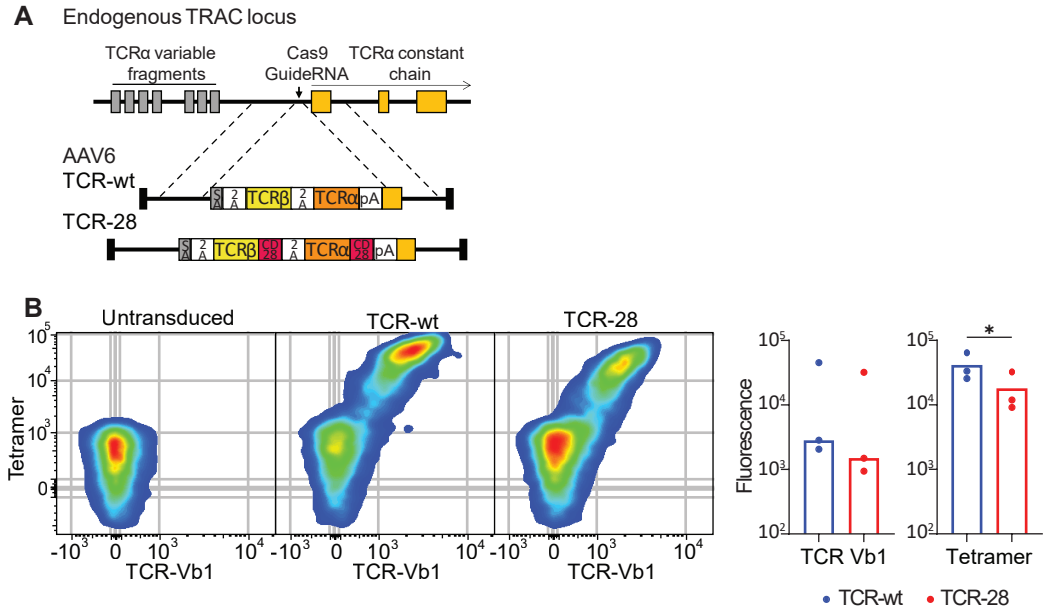

A, diagram of genetic engineering strategy illustrating knock in of NY-ESO-1 TCR-wt or TCR-28 via AAV6 mediated template delivery into the endogenous TRAC locus. **B,** flow cytometry plots of TRAC-edited T-cells transduced with no AAV (left), AAV encoding TCR-wt (middle), or AAV encoding TCR-28 (right) stained for NY-ESO-1 tetramer and TCR-Vβ1. Data representative of 3 donors. **C,** Summary of MFI of TRAC-edited T-cells transduced with AAV encoding TCR-wt or TCR-28 stained for NY-ESO-1 tetramer and TCR-Vβ1.

Extended Data Figure 3.2

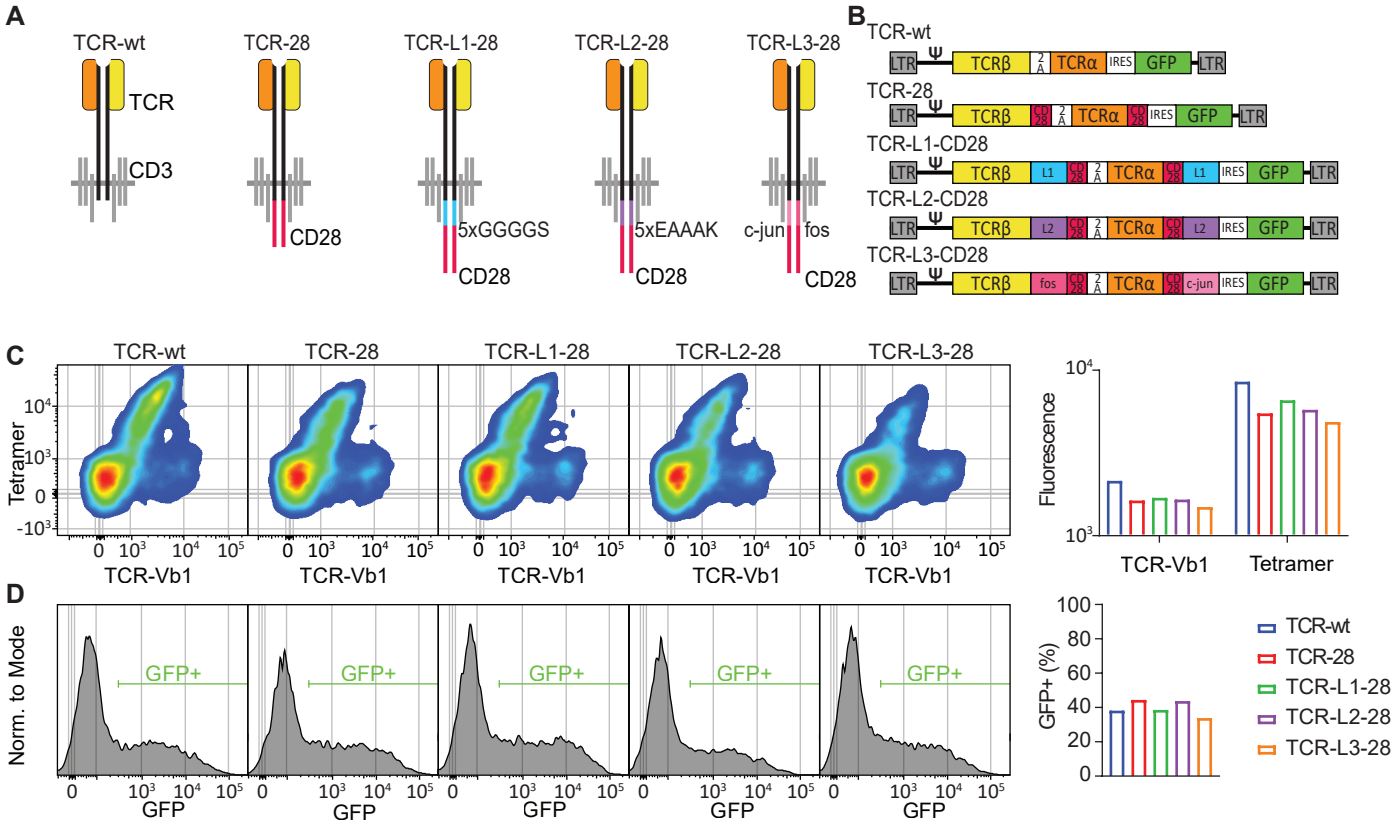

A, diagrams of TCR CD28 fusion designs incorporating either a flexible linker (TCR-L1-28), a rigid alpha-helix linker (TCR-L2-28) or a rigid beta-sheet linker (TCR-L3-28). **B,** diagrams of retroviral constructs encoding the TCR with linkers illustrated in A. **C, D** left, flow cytometry plots of TRAC-edited T-cells transduced with wildtype TCR (TCR-wt), TCR-CD28 fusion (TCR-28), TCR-CD28 fusion with Linker 1 (TCR-L1-28), TCR-CD28 fusion with Linker 2 (TCR-L2-28), TCR-CD28 fusion with Linker 3 (TCR-L3-28) stained for NY-ESO-1 tetramer and TCR-Vβ1 (C). **D,** diagram of GFP expression of cells in C. Right, summary of MFI of modified T-cells stained for NY-ESO-1 tetramer and TCR-Vβ1 (C, right) or GFP expression (D, right).

and NY-ESO-1 illustrated minimal anti-tumour T-cell activity (Ext. Data Fig 3.3A). To benefit from CD4 T-cell function, we co-expressed the co-receptor CD8αβ alongside the CD8 T-cell derived TCR as reported by multiple groups[152, 153] (Ext. Data Fig 3.3B). In both TCR-28 and TCR-wt T-cells, only CD8 T-cells and CD4 T-cells co-endowed with CD8αβ upregulated activation markers (CD25 and CD69) in response to on-target stimulation (Ext. Data Fig 3.3C, D). We confirmed that both TCR-wt^{CD8} and TCR-28^{CD8} secreted increased amounts of IL-2 consistent with increased CD4+ involvement (Fig 3.1G). Based on these findings, we used CD8αβ-endowed T-cells for future studies.

TCR-28 does not lead to improved anti-tumour efficacy in vivo

In NSG mice engrafted with human multiple myeloma (U266), melanoma (SK-Mel-37), cell lines that endogenously express HLA-A2 and NY-ESO-1, TCR-wt^{CD8} and TCR-28^{CD8} engineered T-cells exhibited comparable dose-dependant anti-tumour efficacy (Fig. 3.2A, B). To evaluate whether TCR-28^{CD8} conferred any benefits on T-cells *in* vivo and exclude antigen-loss as a confounding variable, SK-Mel-37 cells were isolated from relapsing mice in another donor. In an *in vitro* cytotoxicity assay, no decrease in sensitivity to fresh T-cell mediated cytotoxicity was observed (Fig. 3.2C). Consistent with the observed lack of benefit of TCR-CD28 fusion, in lung tissue isolated from melanoma-implanted mice treated with TCR-wt^{CD8} and TCR-28^{CD8} at day 24 post T-cell treatment, the number of isolated T-cells, their expression of PD-1 or differentiation markers were not significantly different (Fig 3.2D). Having confirmed that TCR-CD28 fusions are feasible, but not lead to improved *in vivo* outcomes, we evaluated an alternative strategy of delivering CD28 to the TCR/CD3 complex.

Figure 3.2: TCR-28 does not lead to improved anti-tumour efficacy in vivo

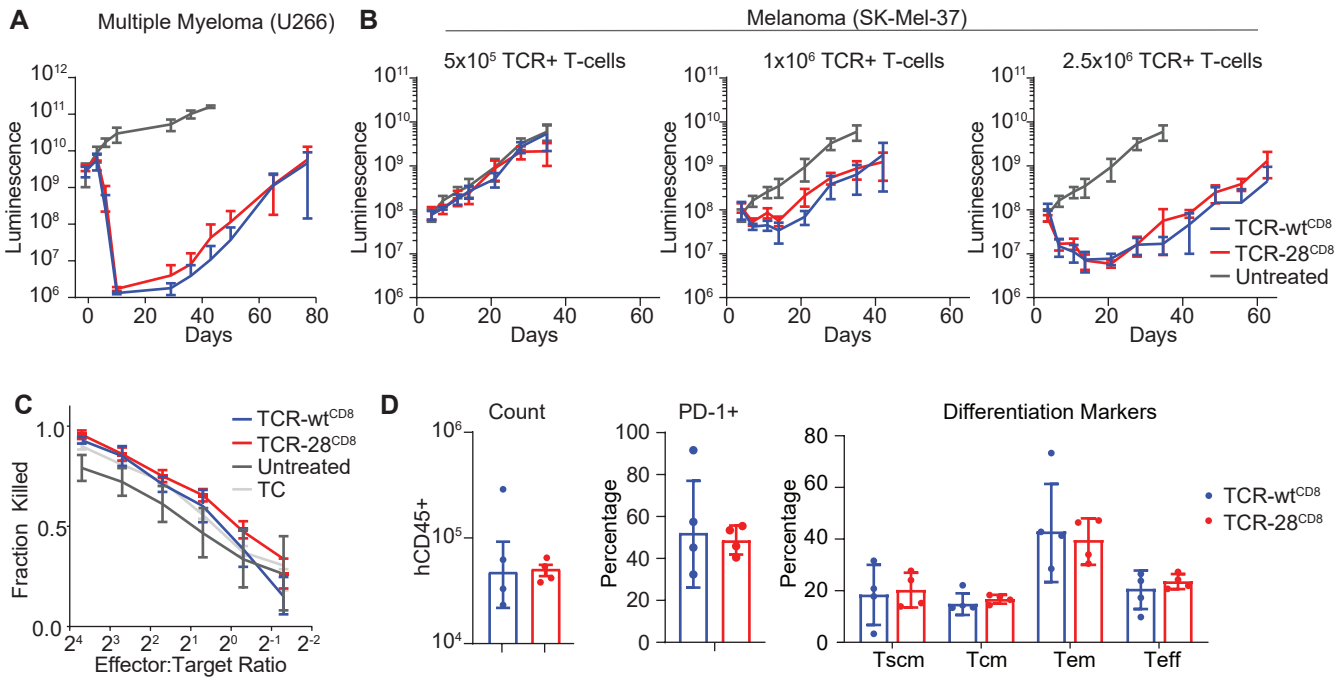

A, bioluminescence of NSG mice engrafted with $5x10^5$ U266 cells via tail IV, treated with $7.5x10^5$ TCR+ TCR-wt^{CD8} or TCR-28^{CD8} T-cells via tail IV 4 days post tumour engraftment. **B,** bioluminescence of NSG mice engrafted with $5x10^5$ SK-Mel-37 cells via tail IV, treated with labelled dose of TCR+ TCR-wt^{CD8} or TCR-28^{CD8} T-cells via tail IV 4 days post tumour engraftment. $1x10^6$ TCR+ T-cell dose is representative of 4 independent experiments/donors. **C,** *in vitro* cytotoxicity assay performed with freshly produced TCR-wt^{CD8} T-cells on lung-isolated adherent cells cultured for 7 days post isolation from mice treated with TCR-wt^{CD8} or TCR-28^{CD8}. **D,** absolute counts of human CD45+ cells(left), percentage of CD45+ expressing PD-1 (middle), and fraction of cells expressing Tscm (CD62L+, CD45Ra+), Tcm(CD62L+, CD45Ra-), Tem (CD62L-, CD45Ra-) and Teff (CD62L-, CD45Ra-) markers (right) of cells isolated from lungs treated with TCR-wt^{CD8} or TCR-28^{CD8} T-cells. Data is pooled from two mice isolated per condition at each of day 17 and day 20 post T-cell injection. Data are mean ± sem.

Extended Data Figure 3.3

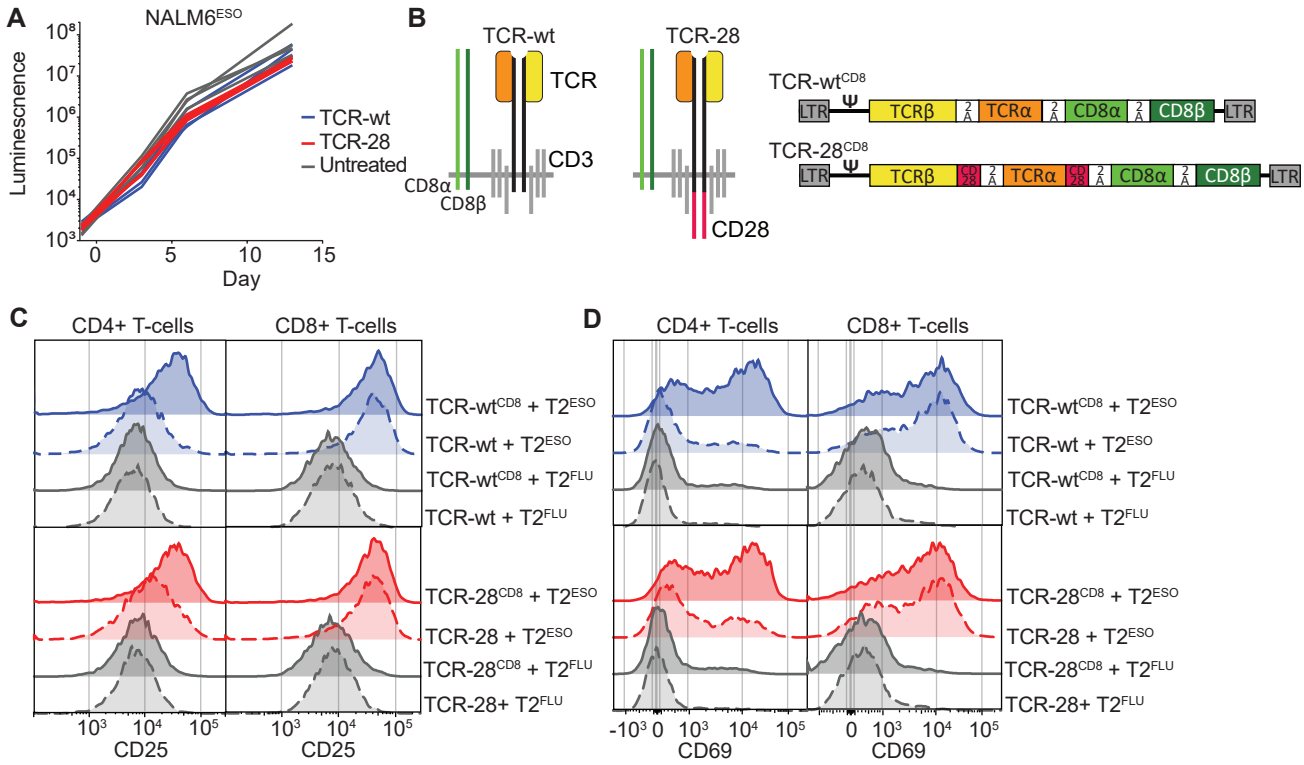

A, bioluminescence of NSG mice engrafted with 5x10^5 NALM6^{ESO} cells via tail IV, treated with 1x10^6 TCR+ TCR-wt or TCR-28 T-cells via tail IV 4 days post tumour engraftment. **B,** left, diagram of TCR-wt and TCR-28 expression cells co-expressing CD8αβ. Right, diagram of retroviral construct encoding TCR-wt or TCR-28 and CD8αβ. **C, D,** flow cytometry histograms for CD25 (C) and CD69 (D) on CD4 and CD8 T-cells 24hrs post stimulation with T2 cells pulsed with 10μM NY-ESO-1 or FLU peptide.

Endowment of CD28 co-stimulation onto CD3 chains leads to improved in vitro proliferation but does not lead to increased efficacy in vivo

We further evaluated a strategy wherein CD28 is fused to members of the CD3 complex, endogenously associating it with the TCR on the T-cell membrane. Since CD28 acts as a dimer, we focused our efforts on CD3ζ and CD3ε which are both found in duplicate within the TCR/CD3 complex (Fig. 3.3A, B). We generated retroviral constructs in which the CD28 was fused to the C-terminus of CD3 (membrane-distal) or between the transmembrane and the ITAM-containing cytosolic domains (membrane-proximal) along with an LNGFR reporter gene (Fig. 3.3A, B). Using CRISPR Cas9-mediated editing, we knocked out the endogenous *CD3Z* or *CD3E* genes, and were successfully able to recapitulate cell-surface expression of the CD3 complex incorporating the modified CD3 constructs (Fig 3.3C, D). Using the LNGFR reporter gene, modified cells were further sorted to ensure each cell contained the modified CD3 construct of interest (Fig 3C, D). To compare the various modified CD3 constructs, IL-2 secretion subsequent to plate-bound OKT3 stimulation was measured in a TCR-target independent manner. T-cells containing CD3ζ or CD3ε with proximal CD28 ($CD3\zeta^{pCD28}$ and $CD3\varepsilon^{pCD28}$) both exhibited increased IL-2 secretion compared to cells transduced with a control LNGFR vector retaining their endogenous CD3 chains, indicative of successful CD28 co-stimulation (Fig. 3.3E). As $CD3\zeta^{pCD28}$ yielded significantly more IL-2 than $CD3\varepsilon^{pCD28}$, that construct was used for subsequent experiments (Fig. 3.3E). T-cells with their endogenous *TRAC* and *CD3Z* genes knocked out, an NY-ESO-1 specific TCR knocked into their TRAC locus, and further transduced with a retrovirus encoding CD8αβ and either $CD3\zeta^{pCD28}$ or $CD3\zeta^{wt}$ exhibited no differences in ability to kill T2 cells

Figure 3.3: Endowment of CD28 co-stimulation onto CD3 chains leads to improved in vitro proliferation but does not lead to increased efficacy in vivo

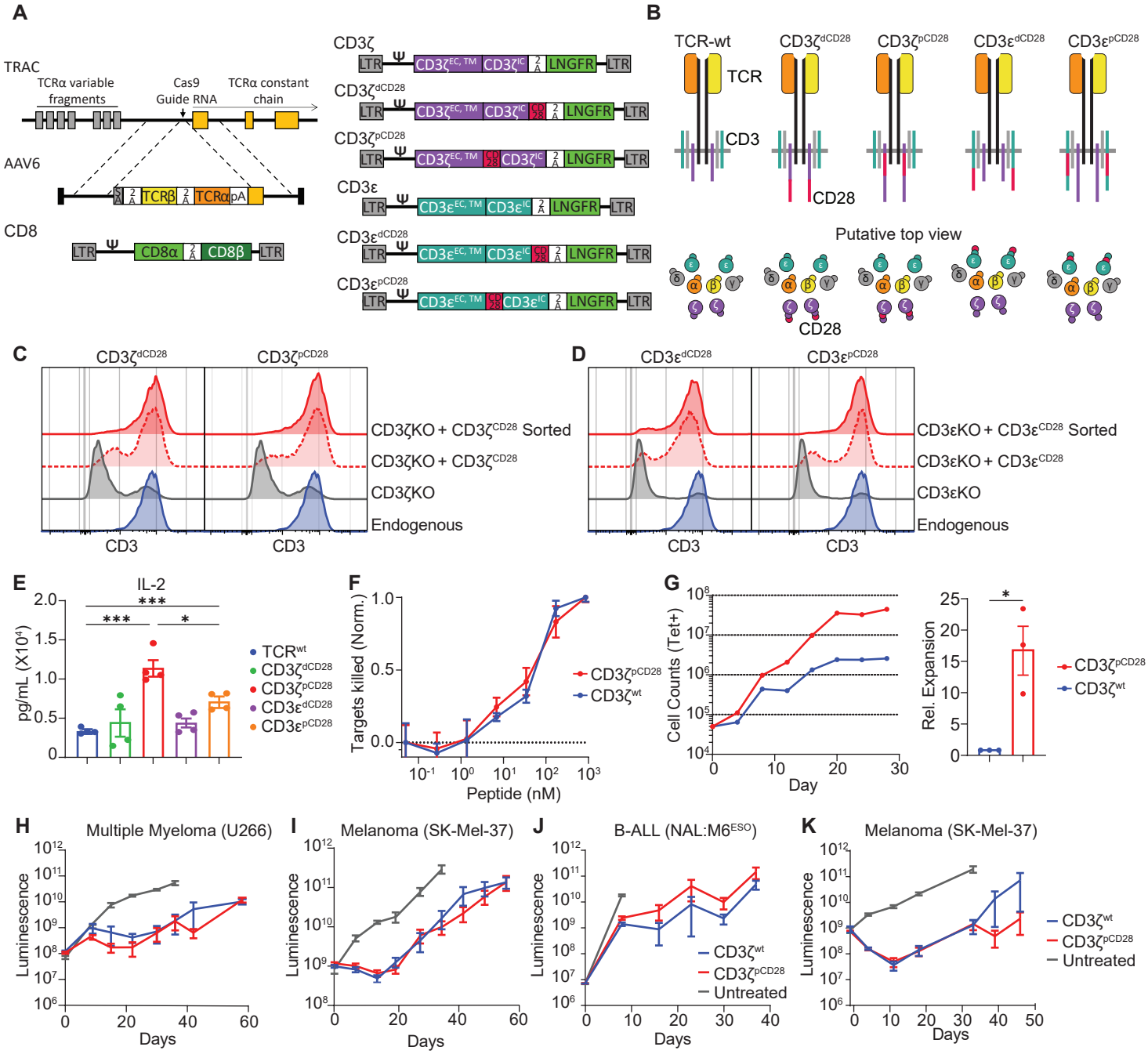

A, left, diagram of genetic engineering strategy illustrating knock in of NY-ESO-1 TCR via AAV6 mediated template delivery, retrovirus encoding CD8α and CD8β, and right, retroviruses encoding control or modified CD3ζ and CD3ε chains with an LNGFR reporter. **B,** putative structure of TCR/CD3 complex incorporating control or modified CD3ζ and CD3ε chains. CD28 intracellular domain illustrated by red bars or red circles. **C, D,** flow histogram unmodified cells (blue), CD3ζ (grey, C) or CD3ε (grey, D) knockout T cells, CD3ζ (dashed red, C) or CD3ε (dashed red, D) knockout T cells transduced with retroviral construct, or CD3ζ (red, C) or CD3ε (red, D) knockout T cells transduced with retroviral construct and sorted for LNGFR expression were stained with anti CD3 antibody at day 5 post electroporation with appropriate guide or mock. Data representative of 3 human donors. **E,** IL-2 cytokine levels detected in supernatant 24 hours after sorted, modified T-cells are plated onto OKT3-coated plates. **F,** cytotoxicity of NY-ESO-1 $CD3\zeta^{KO}$ T-cells, transduced with CD8αβ and $CD3\zeta^{wt}$ or $CD3\zeta^{pCD28}$ and sorted for LNGFR against T2 cells pulsed with a titrated concentration of NY-ESO-1 peptide. Data representative of 2 donors. **G,** left, representative expansion of NY-ESO-1 $CD3\zeta^{KO}$ T-cells, transduced with $CD3\zeta^{wt}$ or $CD3\zeta^{pCD28}$ stimulated with $NALM6^{ESO}$ target cells twice weekly. Right, summary of relative expansions of $CD3\zeta^{wt}$ or $CD3\zeta^{pCD28}$ modified T-cells from three biological donors. **H, I, J** bioluminescence of NSG mice engrafted with $5x10^5$ U266 cells (**H**), SK-Mel-37 (**I**) or $NALM6^{ESO}$(**J**) via tail IV, treated with $1x10^5$(**H**), $1x10^6$(**I**), or $2x10^5$(**J**) NY-ESO-1+ $CD3\zeta^{KO}$ T-cells, transduced with CD8αβ and $CD3\zeta^{wt}$ or $CD3\zeta^{pCD28}$ and sorted for LNGFR+ via tail IV 4 days post tumour engraftment. I is representative of 4 independent donors, J is independent of 2 independent donors. **K,** bioluminescence of NSG mice engrafted with $5x10^5$ SK-Mel-37 , treated with $1x10^6$ high affinity NY-ESO-1+ $CD3\zeta^{KO}$ T-cells, transduced with $CD3\zeta^{wt}$ or $CD3\zeta^{pCD28}$ and sorted for LNGFR+ via tail IV 4 days post tumour engraftment. Data are mean ± sem. * $p<0.05$, ** $p<0.01$, *** $p<0.001$, **** $P<0.0001$.

at titrated peptide concentrations, at an effector to target ratio of 1:1 (Fig 3.3F). CD3ζ^{pCD28} endowed cells showed increased proliferative capability upon twice weekly with NALM6^{ESO} cells, with an average expansion of 16-fold over control cells modified with CD3ζ^{wt} (Fig 3.3G). *In vivo* xenograft models of human multiple myeloma (U266), melanoma (SK-Mel-37), and a B-ALL (NALM6^{ESO}), CD3ζ^{pCD28} failed to show improved tumour control over CD3ζ^{wt} controls (Fig. 3.3H, I, K, Ext. Data Fig 3.4A). Cell isolated from the bone marrow of NALM6-containing mice illustrated comparable tumour and T-cell counts, PD-1 expression levels, and T-cell differentiation patterns between CD3ζ^{pCD28} and CD3^{wt} (Ext. Data Fig. 3.4B).

To exclude that the absence of improved *in vivo* efficacy is an artifact of the TCR chosen or due to the co-transduction with the CD8αβ construct, T-cells were alternatively endowed with a CD8-independent NY-ESO-1 TCR. Both CD4 and CD8 T-cells endowed with this alternative NY-ESO-1 TCR ("TCR-alt"), exhibited increased sensitivity, exhibiting increased cytotoxicity against T2 cells pulsed with titrated peptide concentrations compared to TCR-wt^{CD8} (Ext Data Fig. 3.4C). T-cells endowed with this alterative TCR and CD3ζ^{pCD28} or CD3ζ^{wt} similarly showed no increase in anti-tumour efficacy in a mouse xenograft model of disseminated human melanoma.

Extended Data Figure 3.4

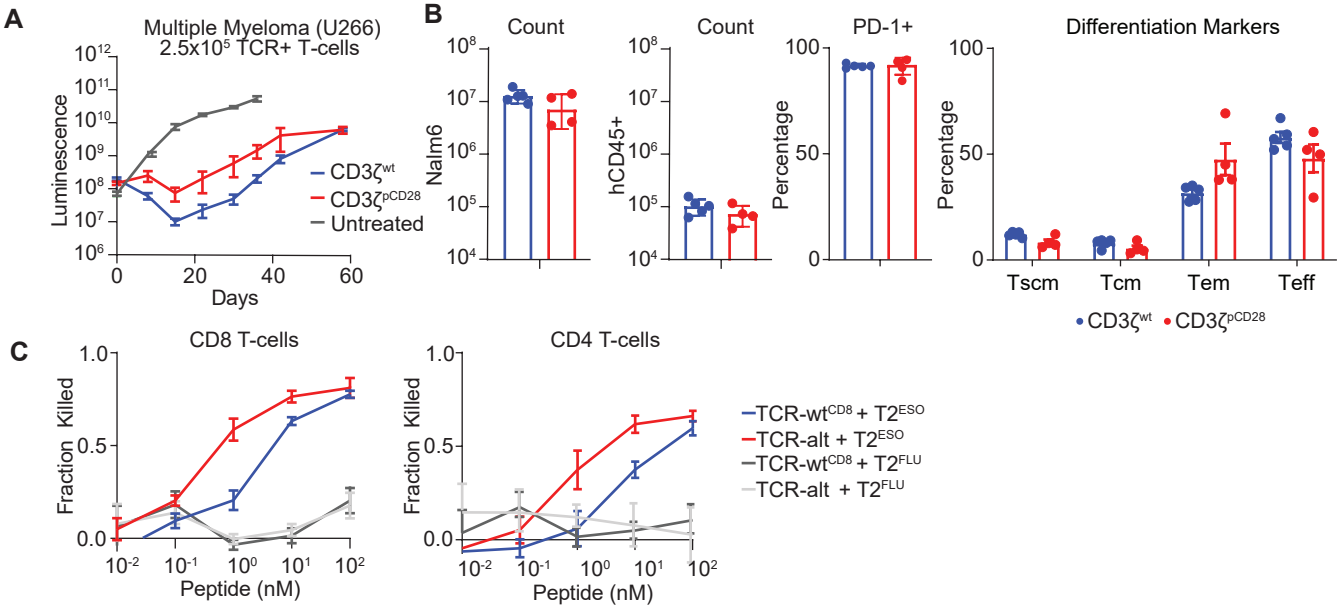

A, bioluminescence of NSG mice engrafted with 5x10^5 U266 cells via tail IV, treated with 2.5x10^5 NY-ESO-1+ CD3ζ^{KO} T-cells, transduced with CD8αβ and CD3ζ^{wt} or CD3ζ^{pCD28} and sorted for LNGFR+ via tail IV 4 days post tumour engraftment. **B,** absolute counts of GFP+ hCD45dim NALM6 cells and GFP- hCD45+ cells(left), percentage of hCD45+ expressing PD-1 (middle), and fraction of cells expressing Tscm (CD62L+, CD45Ra+), Tcm(CD62L+, CD45Ra-), Tem (CD62L-, CD45Ra-) and Teff (CD62L-, CD45Ra-) markers (right) of cells isolated from bone marrow at day 15 of NALM6^{ESO}-engrafted mice treated with TCR-wt^{CD8} or TCR-28^{CD8} T-cells. **C,** *in vitro* cytotoxicity assay of T-cells transduced with NY-ESO-1 and CD8αβ or high affinity NY-ESO-1 TCR sorted for CD4 or CD8 against T2 cells pulsed with titrated NY-ESO-1 or off-target FLU peptide concentrations at an E:T ratio of 1:1. Data are mean ± sem.

Discussion

We illustrated that the fusion of CD28 onto either the TCR α and β chains or CD3 chains is feasible and leads to cell surface expression of the modified TCR/CD3 complex. While the TCR-28 fusion endowed cells have mildly augmented cell surface staining of the TCRβ chain and tetramer binding, this decrease does not detrimentally affecT-cell properties *in vivo* and *in vitro*. We found that adding flexible, α-helical or β-sheet linkers between the TCR chains and CD28 still led to a decrease in surface staining, consistent with a CD28-mediated phenotype. There is evidence that the PI3K domain in CD28 leads to internalisation, which could be an explanation for the decreased cell surface staining and would suggest that TCR fusions harbouring a mutant $CD28^{Y191F}$ would not exhibit decreased cell surface expression[154]. Alternatively, it is known that CD28 contains positively charged amino acids in its cytoplasmic tail that induce its association with the inner leaflet of the cell membrane[155]. As the TCR chains have very short intracellular domains, this novel association could be leading to a disruption in the TCR/CD3 complex, which may be exhibited by the observed decreased staining. As both CD3ε and CD3ζ similarly possess positive charges that associate their cytoplasmic tails to the membrane[56], the TCR/CD3 structure already evolved to accommodate this interaction, the addition of CD28 may not lead to a significant stability impact on these molecules consistent with the lack of decreased cell surface staining.

Consistent with CD28-derived co-stimulation, IL-2 secretion was increased upon stimulation of T-cells endowed exogenous CD28 in their TCR/CD3 complex, and increased proliferative capacity was observed in T-cells endowed with $CD3\zeta^{pCD28}$ was measured upon repetitive stimulation [156]. Further research is needed to identify why the

improved *in vitro* cytokine secretion and proliferation did not translate into improved *in vivo* anti-tumour efficacy. The data suggests that the CD28 co-stimulation delivered by this design is sub-optimal, and while sufficient to augment T-cell proliferation at high T-cell concentrations ($1x10^6$/mL) with excess nutrients *in vitro*, under more dilute and challenging *in vivo* conditions, the CD28 co-stimulation was not sufficient. Recent studies in the CAR field have highlighted the role of the extracellular "hinge" and transmembrane region of CD28 in CAR T-cell efficacy, which suggests that the cytoplasmic tail of CD28, as used here, may be missing key features required for full co-stimulation[108, 109].

In attempt to validate the observations, multiple confounding explanations have been excluded by our study. Our work excluded antigen loss as a confounding mechanism, as fresh T-cells illustrated comparable cytotoxicity against both mouse-isolated relapsing tumours and tissue cultured cells. Similarly, as T-cells have been shown to have different requirements between liquid and solid tumours[157], we evaluated the T-cells in both and showed no increased efficacy in either model, suggesting that the tumour microenvironment is not a major contributor to the lack of increased efficacy. To exclude the possibility that the TCR chosen is not representative, an alternative high affinity one was cloned[158], which confirmed our findings. One limitation that was not excluded was the absence of an extended immune system beyond the injected human T-cells, as NSG mice were used. The investigation of human tumours and human T-cells in mice must be performed in immunocompromised mice to prevent graft rejection, which allows for the study of human cells, but precludes the evaluation in a immune-replete

model. It is likely that additional immune system components are required for T-cells to exert long-term TCR mediated control.

Other groups have designed TCRs that include co-stimulatory domains previously, however those TCRs were specifically designed to not associate with the endogenous CD3 complex, allowing for no mispairing without the need for genetic engineering[130, 132]. Comparisons were limited to comparing TCRs with on-board co-stimulation that do not miss pair to wildtype TCRs that dimerize with the endogenous TCR chains preventing an evaluation of the true benefit of co-stimulation *in vivo*. This is the first paper to take advantage of genetic engineering strategies to explicitly evaluate the benefits of co-stimulation when delivered to the TCR without a confounding affect on mispairing. In our precise models, we find no benefit from fused co-stimulation, suggesting that the prior findings were largely due to mispairing avoidance. The findings here are in contrast to a recent report on artificial T-cell–activating adapter molecules (ATAMs), where a CD3ζ-CD28 fusion was not associated with any increased *in vitro* proliferation or IL-2 secretion[159]. This discrepancy can be explained by the use of CRISPR/Cas9 in this study to remove the endogenous CD3ζ, while in the other work the engineered CD3ζ had to compete with the endogenous CD3ζ for association with the TCR/CD3 complex and likely was found as a heterodimer with the endogenous CD28-less CD3ζ.

This study highlights the benefits of carefully genetically engineered studies to uncover novel biology and more potent therapeutics. Overall, while CD28 fusions did not lead to increased efficacy in challenging *in vivo* models, there was also no decrease in

functionality nor were any safety concerns identified, suggesting that the identified sites should be considered for other TCR engineering strategies, which may be more potent.

Extended thoughts: CD4+ T-cells transduced with CD8-derived TCR and exogenous CD8αβ exhibit augmented accumulation in vivo

Recent work has illustrated that CD8αβ overexpression on CD4+ T-cells expressing an exogenous CD8 T-cell derived TCR (TCR_{CD8}) leads to increased activity[152, 153]. However, those studies did not perform comparisons to a CD4-derived TCR (TCR_{CD4}) to evaluate whether full CD4 activity was restored. As part of efforts to exclude additional confounding factors masking possible benefits of co-stimulation, a previously reported CD4 T-cell -derived TCR targeting an antigen on SK-Mel-37 was introduced into T-cells[160]. $NALM6^{ESO}$ cells, which express HLA-A2 and exogenous NY-ESO-1, were only lysed by an NY-ESO-1 specific TCR_{CD8} on CD8 T-cells or on CD4 T-cells co-expressing CD8αβ. Similarly, SK-Mel-37 melanoma cells were lysed by both an NY-ESO-1 specific TCR_{CD8} on CD8 T-cells and on CD4 T-cells co-expressing CD8αβ, but also by an NY-ESO-1 specific TCR_{CD4} on CD4 T-cells. (Fig 3.4, B).

To compare the *in vivo* efficacy of CD4 T-cells endowed with an NY-ESO-1 specific TCR_{CD8} and exogenous CD8αβ to CD4 T-cells endowed with an NY-ESO-1 specific TCR_{CD4}, melanoma engrafted NSG mice were treated 4 days later with $1x10^6$ total TCR+ T-cells, composed of either bulk CD4 and CD8 T-cells transduced with an NY-ESO-1 specific TCR_{CD8} and exogenous CD8αβ, or $1x10^6$ total TCR+ coreceptor matched T-cells, composed of CD8 T-cells and CD4 T-cells transduced with an NY-ESO-1 specific TCR_{CD8} and TCR_{CD4}, respectively. The separately transduced T-cells

were pooled together at the same ratio CD4:CD8 ratio identified in the bulk-transduced condition to ensure comparability. There was no difference in anti-tumour efficacy of T-cells endowed with a TCR_{CD8} and exogenous CD8αβ or T-cells endowed with co-receptor matched TCRs (Fig 3.4, C). While no difference in tumour luminescence was observed, cells isolated from the spleens and lungs of treated mice illustrated that co-receptor matched T-cells were present in much higher numbers in both tissues suggesting that CD8αβ expression on CD4 TCR_{CD8} T-cells was not sufficient to fully recapitulate their function (Fig 3.4, D).

In light of these findings, $CD3\zeta^{pCD28}$ was re-evaluated in an *in vivo* melanoma model. NSG mice were engrafted with SK-Mel-37 melanoma via tail vein iv, and subsequent treated with T-cells engineered with co-receptor matched TCRs 4 days later. $CD3\zeta^{pCD28}$ did not lead to improved tumour control as measured by luminescence compared to CD3ζ endowed T-cells (Fig 3.4, E).

This findings suggest that while the expression of CD8αβ on CD4 T-cells endowed with TCR_{CD8} does allow these cells to exert some functions, their capabilities are limited. This could be due to decreased Lck loading onto the exogenous CD8αβ proteins due to competition with CD4, which is known to bind Lck with higher affinity[59]. The presence of both CD4 and CD8αβ may also decrease the availability of free Lck, which has been suggested to be more active than co-receptor bound Lck[59]. This hypothesis can be tested by comparing CD4 T-cells expressing exogenous CD8αβ with their endogenous co-receptor ablated or intact.

Figure 3.4: CD4+ T-cells transduced with a CD8-derived TCR and exogenous CD8 exhibit augmented accumulation in vivo

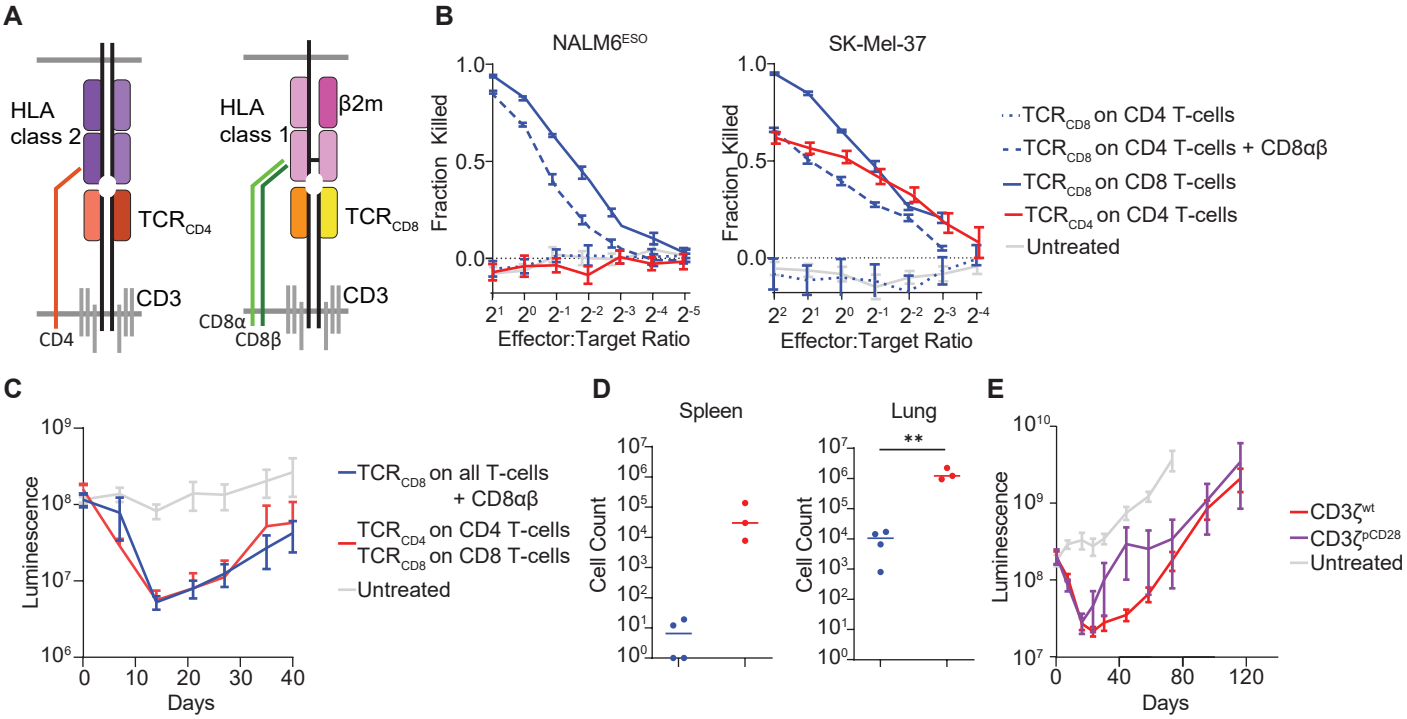

A, diagram of CD4 or CD8 T cell TCR binding an HLA class 2 or class 1 antigen with the CD4 or CD8 co-receptor participating, respectively. **B,** 18-hour *in vitro* CTL assay comparing CD8 T-cell isolated TCR (TCR_{CD8}) expressed on CD8 T-cells, TCR_{CD8} in CD4 T-cells with or without exogenous CD8αβ, or a CD4 T-cell isolated TCR (TCR_{CD4}) expressed on CD4 T-cells in $NALM6^{ESO}$ (HLA-A2+, HLA- DRA1-) and SK-Mel-37 (HLA-A2+, HLA- DRA1+). **C,** bioluminescence of NSG mice engrafted with melanoma (SK-Mel-37) monitored over 40 days treated with either bulk T-cells transduced with TCR_{CD8} and exogenous CD8αβ (blue), or co-receptor matched TCR T-cells (red). **D,** CD3+ T-cell counts isolated from spleen and lung of NSG mice engrafted with melanoma at day 40 post T-cell treatment. **E,** bioluminescence of NSG mice engrafted with melanoma (SK-Mel-37) monitored over 120 days treated or co-receptor matched TCR T-cells (red) with their endogenous CD3ζ edited and replaced by retrovirally expressed $CD3\zeta^{pCD28}$ or control $CD3\zeta^{wt}$. Data are mean ± sem. * $p<0.05$, ** $p<0.01$, *** $p<0.001$, **** $P<0.0001$.

The mismatch between the observed, unchanged, tumour growth and increased cell accumulation in co-receptor matched T-cells also raises the question of whether the tumour relapses can be attributed to a limitation of the model, leading to T-cell failure. It is known that HLA levels are downregulated *in vivo*[161], and while this thesis has excluded the permanent loss of HLA, since tumour samples can still be lysed *in vitro*, it does not exclude a transient loss that significantly decreases a tumour's sensitivity to T-cell mediated lysis *in vivo.* The evaluation of these engineering strategies in a more immunologically complete model, including NK cells, would exclude HLA downregulation as a resistance mechanism.

Chapter 4 – Development and evaluation of TCR orthogonal co-stimulatory molecule driving both CD28 and 4-1BB co-stimulation

In light of the limited *in vivo* efficacy exhibited by TCR T-cells endowed with CD28 co-stimulation directly on the TCR/CD3 chains, we set out to design a TCR orthogonal co-stimulatory molecule. As the CD28 and 4-1BB costimulatory pathways have been shown to have synergistic properties in a number of biological settings[84, 85, 162, 163] and in engineering T-cells[98, 99, 164-166], we combined a ligand for CD28 with the signaling domain of 4-1BB, inventing "80BB". We chose CD80 as the CD28 ligand for its dimeric structure, knowing that 4-1BB signaling domains function satisfactorily in this format[91, 167].

We chose to take advantage of a recently published anti-CD19 HLA-independent TCR (19-HIT)[129], which takes advantage of endogenous CD3 complex to acquire high sensitivity and likewise does not possess autochthonous costimulatory machinery. Using this 19-HIT molecule allowed us to take advantage of a wide assortment of well validated models and tools developed for studying anti-CD19 CARs.

80BB augments HIT T-cell anti-tumour potency

We designed the chimeric 80BB receptor by fusing the extracellular and transmembrane domains of the human CD80 ligand to the intracellular domain of the human 4-1BB receptor (Fig. 4.1A), hypothesizing that it could at once serve as a CD28 agonist and a 4-1BB costimulatory receptor. To investigate its functional properties, we expressed it in human peripheral blood T-cells engineered with a HIT receptor, a chimeric TCR that signals through the CD3 complex and does not possess a

costimulatory endodomain[129]. We targeted the anti-CD19 HIT receptor (19-HIT) cDNA to the *TRAC* locus as previously reported[139], and retrovirally transduced 80BB cDNA (Extended Data Fig. 4.1A). 80BB was well expressed on T-cells, resulting in high CD80 staining, typically 40-fold above endogenous CD80 expression (Fig. 4.1A). Upon its transduction, 80BB expression did not alter the cytolytic activity of HIT T-cells against the CD19+ NALM6 cells (19-HIT^{80BB} vs 19-HIT, Ext. Data Fig. 4.1B). Upon repeated exposure to antigen, however, 80BB considerably augmented T-cell expansion and accumulation, achieving >15-fold higher T-cell numbers by day 14 after 7 repeated antigen stimulations with NALM6 cells (Fig. 4.1B). Furthermore, these 19-HIT^{80BB} cells retained their cytolytic function (Fig. 4.1C), unlike 19-HIT T-cells which started exhibiting diminished tumour lysis by the third tumour stimulation and eventually failed to clear subsequent challenges. Furthermore, 19-HIT^{80BB} T-cells displayed sustained cytolytic function in both CD4 and CD8 T-cell fractions (Ext Data Fig. 4.1C). 19-HIT^{80BB} also exhibited greater mitochondrial and glycolytic capacities after multiple stimulations (n=3), compared to 19-HIT-cells (Fig. 4.1D).

Encouraged by these findings, we proceeded to an initial *in vivo* evaluation of 19-HIT^{80BB} function in the well-established NALM6 leukemia model in immunodeficient NSG mice[164]. NALM6 is an acute lymphoblastic leukemia that does not express CD80, CD86, 4-1BBL, PD-L1 or CTLA4 (Ex. Data Fig. 4.1D). We administered low doses of 19-HIT T-cells to assess if their efficacy was enhanced by co-expressing 80BB. At doses where treatment with 19-HIT T-cells without co-stimulation provided minimal ($1x10^5$/mouse) or no survival advantage ($0.5x10^5$/mouse) relative to untreated control

Figure 4.1: CD80-4-1BB synthetic costimulatory molecule (80BB) enhances HLA Independent TCR (HIT) T cell anti-tumour function

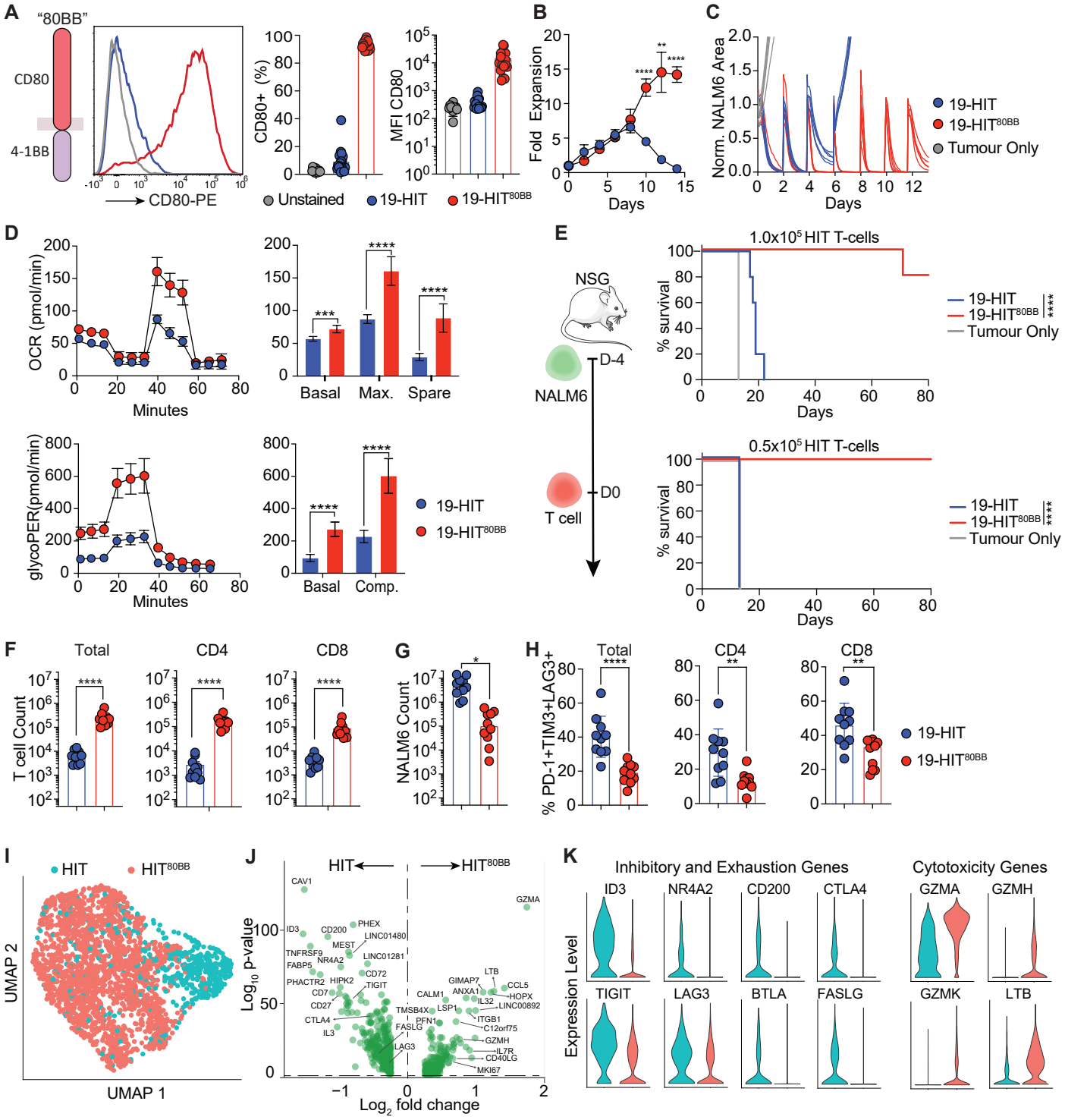

A, Left, diagram depicting the fusion of the extracellular domain and transmembrane domain of CD80 with the intracellular domain of 4-1BB to generate the CD80-4-1BB synthetic costimulatory molecule (80BB). Middle, representative flow cytometry profile of CD80 on the surface of 19-HIT T cells with (red) or without retrovirally transduced 80BB (19-HIT^{80BB}, blue). Right, CD80 percentages and MFI of 19-HIT and 19-HIT^{80BB} T cells. Data were collected 4 days post 80BB transduction. Each dot represents an independent donor. **B,** T cell fold expansion upon repetitive antigen stimulation using NALM6 target cells every second day at an E:T ratio 1:2. Data are representative of 3 donors. **C,** Serial *in vitro* cytotoxicity assay using NALM6. Fresh target cells were added every 2 days. Data are representative of 13 donors. **D,** Mitochondrial stress (top), and glycolytic rate (bottom) Seahorse assays were performed after 3 rounds of stimulation with NALM6 cells. "Max" refers to the maximum respiratory capacity and "Comp" refers to the compensatory glycolytic rate. Data are representative of 3 donors. **E,** Left, diagram depicting *in vivo* treatment of NALM6-bearing mice with 19-HIT or 19-HIT^{80BB} T cells. Right, Kaplan–Meier survival analysis of NALM6 bearing mice treated with $1.0x10^5$ (top) or $0.5x10^5$ (bottom) 19-HIT or 19-HIT^{80BB} T cells (n=5 mice/group). Data are representative of 3 donors. **F,** Absolute counts of T cells (left), CD4+ T-cells (middle), CD8+ T-cells (right). **G**, Absolute count of NALM6. **H**, Percentages of T-cells co-expressing inhibitory markers PD-1, LAG3, TIM3 in total T-cells (left), CD4 (middle) and CD8 (right). **F-H,** T cells were isolated from the bone marrow of NALM6-bearing mice nine days post 19-HIT or 19-HIT^{80BB} T cell treatment. **I,** UMAP projection of 2591 T cells isolated from the bone marrow of NALM6-bearing mice nine days post 19-HIT or 19-HIT^{80BB} treatment. **J,** Volcano plot of differentially expressed genes between 19-HIT and 19-HIT^{80BB} T cells. **K,** Violin plots of selected genes significantly up or downregulated in 19-HIT and 19-HIT^{80BB} highlighting Inhibitory, Exhaustion and Cytotoxicity genes. **(F-K)** Data are pooled from 5 mice treated with $1x10^5$ and 5 mice with $0.5x10^5$ T cells. *P* values were determined by two-tailed t-test **(A, B, D, F, G, H)**, log-rank Mantel–Cox test **(E)** or Wilcoxon rank sum test (**J, K**). Data are mean ± sem. * $p<0.05$, ** $p<0.01$, *** $p<0.001$, **** $P<0.0001$.

Extended Data Figure 4.1

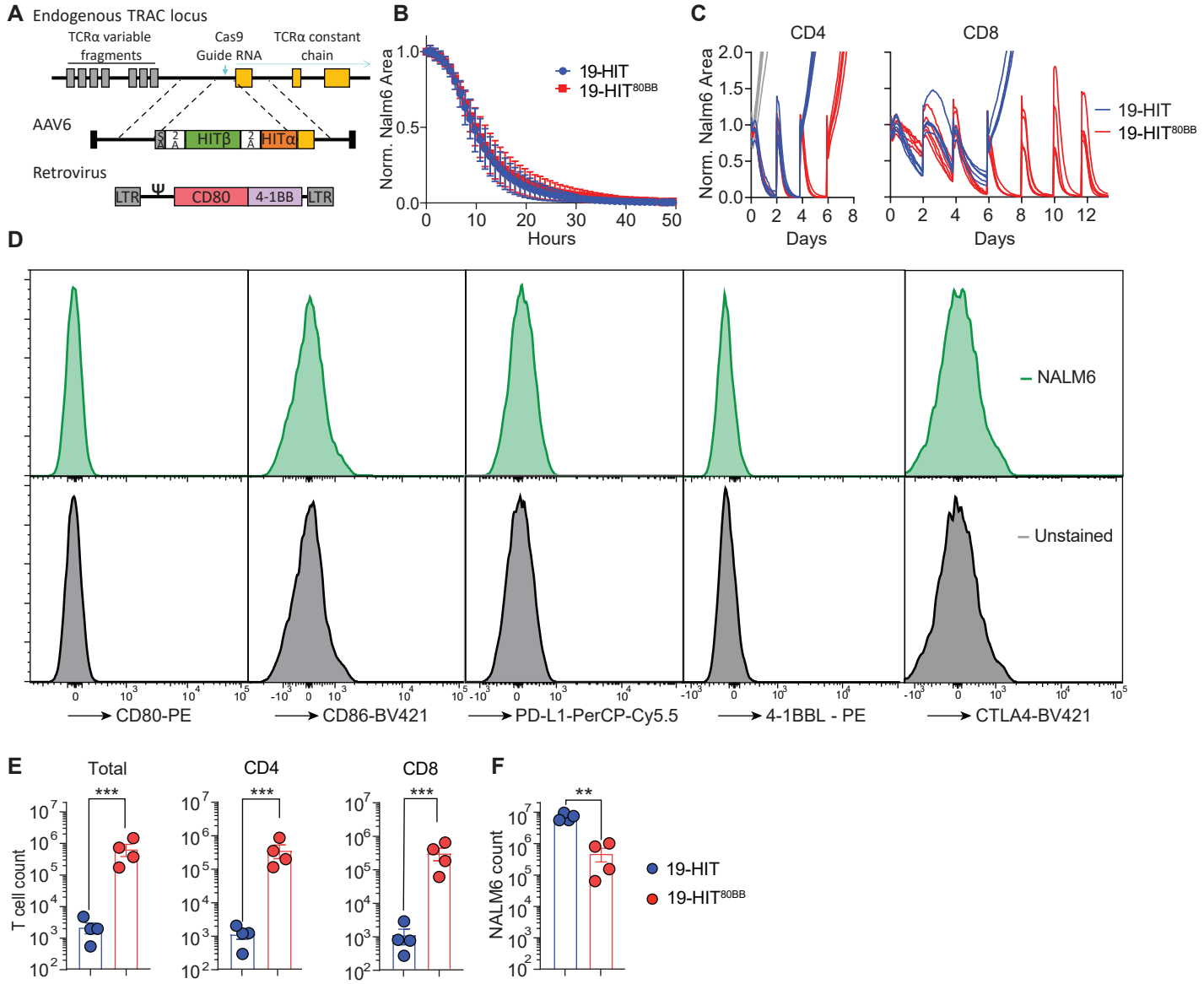

A, Diagram illustrating genetic T cell engineering strategy of HIT and HIT^{80BB} T cells. The alpha and beta chains of HIT directed against CD19 were targeted into the *TRAC* locus as previously described[34]. 80BB construct was delivered using the gamma retroviral vector SFG. **B,** 48-hour serial in vitro cytotoxicity assay using NALM6 targets. Cells were plated at an effector: target ratio of 1:2. **C**, Serial in vitro cytotoxicity assay with fresh NALM6 cells added every 2 days, starting with sorted CD4 (left) and CD8 T-cells (right). Data are representative of 4 replicates. **D**, Flow cytometry profiles of CD80, CD86 and PD-L1, 4-1BBL and CTLA4 on NALM6 cells. **E,** Absolute count of total (left), CD4 (middle) and CD8 (right) T cells. F, Absolute count of NALM6 **E, F** Cells were isolated from bone marrow of NALM6 bearing mice seventeen days post HIT or HIT^{80BB} treatment. n=4 mice/group treated with 1x10^5 HIT+ T-cells/mouse**.** *P* values were determined by two-tailed t-test **(E, F).** * p<0.05, ** p<0.01, *** p<0.001, **** P<0.0001.

mice, 19-HIT^{80BB} T-cells markedly improved survival establishing that 80BB did increase anti-tumour potency *in vivo* (Fig. 4.1E).

Analysis of bone marrow 9 days after 19-HIT T-cell infusion, demonstrated a greater accumulation of 19-HIT^{80BB} T-cells and a concomitant decrease in tumour cells, consistent with the increased survival (Fig. 4.1E, F, G). Both CD4 and CD8 T-cells were increased in number by 2-2.5-fold ($p<0.01$, Fig. 4.1F), which was further confirmed on day 17 in another experiment with another donor (Ext. Data Fig. 4.1E). These 19-HIT^{80BB} cells also showed reduced expression of PD-1, LAG3, and TIM3 compared to 19-HIT T-cells (Fig. 4.1H). These observations were corroborated by single-cell RNA sequencing performed on 19-HIT and 19-HIT^{80BB} T-cells retrieved on day 9. 19-HIT and 19-HIT^{80BB} T-cells clustered separately (Fig. 4.1I, Ext. Data Fig. 4.2A, B, C) and differed in the expression of genes associated with engineered T-cell dysfunction (ID3, NR4A2, Fig 1K, Ext Data Fig. 4.3A)[168, 169]. We also observed increased expression of inhibitory receptors (CD200, CTLA4, TIGIT, LAG3, BTLA) in HIT-cells and of T-cell division and cytotoxicity genes (MKI67, IL7R, GZMA, GZMH, GZMM, LTB) in HIT^{80BB} (Fig. 4.1J, K, Ext Data Fig. 4.2 D, E, Ext Data Fig. 4.3A, B), consistent with the increased accumulation and prolonged functional maintenance of HIT^{80BB} T-cells (Fig. 4.1B-H). Altogether, our *in vitro* and *in vivo* characterization of HIT^{80BB} T-cells underscores the benefits of expressing 80BB in adoptively transferred T-cells to sustain their accumulation and function.

Extended Data Figure 2

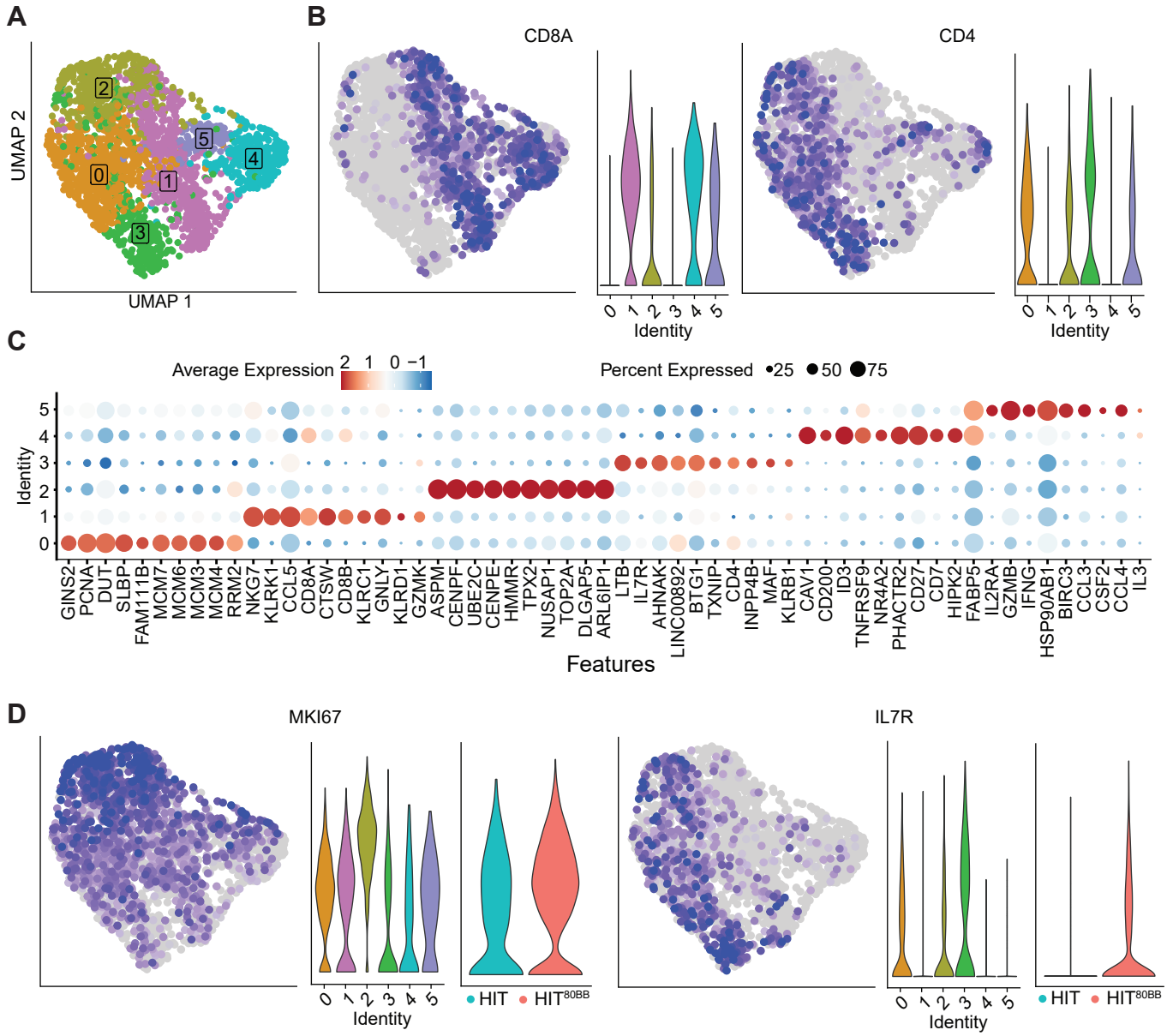

A, UMAP projection of 2591 cells isolated from bone marrow of NALM6 bearing mice nine days post HIT or HIT^{80BB} treatment. Cells are coloured based on Suerat assigned cluster identities. Clusters 0, 1, 2, 3 and 5 are composed of HIT^{80BB} cells. Cluster 4 is predominantly composed of HIT cells. **B,** Feature and violin plots of CD8A (left), CD4 (right) transcripts. **C,** Dot plot of top 10 differentially enriched genes in each cluster. Colour of dot indicates expression level, and size of dot indicated percentage of cells expressing marker. **D,** Feature and violin plots of MKI67 (left), IL7R (right). For violin plots, cells are plotted segregated by cluster and by treatment type.

Extended Data Figure 3

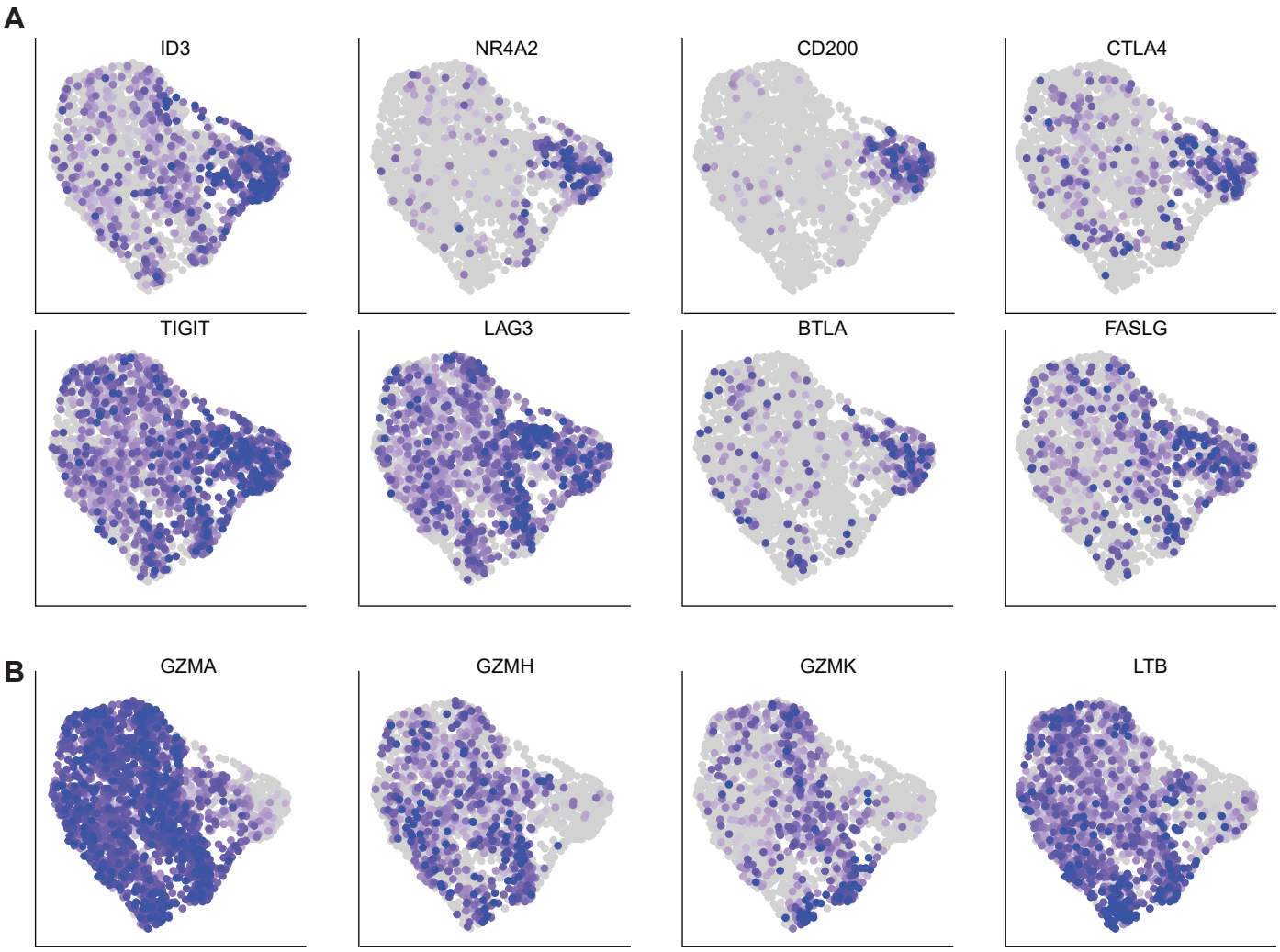

A, B Feature plots of inhibitory and exhaustion (**A**) and cytotoxicity (**B**) genes corresponding to violin plots in fig. 1K.

80BB directs both CD28 and 4-1BB costimulation

To determine whether 80BB acts through both the 4-1BB and CD28 co-stimulatory pathways, we investigated deletional mutants lacking the ability to engage either one. To validate the functionality of the 4-1BB moiety of 80BB, we compared HIT-cells expressing either 80BB (HIT^{80BB}), a truncated variant lacking the intracellular 4-1BB domain ($HIT^{\Delta CD80}$) or full-length CD80 ($HIT^{FL\text{-}CD80}$) *in vitro* and *in vivo*. All four molecules were well expressed at the T-cell surface (Ext. Data Fig. 4.4A). T-cells endowed with 80BB, ΔCD80 or FL-CD80 all produced increased levels of interleukin-2 (IL-2) upon exposure to antigen compared to HIT T-cells (Fig. 4.2A, left panel). However, secretion of IL-13, a cytokine more closely associated with 4-1BB signalling[170], was comparable between HIT, ΔCD80 and FL-CD80 and only increased in HIT^{80BB} T-cells, suggesting 4-1BB signaling (Fig. 4.2A, right panel). Further consistent with 4-1BB co-stimulation[91, 171], HIT^{80BB} cells exhibited greater basal, maximal, and spare respiratory capacity after three rounds of tumour stimulation relative to $HIT^{\Delta CD80}$ and $HIT^{FL\text{-}CD80}$ T-cells (Fig. 4.2B). $HIT^{\Delta CD80}$ and $HIT^{FL\text{-}CD80}$ cells also exhibited reduced glycolysis compared to cells endowed with full-length 80BB (Fig. 4.2B), highlighting the breadth of metabolic benefits endowed by 80BB. It is noteworthy that ΔCD80 or FL-CD80 still tended to display greater respiratory capacities and glycolytic rates compared to HIT alone, pointing to a 4-1BB-independent metabolic effect of 80BB dependent on its CD80 moiety engaging CD28. $HIT^{\Delta CD80}$ and $HIT^{FL\text{-}CD80}$ cells exhibited a reduced ability to control tumour growth in the NALM6 B-ALL mouse model compared to HIT^{80BB} T-cells, further confirming *in vivo* the activity of the 4-1BB moiety (Fig. 4.2C). T-cells expressing either ΔCD80 or FL-CD80 were more effective *in vivo* than control HIT T

Figure 4.2: 80BB provides dual 4-1BB and CD28 costimulation required for optimal anti-tumour function

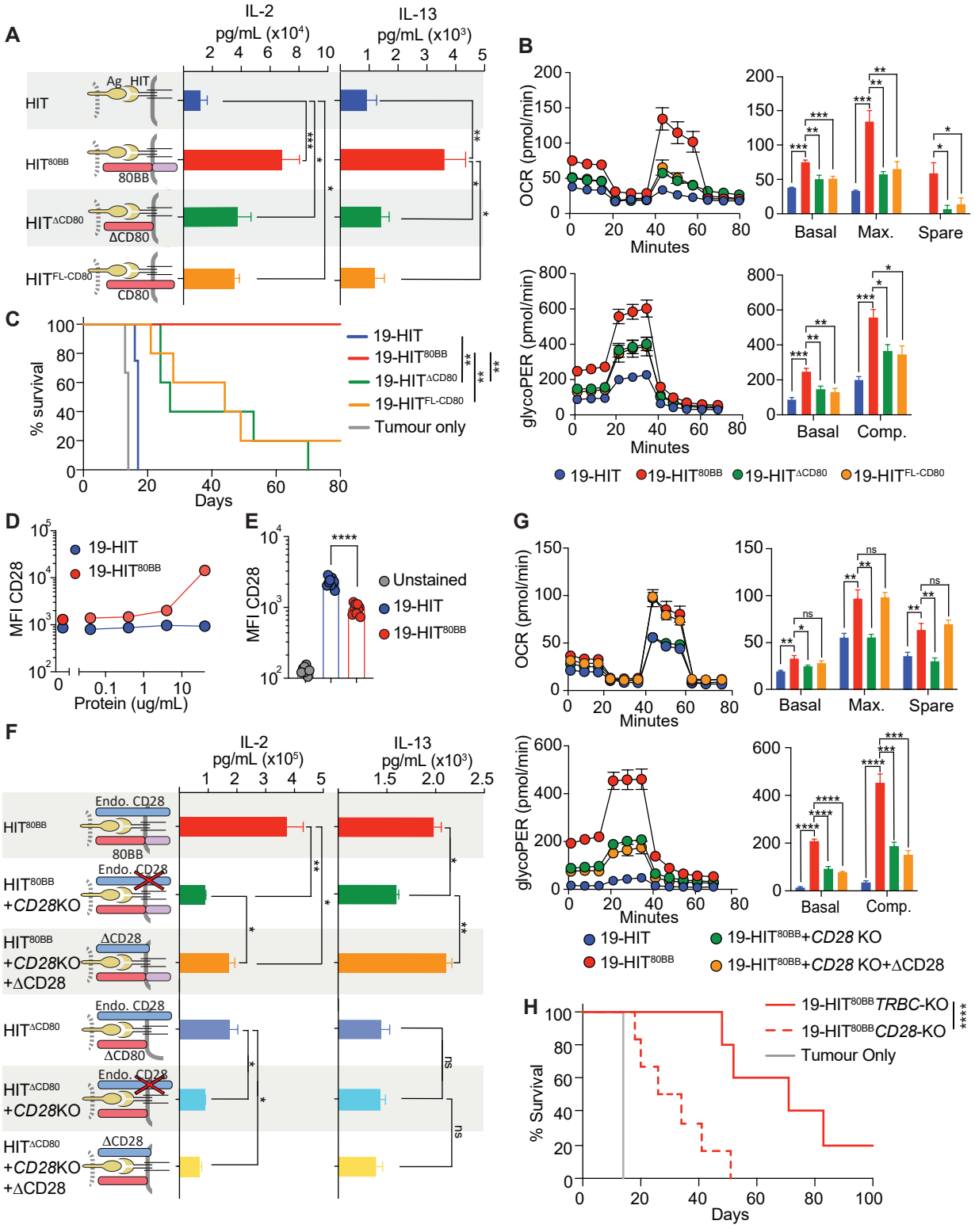

A, Left, diagrams depicting 19-HIT, 19-HIT^{80BB}, 19-HIT expressing CD80 lacking the intracellular domain (19-HIT$^{\Delta CD80}$) and 19-HIT expressing full-length CD80 (HIT$^{FL\text{-}CD80}$). Right**,** human IL-2 and IL-13 supernatant concentration 24 h post co-culture with NALM6 target cells at E:T ratio of 1:2. n= 13 for 19-HIT, 19-HIT^{80BB}, and 19-HIT$^{\Delta CD80}$; n=4 for 19-HIT$^{FL\text{-}CD80}$. **B,** Mitochondrial stress (top) and glycolytic rate (bottom) Seahorse assays were performed after 3 rounds of stimulation with NALM6 cells. Data are representative of 3 donors. **C,** Kaplan–Meier survival analysis of NALM6-bearing mice treated with 1x10^5 19-HIT, 19-HIT^{80BB}, 19-HIT$^{FL\text{-}CD80}$ or 19-HIT$^{\Delta CD80}$ T cells (n=5 mice/group). **D,** Human CD28-Fc binding assay. T cells were incubated with increasing concentrations of CD28-Fc and then stained with PE-anti-Fc. Data are representative of 2 donors. **E,** MFI of CD28 surface staining 4 days after 19-HIT and 19-HIT^{80BB} transduction. **F,** Left, diagrams depicting 19-HIT^{80BB}, 19-HIT^{80BB} + *CD28* KO, 19-HIT^{80BB} + *CD28* KO transduced with CD28 lacking the intracellular domain (ΔCD28; HIT^{80BB} + *CD28* KO+ΔCD28), HIT$^{\Delta CD80,}$ HIT$^{\Delta CD80}$+*CD28* KO and HIT$^{\Delta CD80}$+ ΔCD28. Right, human IL-2 and IL-13 supernatant concentration 24 h post co-culture with NALM6 target cells at E:T ratio of 1:2. Data are representative of 3 donors. **G,** Mitochondrial stress (top) and glycolytic rate (bottom) Seahorse assays performed after 3 rounds of cell stimulation with NALM6. Data are representative of 3 donors. **H,** Kaplan–Meier survival analysis of NALM6-bearing mice treated with 1x10^5 19-HIT^{80BB} with KO-*TRBC* (control, n =5 mice) or KO-*CD28* (n=6 mice). *P* values were determined by Mann Whitney test (**A**), two-tailed t-test **(B, E, G, F),** or log-rank Mantel-Cox test **(C, H)**. Data are mean sem. * p<0.05, ** p<0.01, *** p<0.001, **** P<0.0001.

cells, corroborating the *in vitro* findings showing that 80BB support of T-cell function extends beyond its 4-1BB function.

To establish the nature of this additional effect, we first confirmed that 80BB could bind to CD28, which we established by incubating 80BB expressing T-cells with Fc-tagged CD28 protein (Fig. 4.2D, Ext. Data Fig. 4.4B). T-cells expressing 80BB also showed decreased cell surface expression of endogenous CD28 (Fig. 4.2E), consistent with its masking or internalization upon ligation to CD80. CD28 engagement was further supported by measuring decreased antigen-induced IL-2 secretion by HIT^{80BB} T-cells when the endogenous *CD28* was ablated by CRISPR/Cas9 (Fig. 4.2F, Ext. Data Fig. 4.4C). Re-expression of a non-signaling, truncated ΔCD28 (Ext. Data Fig. 4.2D) in CD28 knock-out ($CD28^{KO}$) cells did not fully restore IL-2 secretion (Fig. 4.2F). Conversely, IL-13 secretion, which was also decreased in the absence of CD28, was fully restored upon ΔCD28 expression (Fig. 4.2F), indicating that maximal IL-13 secretion depended on 80BB binding to CD28 but not CD28 signaling. This is consistent with CD28 directly activating downstream IL-2 secretion and indirectly promoting IL-13 secretion by serving as an agonistic ligand for 80BB. Thus, CD28 and 80BB not only interact but serve as reciprocal activating ligands. $HIT^{\Delta CD80}$ cells, which lack the 4-1BB signalling domain, do not exhibit increased IL-2 or IL-13 restoration upon ΔCD28 expression, further agreeing with the need for both CD28 and 80BB-dependent 4-1BB functions to uphold both cytokines' secretion (Fig. 4.2F).

The metabolic contribution of endogenous CD28 was further investigated in *CD28*-edited T-cells. *CD28* disruption resulted in decreased metabolic respiration and glycolytic rates in HIT^{80BB} cells (Fig. 4.2G). Expression of ΔCD28 in *CD28*-edited cells led to an

Extended Data Figure 4.4

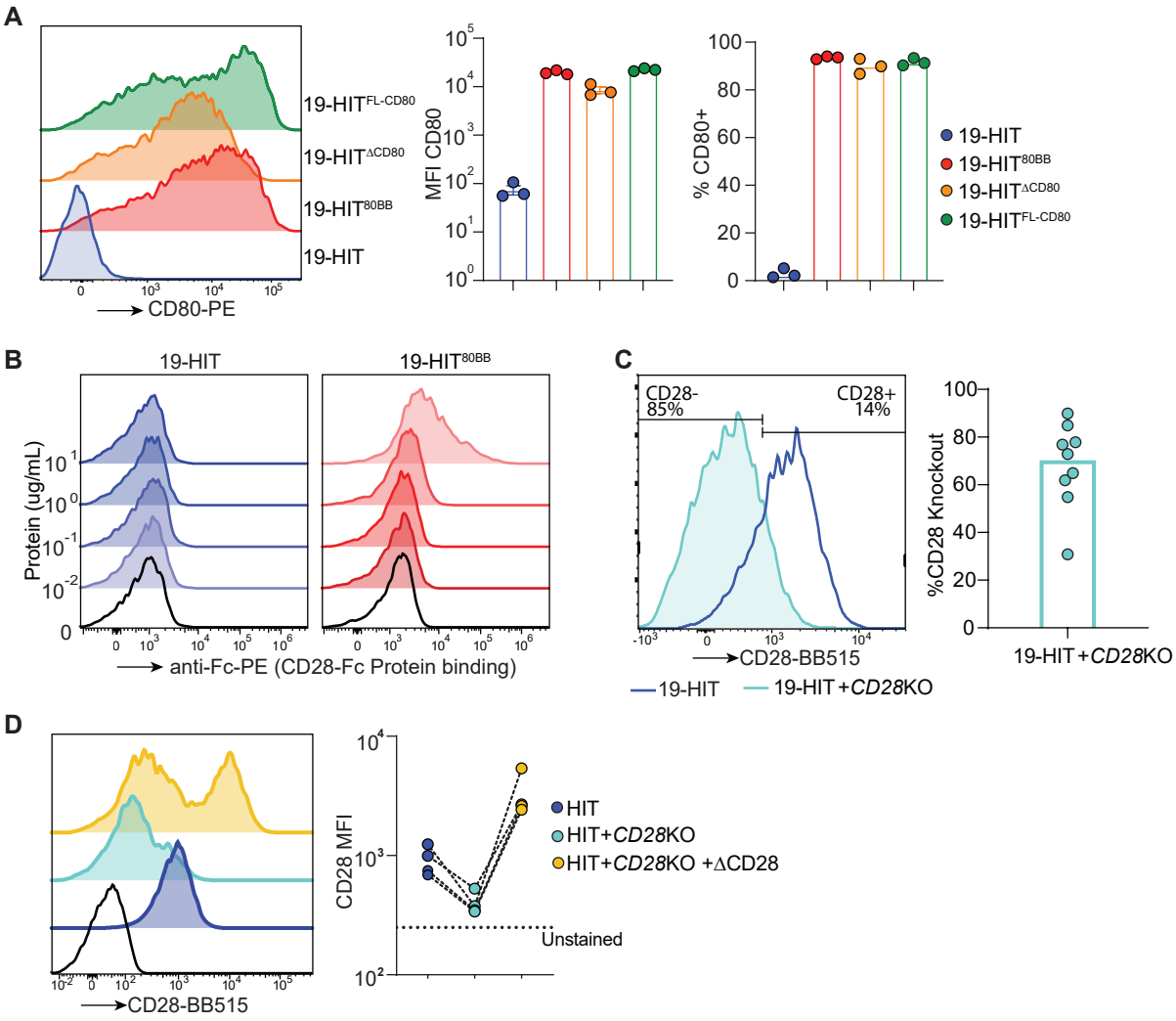

A, Left, representative flow cytometry profiles of HIT, HIT^{80BB}, HIT$^{\Delta CD80}$ and HIT$^{FL\text{-}CD80}$ stained for CD80. Representative of 4 independent donors. Right, summary of CD80 MFI and percentage from 3 independent donors analyzed at same flow cytometry settings. **B**, Flow cytometry plots of CD28-Fc binding assay. T cells were incubated with increasing concentrations of CD28-Fc, and then stained with PE-anti-Fc. **C,** Left, representative flow cytometry plot of HIT and HIT *CD28KO* cells 5 days post CRISPR Cas9 editing. Right, summary of decrease of CD28 surface expression indicating *CD28* knockout in 9 donors. **D**, Left, flow cytometry plot of unstained cells (black), HIT *TRBC* KO (blue), HIT *CD28* KO cells (green) and HIT *CD28* KO ΔCD28 cells (orange). Right, summary of CD28 MFI after CD28*Δ* overexpression in HIT cells. Each dot is an independent donor.

increase in mitochondrial fitness, but no significant effect on glycolytic rate, consistent with previous reports on the metabolic effects of CD28 and 4-1BB co-stimulation[171, 172] (Fig. 4.2G). To evaluate the relevance of endogenous CD28 for *in vivo* therapeutic efficacy, we treated NALM6-bearing NSG mice with HIT^{80BB}, in which endogenous *CD28* was either intact or edited (Ext. Data Fig 4.4C). HIT^{80BB} T-cells performed significantly less well when *CD28* was edited, confirming the dependence of HIT^{80BB} on endogenous CD28 for maximal T-cell activity (Fig. 4.2H).

CTLA4 is an alternate agonist ligand for 80BB

Since the *CD28* KO did not completely abrogate anti-tumour efficacy in (Fig. 4.2F-H), we investigated whether CTLA4, an alternate CD80 ligand could serve as an 80BB agonist. If so, 80BB could then serve as a switch receptor, interacting with the negative regulator CTLA4 to produce an agonistic 4-1BB signal. Incubation of HIT^{80BB} T-cells with soluble Fc-tagged CTLA4 confirmed CTLA4 binding (Fig. 4.3A, Ext. Data Fig. 4.5A), with greater intensity and at lower protein concentrations than binding to CD28 (Fig. 4.2D vs. 4.3A). As CTLA4 is largely confined to intracellular compartment and is only transiently expressed at the cell surface following T-cell activation, we generated a truncated form of CTLA4 (ΔCTLA4) known to constitutively traffic to the cytoplasmic membrane[173]. Following the double transduction of ΔCTLA4 and 80BB encoded by two separate vectors, we observed an inverse correlation between CD80 and ΔCTLA4 cell surface staining intensities (Fig. 4.3B), consistent with the excess ΔCTLA4 precluding the detection of cell surface CD80.

To assess the functional consequences of CTLA4 binding to 80BB, we first overexpressed ΔCTLA4 and measured IL-2 and IL-13 secretion. HIT^{80BB} cells

Figure 4.3: CTLA4 binding to 80BB enhances HIT T cell anti-tumour function

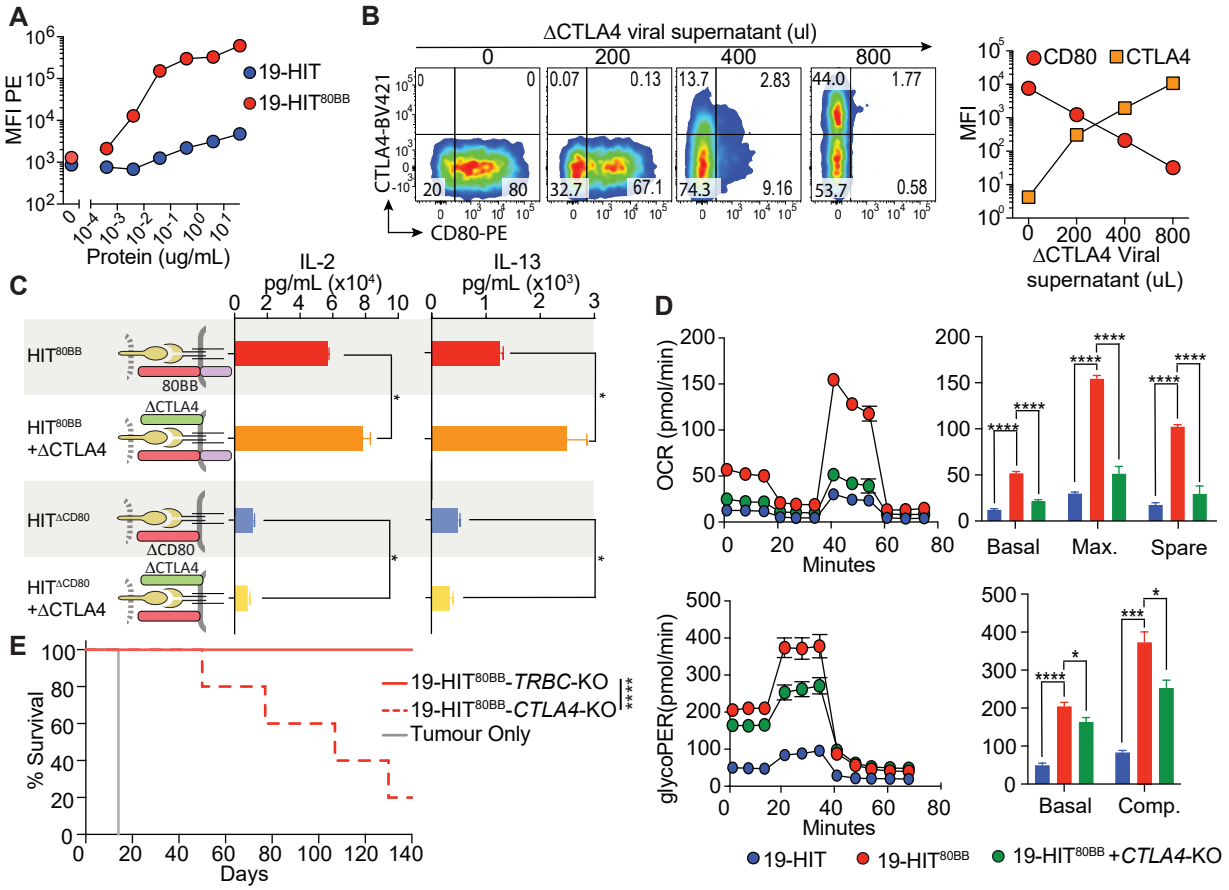

A, Human CTLA4-Fc binding assay. T cells were incubated with increasing concentrations of CTLA4-Fc and then stained with PE-anti-Fc. Data are representative of 2 donors. **B,** flow cytometry profile of CD80 and CTLA4 surface expression. T cells co-transduced with stable amount of viral supernatant encoding for 80BB and a gradient of viral supernatant encoding for truncated CTLA-4 lacking its intracellular domain (ΔCTLA4). Right, MFI of CD80 and CTLA4 surface detection. MFI quantified in right panel. Data are representative of 3 donors**. C**, Diagram depicting 19-HIT^{80BB}, 19-HIT^{80BB} transduced with ΔCTLA4 (HIT^{80BB}+ΔCTLA4), 19-HIT$^{\Delta CD80}$ and HIT$^{\Delta CD80}$+ΔCTLA4. Human IL-2 and IL-13 supernatant concentration 24 h post co-culture with NALM6 target cells at E:T ratio of 1:2. Data are representative of 3 donors. **D,** Mitochondrial stress (top) and glycolytic rate (bottom) Seahorse assays were performed after 3 rounds of cell stimulation with NALM6 target cells. Data are representative of 3 donors. **E**, Kaplan–Meier survival analysis of NALM6-bearing mice treated with 1x10^5 19-HIT^{80BB} with KO *TRBC* (control) or KO *CTLA4* (n=5 mice/group). *P* values were determined by two-tailed t-test (**C**) or log-rank Mantel-Cox test **(E)**. Data are mean ± sem. * p<0.05, ** p<0.01, *** p<0.001, **** P<0.0001.

Extended Data Figure 4.5

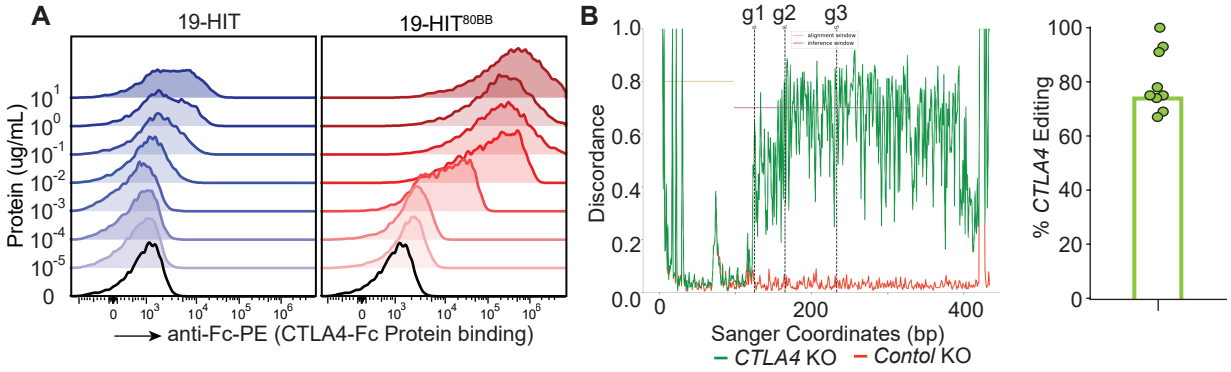

A, Flow cytometry plots of CTLA4-Fc binding assay. Cells were incubated with increasing concentrations of CTLA4-Fc, and then stained with PE-anti-Fc. **B**, Left, trace from inference of CRISPR Edits (ICE) tool (Synthego) highlighting extent of *CTLA4* knockout. Right, summary of extent of *CTLA4* editing indicating *CTLA4* knockout evaluated by ICE from 9 donors.

expressing ΔCTLA4 significantly increased IL-2 and IL-13 secretion, consistent with an agonistic effect of CTLA4 binding to 80BB (Fig. 4.3C). HIT$^{\Delta CD80}$ did not show an increase in IL-2 or IL-13 secretion upon ΔCTLA4 overexpression, confirming the role of intracellular 4-1BB domain in their induction. To establish whether endogenous CTLA4 contributes to 80BB overall activity, we ablated *CTLA4* and assessed the metabolic consequences in HIT^{80BB} cells (Fig. 4.3D, Ext. Data Fig. 4.5B). *CTLA4*-edited HIT^{80BB} cells exhibited decreased respiratory and glycolytic capacities, although still elevated over HIT T-cells (Fig. 4.3D). We further evaluated the contribution of endogenous *CTLA4* on 80BB function *in vivo* by treating NALM6-bearing mice with T-cells in which the endogenous *CTLA4* was either intact or edited (Ext. Data Fig. 4.5B). Tumour elimination was substantially reduced in mice treated with *CTLA4*-edited HIT^{80BB} cells (Fig. 4.3E), confirming the agonistic role of CTLA4 in increasing HIT^{80BB} T-cell potency.

80BB enhances both HIT and TCR-mediated tumour rejection

Having hitherto focused on CD19 HIT T-cells in the well-established NALM6 leukemia model, we sought to expand the spectrum of therapeutic contexts in which 80BB may be useful. We first examined whether 80BB could sustain the therapeutic potency of antigen-targeted HIT T-cells in the context of low target antigen density. Targeting NALM6 variants respectively expressing 2000 or 200 CD19 molecules per cell and administering low HIT T-cell doses ($1x10^5$ and $4x10^5$/mouse, respectively), we found that 80BB expression enhanced tumour elimination in both instances (Fig. 4.4A). We next investigated the activity of 80BB in TCR engineered T-cells. We transduced an NY-ESO-1-specific, HLA-A0201-restricted TCR (Fig. 4.4B), targeting it to the *TRAC* locus,

Figure 4.4: 80BB enhances control of tumours with antigen-low densities and disseminated melanomas

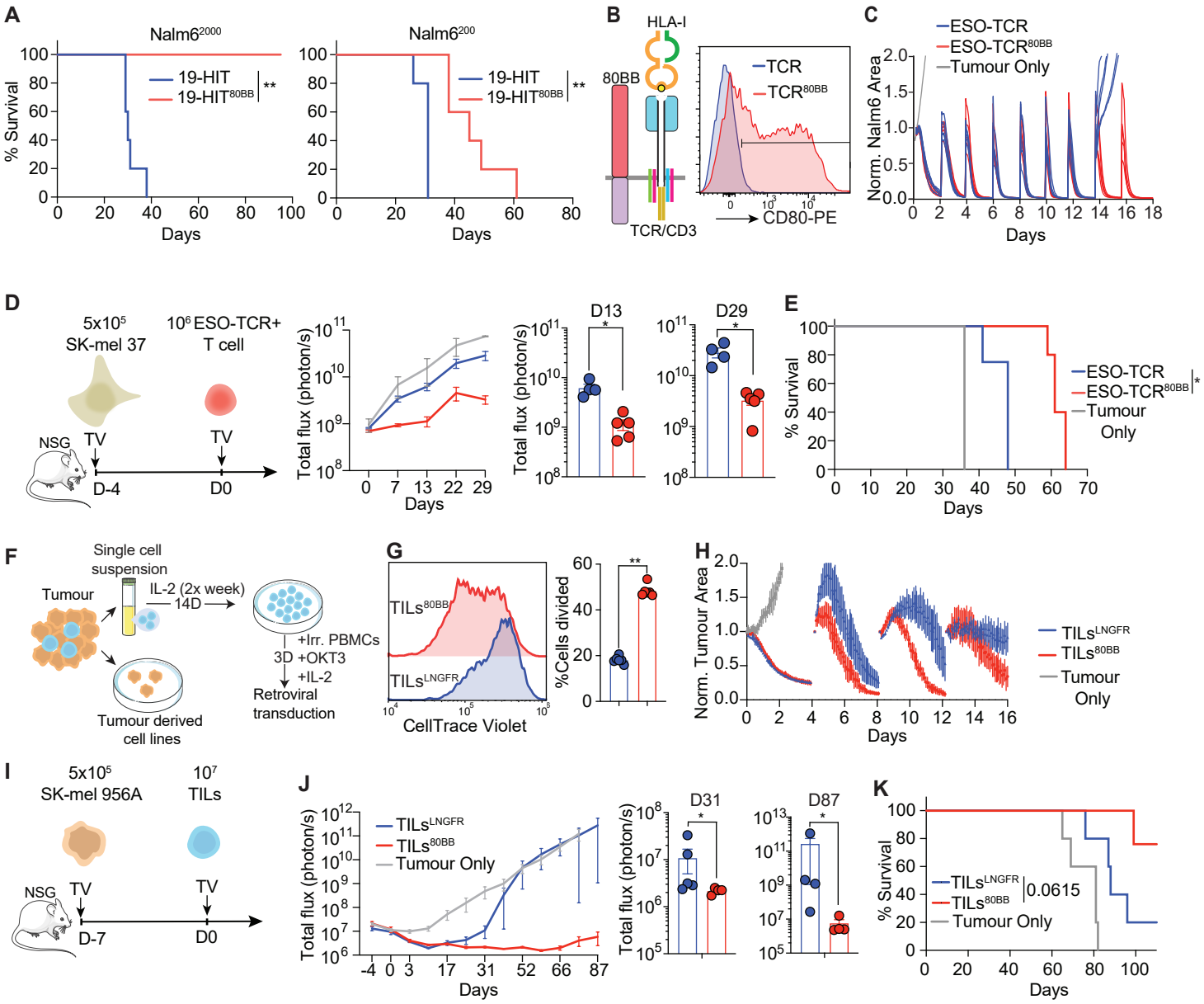

A, Kaplan–Meier survival analysis of NALM6^{2000} (2000 CD19 mol/cell, left) or NALM6^{200} (200 CD19 mol/cell, right) -bearing mice treated with 1x10^5 (left) or 4x10^5 (right); respectively, 19-HIT+ T-cells. n=5 mice/group. **B,** Left**,** diagram of TCR-endowed cell expressing 80BB. Right, representative flow cytometry plot of CD80 expression on NY-ESO-1-TCR+ T-cells. Data are representative of 6 donors. **C,** Serial in vitro cytotoxicity assay of NY-ESO-1-TCR+ T-cells co-cultured with fresh NALM6 cells added every 2 days. Each line represents a technical replicate. **D,** Left, diagram depicting in vivo treatment of SK-Mel37 (HLA.A2.1-NYESO-1+)-bearing mice with NY-ESO-1 TCR+ T cells. Right**,** Tumour burden was monitored using bioluminescence imaging (total flux); tumour burden at days 13 and 29 post T cell injection is shown. **E,** Kaplan–Meier survival analysis of mice bearing disseminated SK-Mel-37 treated with 1x10^6 NY-ESO-1 TCR or NY-ESO-1 TCR^{80BB} (n=5 mice/group for NY-ESO-1 TCR and n=4 mice/group for NY-ESO-1 TCR^{80BB}). **F**, Diagram of TIL rapid expansion protocol and retrovirus transduction with LNGFR (control, TILs^{LNGFR}) or 80BB (TILs^{80BB}). **G,** flow cytometry profile (left) and quantification (right) of CellTrace violet labeled TILs 5 days post-stimulation with autologous patient-derived tumour (SK-Mel-956A). **H,** Serial in vitro cytotoxicity assay with fresh SK-Mel-956A cells added every 4 days to the culture. **I,** Diagram depicting *in vivo* treatment of SK-Mel-956A-FFluc-bearing mice with 1x10^7 TILs^{LNGFR} or TILs^{80BB}. **J, K,** SK-Mel-956A-FFluc-bearing mice treated with 10^7 TILs^{LNGFR} or TILs^{80BB} (n=5 mice/group for TILs^{LNGFR} and n= 4 mice/group for TILs^{80BB}). **J**, Tumour burden monitored using bioluminescence image (total flux). Tumour burden at days 31 and 87 post T cell injection is shown. **K**, Kaplan–Meier survival analysis. *P* values were determined by log-rank Mantel-Cox test (**A, E, K**), or Mann Whitney test (**D, G, J**). Data are mean ± sem. * p<0.05, ** p<0.01, *** p<0.001, **** P<0.0001

along with the CD8α and CD8β coreceptors, with or without 80BB (Ext. Data Fig 4.6A). Similar to its effect in HIT T-cells, 80BB enhanced the ability of NY-ESO-1 specific T-cells to control tumour in a serial cytotoxicity assays (Fig. 4.4C). We further confirmed the therapeutic benefits of 80BB in an *in vivo* disseminated melanoma model using HLA-A0201+/NY-ESO-1+ SK-Mel-37 melanoma cells. We found that 80BB transduced NY-ESO-1-targeted T-cells expression significantly controlled tumour at early time points and delayed tumour growth (Fig. 4.4D). Mouse survival was significantly improved but did not achieve long-term remissions (Fig. 4.4E), which may be due to HLA down-regulation *in vivo* (Ext. Data. Fig. 4.6B), a phenomenon previously observed in clinical and pre-clinical studies[37].

Since the efficacy of single TCR targeting may be limited in solid tumours, the latter finding prompted us to explore whether 80BB could boost the function of not-otherwise engineered T-cells expressing their endogenous TCRs. Adoptive transfer of *ex vivo* expanded tumour-infiltrating lymphocytes is a promising cellular therapy in metastatic melanoma[31]; thus, we examined whether 80BB could enhance the function of polyclonal T-cells harbouring their endogenous TCR in a pre-clinical tumor model. We thus expanded T-cells from a metastatic melanoma specimen resected from a patient with no prior systemic therapy, using a rapid expansion protocol (REP) and transduced them 3 days after OKT3 activation with either 80BB or a control vector encoding LNGFR (Fig. 4.4F). We verified that these REP-expanded tumour-infiltrating lymphocytes (TILs) expressed CD28 and were effectively transduced (Ext. Data Fig. 4.6C, D). These TIL^{80BB} were lytic against autologous melanoma and showed increased expansion over 5 days following exposure to autologous tumour stimulation (Fig. 4.4G, Ext. Data Fig. 4.6E). In an *in*

Extended Data Figure 4.6

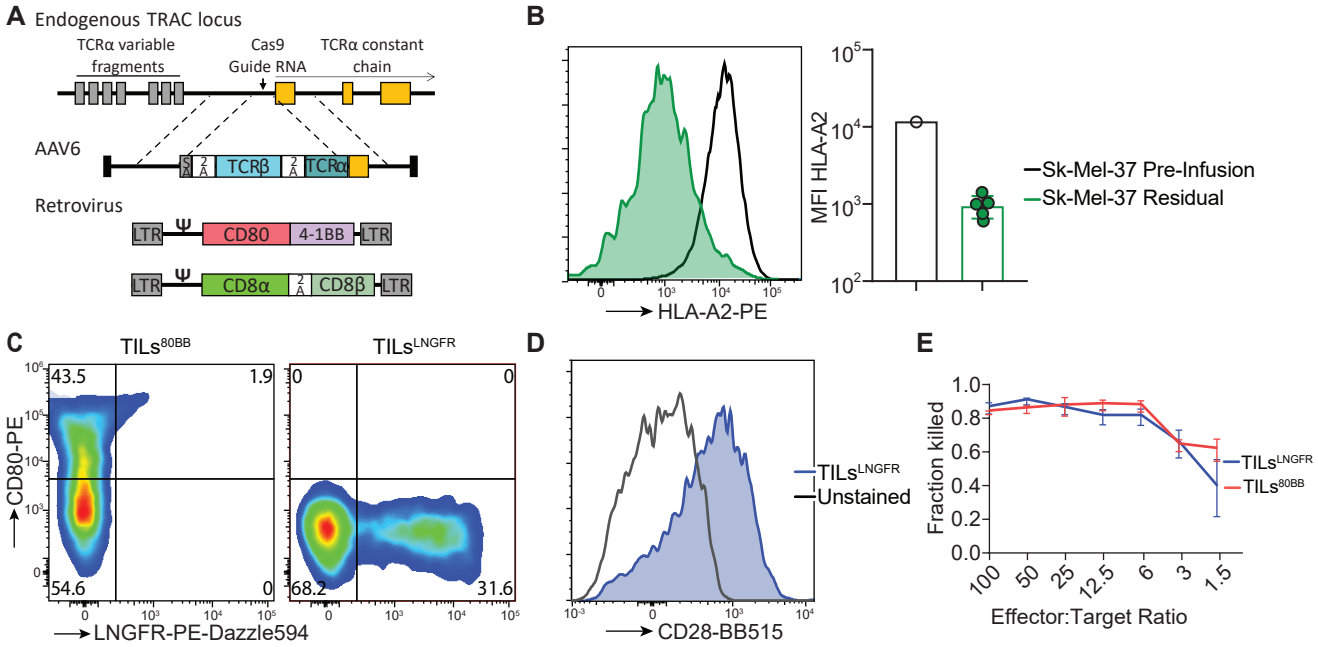

A, Diagram depicting TCR T-cell engineering. The alpha and beta chains of an NY-ESO-1 directed TCR were targeted into the *TRAC* locus as previously described[34]. 80BB and CD8α-P2A-CD8β constructs were delivered using the gamma retroviral vector SFG. **B**, Left, flow profile of HLA-A2 surface expression on SK-Mel-37 cells isolated from mice or from *in vitro* culture. Data pooled from 5 mice. Right, quantification of HLA-A2 MFI, each dot represents one mouse. **C**, Flow profile of transduced TILs transduced for 80BB (left) and LNGFR (right). **D,** Flow profile of post-rapid expansion protocol TIL^{LNGFR} cells stained for CD28 expression. **E**, Fraction of cells killed after 18hrs of co-culture of transduced TILs and autologous tumour cells.

vitro repetitive challenge experiment with autologous tumour, TIL^{80BB} and TIL^{LNGFR} showed comparable tumour lysis at the first tumour challenge, but $TILs^{80BB}$ exhibited greater cytolytic potential in subsequent rechallenges (Fig. 4.4H). In an *in vivo* autologous tumour xenograft model, TIL^{80BB} provided superior survival compared to TIL^{LNGFR}, which only achieved a transient early response (Fig. 4.4I, J and K). In summary, our studies support the effectiveness and usefulness of expressing 80BB to support the function of T-cells engaging their target through CD3-dependent receptors for antigen, including HIT and TCR engineered T-cells.

Discussion

We demonstrate, in several tumour models, the therapeutic benefit of expressing 80BB in HIT or TCR-engineered T-cells. 80BB is a novel chimeric molecule capable of activating both CD28 and 4-1BB costimulatory pathways. It acts as an agonist for endogenous CD28 and provides a 4-1BB effect upon binding to either CD28 or CTLA4. HIT^{80BB} cells consistently showed robust T-cell expansion while maintaining improved T-cell metabolic fitness and tumour lysis capabilities. *In vivo,* HIT^{80BB} showed long-term tumour control at stress-level doses of T-cells, which HIT T-cells lacking 80BB could not achieve. We found increased HIT^{80BB} accumulation in the bone marrow of leukemic mice at day 9, accompanied by lesser expression of inhibitory markers and transcription factors associated with T-cell dysfunction (Fig. 4.1)[168, 169, 174]. Our studies underscore the benefit of co-expressing 80BB with an NY-ESO-1 specific TCR to control a systemic melanoma in immunodeficient mice. T-cell potentiation was also obtained in polyclonal TILs of a melanoma patient, resulting in improved control of autologous melanoma (Fig 4.4). While we only investigated 80BB with TCR or HIT T-cells, we anticipate that 80BB will

in principle enhance the potency of any of the CD3-dependent CARs recently published[129, 175-179]. Overall, our findings underscore the efficacy and versatility of the 80BB molecule.

Based on protein binding assays, genetic ablation, and over-expression studies, we established that 80BB has the ability to bind to CD28 and CTLA4 whereupon it mimics 4-1BB co-stimulation as reflected in cytokine secretion, metabolic fitness, and enhanced tumour elimination (Fig. 4.2). As 80BB can interact with CD28, which is constitutively expressed in early differentiated T-cells, and CTLA4, which is transiently expressed upon T-cell activation and is enriched in terminal effector and exhausted T-cells[174], 80BB has the potential to support T-cell function at different stages of T-cell differentiation. Our studies in the NALM6 model demonstrate that 80BB-mediated enhancement of tumour rejection does not require the expression of 80BB ligands by the targeted tumour cell.

Various synthetic engineering approaches have been previously developed to support the survival or function of natural or TCR-engineered T-cells, some of which aimed to provide costimulatory support to T-cells. Chimeric co-stimulatory receptors allow for tumour-antigen (G_{D2}, CD19, or FOLR1) induced delivery of costimulation[35, 123, 180]. Unlike 80BB, CCRs are dependent on antigen expression by tumour cells. TCR-engineered T-cells may be protected from TGFβ inhibition or Fas-mediated apoptosis by dominant-negative receptors[181, 182]; these receptors abate inhibitory signals but do not deliver agonistic co-stimulation. The fusion of a co-stimulatory signalling motif to a dominant negative receptor or an inhibitory receptor, such as CD200R, Fas, TGFß-R2 or PD-1 can protect from inhibition and further provide supportive co-stimulation leading to more functional T-cells in preclinical models[125, 127, 183, 184]. These switch receptors require

expression of their specific ligands in the tumour microenvironment to deliver their costimulatory signal. The incorporation of costimulatory domains directly into TCR α or β chains has also been attempted. In preclinical models with conventional TCRs, such fusions have resulted in decreased antigen sensitivity[130, 132]. In conjunction with the STAR receptor, however, fusing the OX40 signaling domain to TCR α and β chains suggested enhanced tumour control in murine models and has yielded promising early results in a small cohort of B-ALL patients[185]. Nonetheless, the degree to which chimeric TCR α and β chains augment T-cell potency remains to be elucidated.

Clinically investigated strategies to enhance the efficacy of TCR-directed T-cells are overall confined to TILs, which are typically dependant on exogenous IL-2 for their engraftment and persistence[31]. As multiple approaches to support T-cells with systemically active cytokines or co-stimulatory agonist antibodies have led to toxicities[31, 87, 186], efforts increasingly focus on T-cell engineering approaches that may be more effective and less toxic. TILs constitutively expressing IL-2 or IL-12 have to date led to limited therapeutic success [33, 34]. Clinical trials to evaluate TCR or chimeric TCR engineered cells or TILs either lacking PD-1[149, 187], co-expressing a CCR[35] or a switch receptor[188] have been recently initiated.

80BB further extends the tools available to support adoptive cell therapies that rely on TCR or chimeric TCR molecules for tumour recognition[37, 42, 189] as an alternative approach to provide T-cell-restricted, antigen-independent costimulatory support. No safety signals such as weight loss, tumour-independent T-cell proliferation or increased rates of GvHD, were observed in mice treated with 80BB-endowed T-cells in either HIT, TCR or TIL settings. 80BB will be especially useful to support HIT T-cells, which are

capable of detecting lower antigen levels than current CARs and are thus poised to reduce antigen-low relapses. The small size of the 80BB cDNA makes it an easy tool to incorporate in a variety of genetic engineering strategies to further expand the efficacy and scope of T-cell therapies.

Extended Thoughts: Safety

Increased T-cell function has been illustrated to lead to increased toxicities, which can largely be grouped into two categories – tumour response dependant toxicities and tumour-response independent toxicities. The first group would include CRS and ICANS, two adverse effects associated with CAR therapies[190, 191], while the second group would include toxicities associated with off-target T-cell stimulation or co-stimulation[192]. This molecule could hypothetically have both types of toxicities, and thus will need to be thoroughly investigated prior to patient use.

As the first set of toxicities will be similar to those induced by CARs, similar models can be used to evaluate their likelihood and treatment strategies. Taking advantage of *nod scid* mice, which have more functional monocytes and macrophages compared to NSG mice, CAR T-cell induced CRS has been modelled in our lab, and similar models can be evaluate 19-HIT^{80BB} safety. These studies can be performed with human T-cells, interacting with human tumours, which precludes species differences as confounders.

A second set of toxicities could hypothetically be caused by non-specific co-stimulation provided by 80BB to other T-cells in trans. As discussed in the introduction, the requirement for co-stimulation is believed to be a key mechanism of limiting off-target T-cell activation, and it is possible that T-cells endowed with 80BB will non-specifically deliver co-stimulation to by-stander T-cells. Human and mouse T-cells have key differences, especially in regards to CD28

expression and co-stimulation[193]. Therefore, the ideal model to evaluate these safety concerns would be a mouse with a fully human immune system, engrafted with human T-cells that have been matured in the mouse and are fully function inside the mouse alongside a fully human immune system. Upon delivery of therapeutic T-cells endowed with 80BB one can then evaluate whether any increased activation is observed in the bystander T-cells (or other immune cells) and whether any toxicity is observed.

While there are some models that allow for the development of a human immune system inside a mouse, these models are cumbersome to work with and involve the implantation of human fetal bone marrow, thymic and liver tissue[194]. Pilot studies can be performed on mouse T-cells in an immune-competent mouse model. While limited by mouse-human differences, these models would still allow for the evaluation of by-stander T-cell activation and could highlight safety issues that need to be addressed.

If safety issues are identified, the 80BB molecule would need to be further engineered. If CRS or ICANNS issues are identified, one can dampen the signalling by mutating key residues of 80BB or by decreasing the affinity of the CD80 domain to CD28 and/or CTLA-4. Alternatively, if 80BB T-cells lead to non-specific by-stander activation, 80BB can be mutated to exhibit decreased surface expression, such as by the addition of CTLA4 intracellular retention domains or through careful promoter engineering which would presumably decrease the likelihood of *trans* interactions.

Chapter 5 - Conclusions and Future Directions

This thesis evaluated various strategies to deliver co-stimulation to TCR T-cells in a target-independent manner. Initial studies focused on whether the addition of CD28 co-stimulation directly onto the TCR/CD3 complex would lead to improved T-cell efficacy in tumour models. While there was some evidence of improved activity *in vitro*, this did not translate to better anti-tumour efficacy *in vivo.* This led to the development of a novel fusion protein that is orthogonal to the TCR, and simultaneously drives both the 4-1BB and CD28 pathways.

This "80BB" molecule led to improved T-cell efficacy *in vitro* and *in vivo*, using fresh healthy-donor isolated T-cells and TILs. T-cells endowed with 80BB were illustrated to have improved proliferative capacity, repetitive cytotoxicity function and improved glycolytic and mitochondrial metabolism after stimulation compared to T-cells without additional co-stimulation. Studies on T-cells isolated from the bone marrows of treated mice highlighted that T-cells endowed with 80BB accumulated to a higher degree *in vivo* and expressed lower levels of activation/exhaustion markers. Having verified the therapeutic benefits of 80BB, this thesis characterized the interaction network of 80BB, and confirmed its dependence on both CD28 and its own 4-1BB intracellular motif to deliver co-stimulation. Furthermore, 80BB was illustrated to interact with both CD28 and CTLA-4, allowing it to drive both target independent co-stimulation and to act as a *switch* receptor upon interaction with CTLA-4. Finally, as 80BB acts in a target agnostic manner, it was shown that patient TILs with polyclonal TCRs can also be endowed with

80BB as part of a rapid expansion protocol (REP), leading to improved anti-tumour efficacy *in vitro* and *in vivo.*

Future Directions

The TCR/CD3 fusion experiments highlighted that the fusion of CD28 onto the TCR or CD3 chains is feasible, and leads to increased IL-2 secretion, suggestive of successful co-stimulation delivery. The lack of *in vivo* benefit can be attributed to either insufficient co-stimulation or to possible modeling limitations. While CD28 is a highly potent co-stimulatory molecule, its possible that its association with the membrane limits its utility when expressed in this context. Future directions would evaluate the use of other well studied co-stimulatory proteins, such as 4-1BB and ICOS, which may be more functional in this format. An alternative strategy would be to mutate key Arginine residues in the CD28 intracellular motif and evaluate whether the mutants are able to lead to improved co-stimulatory function[195].

Another future direction would be to evaluate whether the co-stimulation leads to a more prominent *in vivo* benefit in an immune replete model. This study took advantage of NSG mice to model human tumours and human T-cell anti-tumour responses without the additional confounding effects of a functional mouse immune system that could exert both anti-T-cells effects and anti tumour effects. Conversely, it is possible the lack of complete immune system, especially NK cells, which are known to serve a role in enforcing HLA expression, may be allowing the tumour to down regulate its HLA, to escape T-cell mediated control. This possibility is highlighted by the observed increased T-cell accumulation in co-receptor matched TCR models, without an observed

antitumour function. The relatively modest benefit of the 80BB molecule when endowed onto TCR T-cells compared to its drastic benefits when co-endowed with a 19-HIT receptor further could be explained by possible modelling limitations.

This would suggest that studies with mice that allow for NK cell function may lead to more robust findings. Multiple mouse models with exogenous human IL-15 expression have been developed to allow for human NK cell function in transgenic animals[196-198]. The use of such a model and the co-injection of human NK cells alongside the human engineered T-cells could prevent transient downregulation of HLA from potentially confounding the observes results.

T-cells endowed with 80BB exhibited a well studied increase in potency. The expression of co-stimulatory molecules has been illustrated to have a role in the function of by-stander T-cells, and it is likely that 80BB would illustrate such an effect if tested in an appropriate model. This could be modelled in models of mixed T-cells targeting different antigens on the same tumour with a subset endowed with 80BB. T-cell counts and their phenotypes could be evaluating for evidence of *trans* co-stimulation. A fully murine model, recapitulating the full immune system would further allow the measurement of whether 80BB is able to overcome tumour micro-environment inhibition, including Tregs mediate inhibition. The findings that T-cell intrinsic CTLA-4 is able to lead to positive co-stimulation in T-cells endowed with 80BB, lead to the hypothesis that 80BB would similarly convert inhibitory Treg-derived CTLA-4 signals into positive costimulation. In a mouse model that fully recapitulates the immune system, one can also evaluate whether 80BB endowed T-cells are able to drive the recruitment of additional immune effector cells and lead to antigen spreading.

Tumour infiltrating lymphocytes (TILs) are a powerful anti-cancer tool, composed of T-cells with many specifies. This thesis illustrated that TILs endowed with 80BB exhibited improved anti-tumour efficacy *in vitro* and *in vivo* compared to mock transduced TILs. Further work is needed to more thoroughly characterize the extend of the benefits. In primary T-cells, 80BB led to increased proliferation in response to stimulation, increased glycolytic and metabolic rates, increased cytokine secretion and decreased expression of exhaustion-associated cell markers. These findings should be confirmed in TILs as well. Furthermore, as TILs are a polyclonal population, it would be possible to evaluate whether 80BB specifically augments the efficacy of any specific sub-population, which can be detected by evaluating the changes in TCR variable beta use.

This thesis highlights that TCR targeted T-cell anti-cancer function can be improved using target agnostic costimulatory proteins that do not require any additional inhibitory or targeting antigens to be expressed on the tumour for T-cell costimulation. This promising strategy will be further evaluated in preclinical models, and should be considered for clinical evaluations, especially in the TIL context.

Bibliography

1. Schreiber, R.D., Old, L.J. & Smyth, M.J. Cancer Immunoediting: Integrating Immunity’s Roles in Cancer Suppression and Promotion. *Science* **331**, 1565-1570 (2011).

2. Waldman, A.D., Fritz, J.M. & Lenardo, M.J. A guide to cancer immunotherapy: from T cell basic science to clinical practice. *Nature Reviews Immunology* **20**, 651-668 (2020).

3. Lesch, S. & Gill, S. The promise and perils of immunotherapy. *Blood Adv* **5**, 3709-3725 (2021).

4. Zhang, Y. & Zhang, Z. The history and advances in cancer immunotherapy: understanding the characteristics of tumor-infiltrating immune cells and their therapeutic implications. *Cellular & Molecular Immunology* **17**, 807-821 (2020).

5. Ribas, A. & Wolchok, J.D. Cancer immunotherapy using checkpoint blockade. *Science* **359**, 1350-1355 (2018).

6. June, C.H. & Sadelain, M. Chimeric Antigen Receptor Therapy. *New England Journal of Medicine* **379**, 64-73 (2018).

7. McCarthy, E.F. The toxins of William B. Coley and the treatment of bone and soft-tissue sarcomas. *Iowa Orthop J* **26**, 154-158 (2006).

8. Coley, W.B. The treatment of malignant tumors by repeated inoculations of erysipelas. With a report of ten original cases. 1893. *Clin Orthop Relat Res*, 3-11 (1991).

9. Redelman-Sidi, G., Glickman, M.S. & Bochner, B.H. The mechanism of action of BCG therapy for bladder cancer--a current perspective. *Nat Rev Urol* **11**, 153-162 (2014).

10. Han, J., Gu, X., Li, Y. & Wu, Q. Mechanisms of BCG in the treatment of bladder cancer-current understanding and the prospect. *Biomed Pharmacother* **129**, 110393 (2020).

11. Goldman, B. & DeFrancesco, L. The cancer vaccine roller coaster. *Nature Biotechnology* **27**, 129-139 (2009).

12. Chen, F. et al. Neoantigen identification strategies enable personalized immunotherapy in refractory solid tumors. *The Journal of Clinical Investigation* **129**, 2056-2070 (2019).

13. Carreno, B.M. et al. Cancer immunotherapy. A dendritic cell vaccine increases the breadth and diversity of melanoma neoantigen-specific T cells. *Science* **348**, 803-808 (2015).

14. Kantoff, P.W. et al. Sipuleucel-T immunotherapy for castration-resistant prostate cancer. *N Engl J Med* **363**, 411-422 (2010).

15. Anassi, E. & Ndefo, U.A. Sipuleucel-T (provenge) injection: the first immunotherapy agent (vaccine) for hormone-refractory prostate cancer. *P t* **36**, 197-202 (2011).

16. Sutherland, S.I.M., Ju, X., Horvath, L.G. & Clark, G.J. Moving on From Sipuleucel-T: New Dendritic Cell Vaccine Strategies for Prostate Cancer. *Frontiers in Immunology* **12** (2021).

17. Fu, C., Zhou, L., Mi, Q.S. & Jiang, A. DC-Based Vaccines for Cancer Immunotherapy. *Vaccines (Basel)* **8** (2020).

18. Santos, P.M. & Butterfield, L.H. Dendritic Cell-Based Cancer Vaccines. *J Immunol* **200**, 443-449 (2018).

19. Vo, M.-C. et al. A combination of immunoadjuvant nanocomplexes and dendritic cell vaccines in the presence of immune checkpoint blockade for effective cancer immunotherapy. *Cellular & Molecular Immunology* **18**, 1599-1601 (2021).

20. Calmeiro, J. et al. Pharmacological combination of nivolumab with dendritic cell vaccines in cancer immunotherapy: An overview. *Pharmacological Research* **164**, 105309 (2021).

21. Lorentzen, C.L., Haanen, J.B., Met, Ö. & Svane, I.M. Clinical advances and ongoing trials on mRNA vaccines for cancer treatment. *Lancet Oncol* **23**, e450-e458 (2022).

22. Fiedler, K., Lazzaro, S., Lutz, J., Rauch, S. & Heidenreich, R. mRNA Cancer Vaccines. *Recent Results Cancer Res* **209**, 61-85 (2016).

23. Chow, A., Perica, K., Klebanoff, C.A. & Wolchok, J.D. Clinical implications of T cell exhaustion for cancer immunotherapy. *Nature Reviews Clinical Oncology* **19**, 775-790 (2022).

24. Rudd, C.E., Taylor, A. & Schneider, H. CD28 and CTLA-4 coreceptor expression and signal transduction. *Immunol Rev* **229**, 12-26 (2009).

25. Agata, Y. et al. Expression of the PD-1 antigen on the surface of stimulated mouse T and B lymphocytes. *Int Immunol* **8**, 765-772 (1996).

26. Robert, L. et al. Distinct immunological mechanisms of CTLA-4 and PD-1 blockade revealed by analyzing TCR usage in blood lymphocytes. *Oncoimmunology* **3**, e29244 (2014).

27. Riviere, P. et al. High Tumor Mutational Burden Correlates with Longer Survival in Immunotherapy-Naïve Patients with Diverse Cancers. *Mol Cancer Ther* **19**, 2139-2145 (2020).

28. Paik, J. Nivolumab Plus Relatlimab: First Approval. *Drugs* **82**, 925-931 (2022).

29. Gomes de Morais, A.L., Cerdá, S. & de Miguel, M. New Checkpoint Inhibitors on the Road: Targeting TIM-3 in Solid Tumors. *Curr Oncol Rep* **24**, 651-658 (2022).

30. Dudley, M.E., Wunderlich, J.R., Shelton, T.E., Even, J. & Rosenberg, S.A. Generation of tumor-infiltrating lymphocyte cultures for use in adoptive transfer therapy for melanoma patients. *J Immunother* **26**, 332-342 (2003).

31. Rosenberg, S.A. IL-2: the first effective immunotherapy for human cancer. *J Immunol* **192**, 5451-5458 (2014).

32. Rohaan, M.W. et al. Tumor-Infiltrating Lymphocyte Therapy or Ipilimumab in Advanced Melanoma. *New England Journal of Medicine* **387**, 2113-2125 (2022).

33. Zhang, L. et al. Tumor-infiltrating lymphocytes genetically engineered with an inducible gene encoding interleukin-12 for the immunotherapy of metastatic melanoma. *Clin Cancer Res* **21**, 2278-2288 (2015).

34. Heemskerk, B. et al. Adoptive cell therapy for patients with melanoma, using tumor-infiltrating lymphocytes genetically engineered to secrete interleukin-2. *Hum Gene Ther* **19**, 496-510 (2008).

35. Sukumaran, S. et al. 198 Costimulatory antigen receptor (CoStAR): a novel platform that enhances the activity of tumor infiltrating lymphocytes (TILs). *Journal for ImmunoTherapy of Cancer* **9**, A209-A209 (2021).

36. O'Malley, D. et al. 492 Phase 2 efficacy and safety of autologous tumor-infiltrating lymphocyte (TIL) cell therapy in combination with pembrolizumab in immune checkpoint inhibitor-naïve patients with advanced cancers. *Journal for ImmunoTherapy of Cancer* **9**, A523-A524 (2021).

37. Chandran, S.S. & Klebanoff, C.A. T cell receptor-based cancer immunotherapy: Emerging efficacy and pathways of resistance. *Immunol Rev* **290**, 127-147 (2019).

38. Hong, D.S. et al. Autologous T cell therapy for MAGE-A4+ solid cancers in HLA-A*02+ patients: a phase 1 trial. *Nature Medicine* (2023).

39. Rapoport, A.P. et al. NY-ESO-1-specific TCR-engineered T cells mediate sustained antigen-specific antitumor effects in myeloma. *Nat Med* **21**, 914-921 (2015).

40. Rath, J.A. & Arber, C. Engineering Strategies to Enhance TCR-Based Adoptive T Cell Therapy. *Cells* **9**, 1485 (2020).

41. Poole, A. et al. Therapeutic high affinity T cell receptor targeting a KRASG12D cancer neoantigen. *Nature Communications* **13**, 5333 (2022).

42. Foy, S.P. et al. Non-viral precision T cell receptor replacement for personalized cell therapy. *Nature* (2022).

43. Greenbaum, U., Dumbrava, E.I., Biter, A.B., Haymaker, C.L. & Hong, D.S. Engineered T-cell Receptor T Cells for Cancer Immunotherapy. *Cancer Immunol Res* **9**, 1252-1261 (2021).

44. Shafer, P., Kelly, L.M. & Hoyos, V. Cancer Therapy With TCR-Engineered T Cells: Current Strategies, Challenges, and Prospects. *Frontiers in Immunology* **13** (2022).

45. Driessens, G., Kline, J. & Gajewski, T.F. Costimulatory and coinhibitory receptors in anti-tumor immunity. *Immunol Rev* **229**, 126-144 (2009).

46. Lahman, M.C. et al. Targeting an alternate Wilms' tumor antigen 1 peptide bypasses immunoproteasome dependency. *Sci Transl Med* **14**, eabg8070 (2022).

47. Mariuzza, R.A., Agnihotri, P. & Orban, J. The structural basis of T-cell receptor (TCR) activation: An enduring enigma. *Journal of Biological Chemistry* **295**, 914-925 (2020).

48. Call, M.E. & Wucherpfennig, K.W. Molecular mechanisms for the assembly of the T cell receptor-CD3 complex. *Mol Immunol* **40**, 1295-1305 (2004).

49. Courtney, A.H., Lo, W.L. & Weiss, A. TCR Signaling: Mechanisms of Initiation and Propagation. *Trends Biochem Sci* **43**, 108-123 (2018).

50. Delgado, P. & Alarcon, B. An orderly inactivation of intracellular retention signals controls surface expression of the T cell antigen receptor. *J Exp Med* **201**, 555-566 (2005).

51. Purbhoo, M.A., Irvine, D.J., Huppa, J.B. & Davis, M.M. T cell killing does not require the formation of a stable mature immunological synapse. *Nat Immunol* **5**, 524-530 (2004).

52. Sykulev, Y., Joo, M., Vturina, I., Tsomides, T.J. & Eisen, H.N. Evidence that a single peptide-MHC complex on a target cell can elicit a cytolytic T cell response. *Immunity* **4**, 565-571 (1996).

53. James, J.R. Tuning ITAM multiplicity on T cell receptors can control potency and selectivity to ligand density. *Sci Signal* **11** (2018).

54. Zenner, G., Vorherr, T., Mustelin, T. & Burn, P. Differential and multiple binding of signal transducing molecules to the ITAMs of the TCR-zeta chain. *J Cell Biochem* **63**, 94-103 (1996).

55. Bettini, M.L. et al. Cutting Edge: CD3 ITAM Diversity Is Required for Optimal TCR Signaling and Thymocyte Development. *The Journal of Immunology* **199**, 1555-1560 (2017).

56. Li, L. et al. Ionic CD3−Lck interaction regulates the initiation of T-cell receptor signaling. *Proceedings of the National Academy of Sciences* **114**, E5891-E5899 (2017).

57. Stepanek, O. et al. Coreceptor scanning by the T cell receptor provides a mechanism for T cell tolerance. *Cell* **159**, 333-345 (2014).

58. Borger, J.G., Zamoyska, R. & Gakamsky, D.M. Proximity of TCR and its CD8 coreceptor controls sensitivity of T cells. *Immunol Lett* **157**, 16-22 (2014).

59. Wei, Q. et al. Lck bound to coreceptor is less active than free Lck. *Proceedings of the National Academy of Sciences* **117**, 15809-15817 (2020).

60. Lo, W.L. & Weiss, A. Adapting T Cell Receptor Ligand Discrimination Capability via LAT. *Front Immunol* **12**, 673196 (2021).

61. Mayya, V. & Dustin, M.L. What Scales the T Cell Response? *Trends Immunol* **37**, 513-522 (2016).

62. Conley, J.M., Gallagher, M.P. & Berg, L.J. T Cells and Gene Regulation: The Switching On and Turning Up of Genes after T Cell Receptor Stimulation in CD8 T Cells. *Front Immunol* **7**, 76 (2016).

63. Huang, J. et al. A single peptide-major histocompatibility complex ligand triggers digital cytokine secretion in CD4(+) T cells. *Immunity* **39**, 846-857 (2013).

64. Xiao, Q. et al. Size-dependent activation of CAR-T cells. *Science Immunology* **7**, eabl3995 (2022).

65. van Loenen, M.M. et al. Mixed T cell receptor dimers harbor potentially harmful neoreactivity. *Proc Natl Acad Sci U S A* **107**, 10972-10977 (2010).

66. Morton, L.T. et al. Simultaneous Deletion of Endogenous TCRαβ for TCR Gene Therapy Creates an Improved and Safe Cellular Therapeutic. *Molecular Therapy* **28**, 64-74 (2020).

67. Kuball, J.r. et al. Facilitating matched pairing and expression of TCR chains introduced into human T cells. *Blood* **109**, 2331-2338 (2006).

68. Cohen, C.J., Zhao, Y., Zheng, Z., Rosenberg, S.A. & Morgan, R.A. Enhanced antitumor activity of murine-human hybrid T-cell receptor (TCR) in human lymphocytes is associated with improved pairing and TCR/CD3 stability. *Cancer Res* **66**, 8878-8886 (2006).

69. Cohen, C.J. et al. Enhanced antitumor activity of T cells engineered to express T-cell receptors with a second disulfide bond. *Cancer Res* **67**, 3898-3903 (2007).

70. Thomas, S. et al. Targeting the Wilms Tumor Antigen 1 by TCR Gene Transfer: TCR Variants Improve Tetramer Binding but Not the Function of Gene Modified Human T Cells1. *The Journal of Immunology* **179**, 5803-5810 (2007).

71. Ahmadi, M. et al. CD3 limits the efficacy of TCR gene therapy in vivo. *Blood* **118**, 3528-3537 (2011).

72. Schober, K. et al. Orthotopic replacement of T-cell receptor α- and β-chains with preservation of near-physiological T-cell function. *Nature Biomedical Engineering* **3**, 974-984 (2019).

73. Linsley, P.S. & Ledbetter, J.A. The role of the CD28 receptor during T cell responses to antigen. *Annu Rev Immunol* **11**, 191-212 (1993).

74. Sansom, D.M. & Hall, N.D. B7/BB1, the ligand for CD28, is expressed on repeatedly activated human T cells in vitro. *Eur J Immunol* **23**, 295-298 (1993).

75. Acuto, O. & Michel, F. CD28-mediated co-stimulation: a quantitative support for TCR signalling. *Nature Reviews Immunology* **3**, 939-951 (2003).

76. Beckermann, K.E. et al. CD28 costimulation drives tumor-infiltrating T cell glycolysis to promote inflammation. *JCI Insight* **5** (2020).

77. Klein Geltink, R.I. et al. Mitochondrial Priming by CD28. *Cell* **171**, 385-397.e311 (2017).

78. Kamphorst, A.O. et al. Rescue of exhausted CD8 T cells by PD-1–targeted therapies is CD28-dependent. *Science* **355**, 1423-1427 (2017).

79. Condomines, M. et al. Tumor-Targeted Human T Cells Expressing CD28-Based Chimeric Antigen Receptors Circumvent CTLA-4 Inhibition. *PLoS One* **10**, e0130518 (2015).

80. Maurer, M.F. et al. The engineered CD80 variant fusion therapeutic davoceticept combines checkpoint antagonism with conditional CD28 costimulation for anti-tumor immunity. *Nature Communications* **13**, 1790 (2022).

81. Waite, J.C. et al. Tumor-targeted CD28 bispecific antibodies enhance the antitumor efficacy of PD-1 immunotherapy. *Science Translational Medicine* **12**, eaba2325 (2020).

82. Shuford, W.W. et al. 4-1BB costimulatory signals preferentially induce CD8+ T cell proliferation and lead to the amplification in vivo of cytotoxic T cell responses. *J Exp Med* **186**, 47-55 (1997).

83. Gramaglia, I., Cooper, D., Miner, K.T., Kwon, B.S. & Croft, M. Co-stimulation of antigen-specific CD4 T cells by 4-1BB ligand. *Eur J Immunol* **30**, 392-402 (2000).

84. Maus, M.V. et al. Ex vivo expansion of polyclonal and antigen-specific cytotoxic T lymphocytes by artificial APCs expressing ligands for the T-cell receptor, CD28 and 4-1BB. *Nat Biotechnol* **20**, 143-148 (2002).

85. Melero, I. et al. Amplification of tumor immunity by gene transfer of the co-stimulatory 4-1BB ligand: synergy with the CD28 co-stimulatory pathway. *Eur J Immunol* **28**, 1116-1121 (1998).

86. Chester, C., Ambulkar, S. & Kohrt, H.E. 4-1BB agonism: adding the accelerator to cancer immunotherapy. *Cancer Immunol Immunother* **65**, 1243-1248 (2016).

87. Cabo, M. et al. Trial Watch: Immunostimulatory monoclonal antibodies for oncological indications. *Oncoimmunology* **6**, e1371896 (2017).

88. Choi, Y. et al. T-cell agonists in cancer immunotherapy. *J Immunother Cancer* **8** (2020).

89. Hinner, M.J. et al. Tumor-Localized Costimulatory T-Cell Engagement by the 4-1BB/HER2 Bispecific Antibody-Anticalin Fusion PRS-343. *Clin Cancer Res* **25**, 5878-5889 (2019).

90. Sadelain, M. Chimeric antigen receptors: driving immunology towards synthetic biology. *Curr Opin Immunol* **41**, 68-76 (2016).

91. van der Stegen, S.J., Hamieh, M. & Sadelain, M. The pharmacology of second-generation chimeric antigen receptors. *Nat Rev Drug Discov* **14**, 499-509 (2015).

92. Kuwana, Y. et al. Expression of chimeric receptor composed of immunoglobulin-derived V regions and T-cell receptor-derived C regions. *Biochem Biophys Res Commun* **149**, 960-968 (1987).

93. Gross, G., Waks, T. & Eshhar, Z. Expression of immunoglobulin-T-cell receptor chimeric molecules as functional receptors with antibody-type specificity. *Proc Natl Acad Sci U S A* **86**, 10024-10028 (1989).

94. Brocker, T., Peter, A., Traunecker, A. & Karjalainen, K. New simplified molecular design for functional T cell receptor. *Eur J Immunol* **23**, 1435-1439 (1993).

95. Imai, C. et al. Chimeric receptors with 4-1BB signaling capacity provoke potent cytotoxicity against acute lymphoblastic leukemia. *Leukemia* **18**, 676-684 (2004).

96. Maher, J., Brentjens, R.J., Gunset, G., Riviere, I. & Sadelain, M. Human T-lymphocyte cytotoxicity and proliferation directed by a single chimeric TCRzeta /CD28 receptor. *Nat Biotechnol* **20**, 70-75 (2002).

97. Cappell, K.M. & Kochenderfer, J.N. A comparison of chimeric antigen receptors containing CD28 versus 4-1BB costimulatory domains. *Nat Rev Clin Oncol* **18**, 715-727 (2021).

98. Wang, J. et al. Optimizing adoptive polyclonal T cell immunotherapy of lymphomas, using a chimeric T cell receptor possessing CD28 and CD137 costimulatory domains. *Hum Gene Ther* **18**, 712-725 (2007).

99. Hirabayashi, K. et al. Dual-targeting CAR-T cells with optimal co-stimulation and metabolic fitness enhance antitumor activity and prevent escape in solid tumors. *Nature Cancer* **2**, 904-918 (2021).

100. Kloss, C.C., Condomines, M., Cartellieri, M., Bachmann, M. & Sadelain, M. Combinatorial antigen recognition with balanced signaling promotes selective tumor eradication by engineered T cells. *Nature Biotechnology* **31**, 71-75 (2013).

101. Zhao, Z. et al. Structural Design of Engineered Costimulation Determines Tumor Rejection Kinetics and Persistence of CAR T Cells. *Cancer Cell* **28**, 415-428 (2015).

102. Pegram, H.J. et al. Tumor-targeted T cells modified to secrete IL-12 eradicate systemic tumors without need for prior conditioning. *Blood* **119**, 4133-4141 (2012).

103. Roybal, Kole T. et al. Precision Tumor Recognition by T Cells With Combinatorial Antigen-Sensing Circuits. *Cell* **164**, 770-779 (2016).

104. Juillerat, A. et al. An oxygen sensitive self-decision making engineered CAR T-cell. *Scientific Reports* **7**, 39833 (2017).

105. Hudecek, M. et al. Receptor affinity and extracellular domain modifications affect tumor recognition by ROR1-specific chimeric antigen receptor T cells. *Clin Cancer Res* **19**, 3153-3164 (2013).

106. Ghorashian, S. et al. Enhanced CAR T cell expansion and prolonged persistence in pediatric patients with ALL treated with a low-affinity CD19 CAR. *Nature Medicine* **25**, 1408-1414 (2019).

107. Hudecek, M. et al. The nonsignaling extracellular spacer domain of chimeric antigen receptors is decisive for in vivo antitumor activity. *Cancer Immunol Res* **3**, 125-135 (2015).

108. Majzner, R.G. et al. Tuning the Antigen Density Requirement for CAR T-cell Activity. *Cancer Discov* **10**, 702-723 (2020).

109. Jun Lee, E.H. et al. Antigen-dependent IL-12 signaling in CAR T cells promotes regional to systemic disease targeting. *bioRxiv*, 2023.2001.2006.522784 (2023).

110. Boucher, J.C. et al. CD28 Costimulatory Domain–Targeted Mutations Enhance Chimeric Antigen Receptor T-cell Function. *Cancer Immunology Research* **9**, 62-74 (2021).

111. Guedan, S. et al. Single residue in CD28-costimulated CAR-T cells limits long-term persistence and antitumor durability. *J Clin Invest* **130**, 3087-3097 (2020).

112. Feucht, J. et al. Calibration of CAR activation potential directs alternative T cell fates and therapeutic potency. *Nat Med* **25**, 82-88 (2019).

113. Subklewe, M. BiTEs better than CAR T cells. *Blood Advances* **5**, 607-612 (2021).

114. Molina, J.C. & Shah, N.N. CAR T cells better than BiTEs. *Blood Advances* **5**, 602-606 (2021).

115. Correnti, C.E. et al. Simultaneous multiple interaction T-cell engaging (SMITE) bispecific antibodies overcome bispecific T-cell engager (BiTE) resistance via CD28 co-stimulation. *Leukemia* **32**, 1239-1243 (2018).

116. Warwas, K.M. et al. Co-Stimulatory Bispecific Antibodies Induce Enhanced T Cell Activation and Tumor Cell Killing in Breast Cancer Models. *Frontiers in Immunology* **12** (2021).

117. Sadelain, M., Brentjens, R. & Rivière, I. The basic principles of chimeric antigen receptor design. *Cancer Discov* **3**, 388-398 (2013).

118. Morgan, R.A. et al. Case report of a serious adverse event following the administration of T cells transduced with a chimeric antigen receptor recognizing ERBB2. *Mol Ther* **18**, 843-851 (2010).

119. Fedorov, V.D., Themeli, M. & Sadelain, M. PD-1- and CTLA-4-based inhibitory chimeric antigen receptors (iCARs) divert off-target immunotherapy responses. *Sci Transl Med* **5**, 215ra172 (2013).

120. Srivastava, S. et al. Logic-Gated ROR1 Chimeric Antigen Receptor Expression Rescues T Cell-Mediated Toxicity to Normal Tissues and Enables Selective Tumor Targeting. *Cancer Cell* **35**, 489-503.e488 (2019).

121. Willemsen, R.A. et al. A phage display selected Fab fragment with MHC class I-restricted specificity for MAGE-A1 allows for retargeting of primary human T lymphocytes. *Gene Therapy* **8**, 1601-1608 (2001).

122. Ataie, N. et al. Structure of a TCR-Mimic Antibody with Target Predicts Pharmacogenetics. *J Mol Biol* **428**, 194-205 (2016).

123. Krause, A. et al. Antigen-dependent CD28 signaling selectively enhances survival and proliferation in genetically modified activated human primary T lymphocytes. *J Exp Med* **188**, 619-626 (1998).

124. Liu, X. et al. A Chimeric Switch-Receptor Targeting PD1 Augments the Efficacy of Second-Generation CAR T Cells in Advanced Solid Tumors. *Cancer Res* **76**, 1578-1590 (2016).

125. Oda, S.K. et al. A CD200R-CD28 fusion protein appropriates an inhibitory signal to enhance T-cell function and therapy of murine leukemia. *Blood* **130**, 2410-2419 (2017).

126. Oda, S.K. et al. A Fas-4-1BB fusion protein converts a death to a pro-survival signal and enhances T cell therapy. *Journal of Experimental Medicine* **217** (2020).

127. Roth, T.L. et al. Pooled Knockin Targeting for Genome Engineering of Cellular Immunotherapies. *Cell* **181**, 728-744.e721 (2020).

128. Zhang, T., He, X., Tsang, T.C. & Harris, D.T. Transgenic TCR expression: comparison of single chain with full-length receptor constructs for T-cell function. *Cancer Gene Ther* **11**, 487-496 (2004).

129. Mansilla-Soto, J. et al. HLA-independent T cell receptors for targeting tumors with low antigen density. *Nat Med* **28**, 345-352 (2022).

130. Stone, J.D. et al. A novel T cell receptor single-chain signaling complex mediates antigen-specific T cell activity and tumor control. *Cancer Immunol Immunother* **63**, 1163-1176 (2014).

131. Schaft, N. et al. T cell re-targeting to EBV antigens following TCR gene transfer: CD28-containing receptors mediate enhanced antigen-specific IFNgamma production. *Int Immunol* **18**, 591-601 (2006).

132. Govers, C. et al. TCRs genetically linked to CD28 and CD3ε do not mispair with endogenous TCR chains and mediate enhanced T cell persistence and anti-melanoma activity. *J Immunol* **193**, 5315-5326 (2014).

133. Mavilio, F. et al. Peripheral blood lymphocytes as target cells of retroviral vector-mediated gene transfer. *Blood* **83**, 1988-1997 (1994).

134. Poznansky, M., Lever, A., Bergeron, L., Haseltine, W. & Sodroski, J. Gene transfer into human lymphocytes by a defective human immunodeficiency virus type 1 vector. *J Virol* **65**, 532-536 (1991).

135. Labbé, R.P., Vessillier, S. & Rafiq, Q.A. Lentiviral Vectors for T Cell Engineering: Clinical Applications, Bioprocessing and Future Perspectives. *Viruses* **13** (2021).

136. Ellis, J. Silencing and Variegation of Gammaretrovirus and Lentivirus Vectors. *Human Gene Therapy* **16**, 1241-1246 (2005).

137. Shao, L. et al. Genome-wide profiling of retroviral DNA integration and its effect on clinical pre-infusion CAR T-cell products. *J Transl Med* **20**, 514 (2022).

138. Newrzela, S. et al. Resistance of mature T cells to oncogene transformation. *Blood* **112**, 2278-2286 (2008).

139. Eyquem, J. et al. Targeting a CAR to the TRAC locus with CRISPR/Cas9 enhances tumour rejection. *Nature* (2017).

140. Rodriguez-Marquez, P. et al. CAR density influences antitumoral efficacy of BCMA CAR T cells and correlates with clinical outcome. *Sci Adv* **8**, eabo0514 (2022).

141. Wang, D., Tai, P.W.L. & Gao, G. Adeno-associated virus vector as a platform for gene therapy delivery. *Nat Rev Drug Discov* **18**, 358-378 (2019).

142. Micklethwaite, K.P. et al. Investigation of product-derived lymphoma following infusion of piggyBac-modified CD19 chimeric antigen receptor T cells. *Blood* **138**, 1391-1405 (2021).

143. Porteus, M.H. A New Class of Medicines through DNA Editing. *New England Journal of Medicine* **380**, 947-959 (2019).

144. Ruggiero, E. et al. CRISPR-based gene disruption and integration of high-avidity, WT1-specific T cell receptors improve antitumor T cell function. *Science Translational Medicine* **14**, eabg8027 (2022).

145. Schober, K. et al. Orthotopic replacement of T-cell receptor α- and β-chains with preservation of near-physiological T-cell function. *Nat Biomed Eng* **3**, 974-984 (2019).

146. Zhang, J. et al. Non-viral, specifically targeted CAR-T cells achieve high safety and efficacy in B-NHL. *Nature* **609**, 369-374 (2022).

147. Chang, A. et al. 277 Development of a robust manufacturing process for AB-1015, an integrated circuit T cell (ICT) product, using targeted, CRISPR integration of transgenes by electroporation (CITE) editing. *Journal for ImmunoTherapy of Cancer* **10**, A292-A292 (2022).

148. Nahmad, A.D. et al. Frequent aneuploidy in primary human T cells after CRISPR–Cas9 cleavage. *Nature Biotechnology* **40**, 1807-1813 (2022).

149. Stadtmauer, E.A. et al. CRISPR-engineered T cells in patients with refractory cancer. *Science* **367**, eaba7365 (2020).

150. Yarnall, M.T.N. et al. Drag-and-drop genome insertion of large sequences without double-strand DNA cleavage using CRISPR-directed integrases. *Nat Biotechnol* (2022).

151. Gnjatic, S. et al. NY-ESO-1: review of an immunogenic tumor antigen. *Adv Cancer Res* **95**, 1-30 (2006).

152. Xue, S.A. et al. Human MHC Class I-restricted high avidity CD4(+) T cells generated by co-transfer of TCR and CD8 mediate efficient tumor rejection in vivo. *Oncoimmunology* **2**, e22590 (2013).

153. Bajwa, G., Lanz, I., Cardenas, M., Brenner, M.K. & Arber, C. Transgenic CD8αβ co-receptor rescues endogenous TCR function in TCR-transgenic virus-specific T cells. *J Immunother Cancer* **8** (2020).

154. Céfaï, D. et al. CD28 receptor endocytosis is targeted by mutations that disrupt phosphatidylinositol 3-kinase binding and costimulation. *J Immunol* **160**, 2223-2230 (1998).

155. Yang, W. et al. Dynamic regulation of CD28 conformation and signaling by charged lipids and ions. *Nat Struct Mol Biol* **24**, 1081-1092 (2017).

156. June, C.H., Ledbetter, J.A., Linsley, P.S. & Thompson, C.B. Role of the CD28 receptor in T-cell activation. *Immunology Today* **11**, 211-216 (1990).

157. Larson, R.C. et al. CAR T cell killing requires the IFNγR pathway in solid but not liquid tumours. *Nature* **604**, 563-570 (2022).

158. Robbins, P.F. et al. Single and dual amino acid substitutions in TCR CDRs can enhance antigen-specific T cell functions. *J Immunol* **180**, 6116-6131 (2008).

159. Miyao, K. et al. Introduction of Genetically Modified CD3ζ Improves Proliferation and Persistence of Antigen-Specific CTLs. *Cancer Immunology Research* **6**, 733-744 (2018).

160. Tsuji, T. et al. Heat shock protein 90-mediated peptide-selective presentation of cytosolic tumor antigen for direct recognition of tumors by CD4(+) T cells. *J Immunol* **188**, 3851-3858 (2012).

161. Hazini, A., Fisher, K. & Seymour, L. Deregulation of HLA-I in cancer and its central importance for immunotherapy. *Journal for ImmunoTherapy of Cancer* **9**, e002899 (2021).

162. Gramaglia, I., Cooper, D., Miner, K.T., Kwon, B.S. & Croft, M. Co-stimulation of antigen-specific CD4 T cells by 4-1BB ligand. *European Journal of Immunology* **30**, 392-402 (2000).

163. Kim, J.V., Latouche, J.-B., Rivière, I. & Sadelain, M. The ABCs of artificial antigen presentation. *Nature Biotechnology* **22**, 403-410 (2004).

164. Zhao, Z. et al. Structural Design of Engineered Costimulation Determines Tumor Rejection Kinetics and Persistence of CAR T Cells. *Cancer Cell* **28**, 415-428 (2015).

165. Hamieh, M. et al. CAR T cell trogocytosis and cooperative killing regulate tumour antigen escape. *Nature* **568**, 112-116 (2019).

166. Katsarou, A. et al. Combining a CAR and a chimeric costimulatory receptor enhances T cell sensitivity to low antigen density and promotes persistence. *Sci Transl Med* **13**, eabh1962 (2021).

167. Salzer, B. et al. Engineering AvidCARs for combinatorial antigen recognition and reversible control of CAR function. *Nat Commun* **11**, 4166 (2020).

168. Chen, J. et al. NR4A transcription factors limit CAR T cell function in solid tumours. *Nature* **567**, 530-534 (2019).

169. Good, C.R. et al. An NK-like CAR T cell transition in CAR T cell dysfunction. *Cell* **184**, 6081-6100 e6026 (2021).

170. Nam, K.O., Shin, S.M. & Lee, H.W. Cross-linking of 4-1BB up-regulates IL-13 expression in CD8(+) T lymphocytes. *Cytokine* **33**, 87-94 (2006).

171. Kawalekar, O.U. et al. Distinct Signaling of Coreceptors Regulates Specific Metabolism Pathways and Impacts Memory Development in CAR T Cells. *Immunity* **44**, 712 (2016).

172. Menk, A.V. et al. 4-1BB costimulation induces T cell mitochondrial function and biogenesis enabling cancer immunotherapeutic responses. *Journal of Experimental Medicine* **215**, 1091-1100 (2018).

173. Nakaseko, C. et al. Cytotoxic T lymphocyte antigen 4 (CTLA-4) engagement delivers an inhibitory signal through the membrane-proximal region in the absence of the tyrosine motif in the cytoplasmic tail. *J Exp Med* **190**, 765-774 (1999).

174. van der Leun, A.M. & Schumacher, T.N. An atlas of intratumoral T cells. *Science* **374**, 1446-1447 (2021).

175. Liu, Y. et al. Chimeric STAR receptors using TCR machinery mediate robust responses against solid tumors. *Sci Transl Med* **13** (2021).

176. Helsen, C.W. et al. The chimeric TAC receptor co-opts the T cell receptor yielding robust anti-tumor activity without toxicity. *Nat Commun* **9**, 3049 (2018).

177. Birtel, M. et al. A TCR-like CAR Promotes Sensitive Antigen Recognition and Controlled T-cell Expansion Upon mRNA Vaccination. *Cancer Research Communications* **2**, 827-841 (2022).

178. Baeuerle, P.A. et al. Synthetic TRuC receptors engaging the complete T cell receptor for potent anti-tumor response. *Nat Commun* **10**, 2087 (2019).

179. Xu, Y. et al. A novel antibody-TCR (AbTCR) platform combines Fab-based antigen recognition with gamma/delta-TCR signaling to facilitate T-cell cytotoxicity with low cytokine release. *Cell Discov* **4**, 62 (2018).

180. Omer, B. et al. A Costimulatory CAR Improves TCR-based Cancer Immunotherapy. *Cancer Immunol Res* **10**, 512-524 (2022).

181. Bollard, C.M. et al. Adapting a transforming growth factor beta-related tumor protection strategy to enhance antitumor immunity. *Blood* **99**, 3179-3187 (2002).

182. Yamamoto, T.N. et al. T cells genetically engineered to overcome death signaling enhance adoptive cancer immunotherapy. *J Clin Invest* **129**, 1551-1565 (2019).

183. Anderson, K.G. et al. Engineering adoptive T cell therapy to co-opt Fas ligand-mediated death signaling in ovarian cancer enhances therapeutic efficacy. *J Immunother Cancer* **10** (2022).

184. Lesch, S. et al. PD-1-CD28 fusion protein strengthens mesothelin-specific TRuC T cells in preclinical solid tumor models. *Cell Oncol (Dordr)* (2022).

185. Wang, J. et al. A novel adoptive synthetic TCR and antigen receptor (STAR) T-Cell therapy for B-Cell acute lymphoblastic leukemia. *Am J Hematol* **97**, 992-1004 (2022).

186. Kraehenbuehl, L., Weng, C.-H., Eghbali, S., Wolchok, J.D. & Merghoub, T. Enhancing immunotherapy in cancer by targeting emerging immunomodulatory pathways. *Nature Reviews Clinical Oncology* **19**, 37-50 (2022).

187. Chesney, J. et al. 883TiP A phase I/II open-label study (IOV-GM1-201) of TALEN-mediated PD-1 inactivated autologous tumor-infiltrating lymphocytes (TIL; IOV-4001) in patients with advanced melanoma and NSCLC. *Annals of Oncology* **33**, S952 (2022).

188. Donaghey, J. et al. Abstract 557: Engineering off-the-shelf anti mesothelin t-cell receptor fusion construct (TRuC™) t-cells. *Cancer Research* **82**, 557-557 (2022).

189. Ecsedi, M., McAfee, M.S. & Chapuis, A.G. The Anticancer Potential of T Cell Receptor-Engineered T Cells. *Trends Cancer* **7**, 48-56 (2021).

190. Siegler, E.L. & Kenderian, S.S. Neurotoxicity and Cytokine Release Syndrome After Chimeric Antigen Receptor T Cell Therapy: Insights Into Mechanisms and Novel Therapies. *Frontiers in Immunology* **11** (2020).

191. Jain, M.D., Smith, M. & Shah, N.N. How I Treat Refractory CRS and ICANS Following CAR T-cell Therapy. *Blood* (2023).

192. Hünig, T. The rise and fall of the CD28 superagonist TGN1412 and its return as TAB08: a personal account. *Febs j* **283**, 3325-3334 (2016).

193. Porciello, N. et al. A non-conserved amino acid variant regulates differential signalling between human and mouse CD28. *Nature Communications* **9**, 1080 (2018).

194. Melkus, M.W. et al. Humanized mice mount specific adaptive and innate immune responses to EBV and TSST-1. *Nat Med* **12**, 1316-1322 (2006).

195. Dobbins, J. et al. Binding of the cytoplasmic domain of CD28 to the plasma membrane inhibits Lck recruitment and signaling. *Science Signaling* **9**, ra75-ra75 (2016).

196. Herndler-Brandstetter, D. et al. Humanized mouse model supports development, function, and tissue residency of human natural killer cells. *Proc Natl Acad Sci U S A* **114**, E9626-e9634 (2017).

197. Matsuda, M. et al. Human NK cell development in hIL-7 and hIL-15 knockin NOD/SCID/IL2rgKO mice. *Life Sci Alliance* **2** (2019).

198. Katano, I. et al. Long-term maintenance of peripheral blood derived human NK cells in a novel human IL-15- transgenic NOG mouse. *Sci Rep* **7**, 17230 (2017).